

# **Evidence Report:**

## ***Risk of Injury Due to Dynamic Loads***

### **HUMAN RESEARCH PROGRAM HUMAN FACTORS AND BEHAVIORAL PERFORMANCE ELEMENT**

Revision: A

Approved for Public Release: September 15, 2021

National Aeronautics and Space Administration  
Lyndon B. Johnson Space Center  
Houston, Texas

## **CURRENT CONTRIBUTING AUTHORS:**

Jeffrey T. Somers, NASA, Lyndon B. Johnson Space Center

Teresa Reiber, KBR @ Lyndon B. Johnson Space Center

Nathaniel Newby, KBR @ Lyndon B. Johnson Space Center

Preston Greenhalgh, KBR @ Lyndon B. Johnson Space Center

Keegan Yates, KBR @ Lyndon B. Johnson Space Center

***Trade names and trademarks are used in this report for identification only. Their usage does not constitute an official endorsement, either expressed or implied, by the National Aeronautics and Space Administration.***

# TABLE OF CONTENTS

<b>LIST OF FIGURES .....</b>	<b>7</b>
<b>LIST OF TABLES .....</b>	<b>10</b>
<b>ABBREVIATIONS .....</b>	<b>11</b>
<b>STATUS .....</b>	<b>12</b>
<b>RISK TITLE .....</b>	<b>12</b>
<b>EXECUTIVE SUMMARY .....</b>	<b>12</b>
<b>1.0 EVIDENCE .....</b>	<b>14</b>
1.1 INTRODUCTION .....	14
1.1.1 Context.....	14
1.1.2 Scope of Occupant Protection .....	14
1.1.3 Definition of Dynamic Loading.....	15
1.1.4 Standard Instruments and Methods to Measure Dynamic Loads .....	16
1.1.5 Definition of Injury.....	16
1.1.6 Unique Aspects of Spaceflight Injury Biomechanics.....	19
1.1.7 Operationally Relevant Injury Scale .....	19
1.1.8 Standardized Testing.....	20
1.2 HISTORICAL SPACEFLIGHT EVIDENCE .....	20
1.2.1 U.S. Space Program .....	20
1.2.2 USSR/Russian Space Program.....	21
1.2.3 Chinese Space Program .....	23
1.3 INJURY RISK FACTORS .....	24
1.3.1 Extrinsic Injury Risk Factors .....	25
1.3.1.1 Vehicle Dynamic Profile .....	25
1.3.1.1.1 Introduction .....	25
1.3.1.1.2 Historical Background on Biomechanics Impacts from Spaceflight.....	26
1.3.1.2 Directional Loading .....	30
1.3.1.2.1 +X Axis Loading (Eyeballs In).....	30
1.3.1.2.2 -X Axis Loading (Eyeballs Out).....	31

1.3.1.2.3	<i>±Y Axis Loading (Eyeballs Left/Right)</i> .....	31
1.3.1.2.4	<i>+Z Axis Loading (Eyeballs Down)</i> .....	32
1.3.1.2.5	<i>-Z Axis Loading (Eyeballs Up)</i> .....	35
1.3.1.2.6	<i>Multiaxial Loading and Secondary Impacts</i> .....	35
1.3.1.3	Seat & Harness System .....	36
1.3.1.4	Spacesuit and Helmet .....	44
1.3.1.5	Rigid Suit Elements.....	47
1.3.1.6	Energy Attenuation .....	47
<b>1.3.2</b>	<b>Intrinsic Injury Risk Factors</b> .....	<b>47</b>
1.3.2.1	Age .....	48
1.3.2.2	Sex.....	50
1.3.2.3	Anthropometry .....	52
1.3.2.4	Spaceflight-Induced Physiological Deconditioning .....	52
1.4	Injury Criteria Definition .....	58
<b>1.4.1</b>	<b>Head Injury</b> .....	<b>58</b>
1.4.1.1	Traumatic Brain Injury.....	58
1.4.1.2	Skull Fracture .....	59
1.4.1.3	Head Injury Mechanisms.....	59
1.4.1.4	Head Injury Metrics.....	59
<b>1.4.2</b>	<b>Spinal Injury</b> .....	<b>60</b>
1.4.2.1	Spinal Injury Mechanisms .....	60
1.4.2.1.1	<i>Neck</i> .....	60
1.4.2.1.2	<i>Thoraco-Lumbar Spine</i> .....	60
1.4.2.2	Spinal Injury Metrics .....	60
<b>1.4.3</b>	<b>Upper and Lower Extremity Injury</b> .....	<b>62</b>
1.4.3.1	Upper and Lower Extremity Injury Mechanisms .....	62
1.4.3.2	Upper and Lower Extremity Injury Metrics.....	62
<b>1.4.4</b>	<b>Thorax Injury</b> .....	<b>63</b>
1.4.4.1	Thorax Injury Mechanisms.....	63
1.4.4.2	Thorax Injury Metrics .....	63
<b>1.4.5</b>	<b>Abdominal and Pelvic Injury</b> .....	<b>64</b>

1.4.5.1	Abdominal and Pelvic Injury Mechanisms .....	64
1.4.5.2	Abdominal and Pelvic Injury Metrics .....	65
1.5	INJURY RISK ASSESSMENT METHODS.....	65
<b>1.5.1</b>	<b>Humans .....</b>	<b>66</b>
1.5.1.1	Human Volunteers .....	66
1.5.1.2	Post Mortem Human Surrogates .....	66
1.5.1.3	Human Exposure Data .....	66
1.5.1.4	Injury Risk Curves .....	67
1.5.1.4.1	Head Injury Risk Curves.....	67
1.5.1.4.2	Neck Injury Risk Curves .....	68
1.5.1.4.3	Thoracic Injury Risk Curves.....	69
1.5.1.4.4	Lumbar Spine Injury Risk Curves .....	70
1.5.1.4.5	Lower Extremity Injury Risk Curves .....	70
<b>1.5.2</b>	<b>Human Surrogates .....</b>	<b>73</b>
1.5.2.1	Physical ATDs .....	73
1.5.2.1.1	Hybrid III ATD .....	74
1.5.2.1.2	Automotive ATD.....	74
1.5.2.1.3	Aerospace and Military ATD .....	74
1.5.2.1.4	FAA Hybrid III ATD.....	75
1.5.2.1.5	Pedestrian ATD.....	75
1.5.2.1.6	Various Size ATDs.....	76
1.5.2.1.7	Spaceflight Application ATDs .....	76
1.5.2.1.8	Injury Assessment Reference Values (IARVs) .....	77
1.5.2.1.9	THOR ATD.....	78
1.5.2.1.10	THOR Injury Assessment Reference Values (IARVs).....	79
1.5.2.1.11	EuroSID ATD .....	79
1.5.2.1.12	WorldSID ATD.....	80
1.5.2.1.13	BioRID ATD .....	80
<b>1.5.3</b>	<b>Animal Models.....</b>	<b>81</b>
<b>1.5.4</b>	<b>Numerical Models.....</b>	<b>81</b>
1.5.4.1	Brinkley Dynamic Response Model.....	81

1.5.4.2	ATD Numerical Models .....	83
1.5.4.3	Hybrid III ATD FEM .....	84
1.5.4.4	THOR ATD FEM.....	85
1.5.4.5	Other FEM ATDs.....	86
<b>1.5.5</b>	<b>Human Numerical Models.....</b>	<b>86</b>
1.5.5.1	Total Human Model for Safety (THUMS®) .....	86
1.5.5.2	Global Human Body Model Consortium (GHBMC) .....	87
1.5.5.3	ESI Human Model.....	88
1.5.5.4	MADYMO Human Model .....	89
1.5.5.5	Advantages and Limitations.....	89
<b>1.5.6</b>	<b>Summary.....</b>	<b>90</b>
<b>2.0</b>	<b>RISK IN CONTEXT OF EXPLORATION MISSION AND OPERATIONS .....</b>	<b>91</b>
<b>3.0</b>	<b>DAG REVIEW .....</b>	<b>92</b>
<b>4.0</b>	<b>KNOWLEDGE BASE.....</b>	<b>92</b>
4.1	GAPS.....	92
4.2	STATE of KNOWLEDGE/FUTURE WORK .....	93
<b>5.0</b>	<b>CONCLUSION .....</b>	<b>94</b>
<b>6.0</b>	<b>REFERENCES.....</b>	<b>95</b>
<b>7.0</b>	<b>RESOURCES.....</b>	<b>106</b>

# LIST OF FIGURES

Figure 1: Direction of Acceleration Relative to Body.....	15
Figure 2: Acceleration Input to the Sled versus Acceleration of the Body [4].....	16
Figure 3: Stress–Strain Properties of Bone in Tension [10]. ....	18
Figure 4: Three Primary Injury Mechanisms [11].....	18
Figure 5: ORIS and its Components.....	20
Figure 6: Soyuz Drop Test Platform [16]. ....	21
Figure 7: Seat Testing at Various Angles [16]. ....	21
Figure 8: Soyuz Test Condition Causing Spinal Injury [16]. ....	22
Figure 9: Photos of Shenzhou Missions. ....	24
Figure 10: Factors Affecting Risk of Injury from Dynamic Loads. ....	24
Figure 11: Vehicle Shapes [22].....	25
Figure 12: General Occupant Loading Conditions in Capsule Landings.....	26
Figure 13: Volunteers Undergoing an Impact Test in Developmental Pressure Suits, Lap Belts, Shoulder Harness, and Seating System (Credit: USAF). ....	28
Figure 14: A Volunteer Being Tested in a Developmental Pressure Suit While Wearing a Lap Belt, Shoulder Straps, and Inverted-V, Negative-G Straps (Credit: USAF).....	29
Figure 15: Relationship Between End Point Disruption and Vertebral Fracture [51].....	33
Figure 16: Postural Effect on Spinal Injury during +Z Loading [51].....	34
Figure 17: F-4 Ejection Seat Posture [52].....	36
Figure 18: Car Crash with Restrained Driver [57]. ....	37
Figure 19: Car Crash with Unrestrained Driver [57].....	37
Figure 20: Head Injury Criterion (HIC) 15 Injury Risk Functions [60]. ....	38
Figure 21: NASCAR Injury Distribution [41]. ....	38
Figure 22: NASCAR Head Injury Risk [41].....	39
Figure 23: Harness Configurations [62]. ....	40
Figure 24: Impact Vehicle Test Apparatus .....	41
Figure 25: Contour Body Support Seat [64]. ....	41
Figure 26: Kazbek Seat for Soyuz Vehicle [61]. ....	41
Figure 27: Comparison of B-2 Ejection Seat Cushions. Original Cushion (left) and Proposed cushion (right) [78].....	44
Figure 28: SMC Mounting Locations. ....	45
Figure 29: Suited Model [84]. ....	46
Figure 30: Bone Strength Decreases with Age [57]. ....	48
Figure 31: Failure of Male Cervical Spine [98]. ....	48
Figure 32: Comparison of Probability Curves and $\pm$ 95% Confidence Intervals for Upright Tests [87]. ....	49
Figure 33: Force, Moment, and Lower Neck Injury Criteria Risk Curves for Combined (black) and Female-Only (pink) Datasets.....	51
Figure 34: Bone Strength is Dependent on BMD and Geometry [131]. ....	53
Figure 35: Changes in BMD after Long-Duration Spaceflight [142].....	54

Figure 36: Compression Strength of Trabecular Bone from Lumbar Spine Correlates with Loading Direction and with Bone Mineral Density [145].	55
Figure 37: Ground Version of the Advanced Resistive Exercise Device (ARED) [146].	56
Figure 38: Relaxed Posture During Impact [149].	57
Figure 39: Tense Posture During Impact [149].	57
Figure 40: Available Injury Assessment Methods.	65
Figure 41: Probability of Human Head Injury Based on Head Injury Criterion (HIC) [226].	67
Figure 42: Risk of Concussion Based on Combined Rotational and Linear Accelerations of the Head [171].	68
Figure 43: Risk of Neck Injury From Force (left) and Moment (right) Derived using PMHS [195].	68
Figure 44: Lower Neck Injury Criteria and Injury Probability Derived from Rear-Impact Tests on PMHS [195].	69
Figure 45: Probability of Neck Injury due to Neck Axial Compression [227].	69
Figure 46: Injury Risk Function for PMHS Sternal Compression [228].	70
Figure 47: Injury Probability as a Function of Axial Force to the Thoracic and Lumbar Spine Regions [197].	70
Figure 48: Probability of AIS 2+ and 3+ Knee, Thigh, or Hip Injuries as a Function of Axial Femur Force [202].	71
Figure 49: Risk of AIS 2+ Tibial Plateau or Condyle Injury as a Function of Upper Tibia Axial Force for a 50th Percentile Male [202].	71
Figure 50: Risk of AIS 2+ Injury as a Function of Revised Tibia Index [202].	72
Figure 51: Risk of AIS 2+ Injury in Calcaneus, Talus, Ankle, and Midfoot as a Function of Lower Tibia Axial Force [202].	72
Figure 52: AIS2+ Injury of Malleolus and Surrounding Ligaments as a Function of Foot Dorsiflexion Moment (left) Inversion/Eversion (right) [202].	72
Figure 53: Anthropomorphic Test Devices (ATD) A) Hybrid III Frontal Impact Family (L to R: 10-year-old, 50th percentile male adult, 5 <sup>th</sup> percentile female adult, 3-year-old, 6-year-old), B) THOR 50 <sup>th</sup> percentile Frontal Impact ATD, C) ADAM 95 <sup>th</sup> percentile Military Vertical Impact ATD, and D) WorldSID 50 <sup>th</sup> percentile Side Impact Dummy.	74
Figure 54: Federal Aviation Administration (FAA) Hybrid III 50th Male ATD.	75
Figure 55: Hybrid III 50th Percentile Male Pedestrian ATD.	76
Figure 56: THOR-50M.	78
Figure 57: The Worldwide Harmonized Side Impact Dummy (WorldSID) (humaneticsatd.com).	80
Figure 58: BioRID-II (humaneticsatd.com).	81
Figure 59: Lumped Mass Diagram of the Brinkley Dynamic Response Criteria Model.	82
Figure 61: Various Anthropomorphic Test Device (ATD) Models. Shown are A) Livermore Software Technology Corporation (LSTC) Hybrid III 5th percentile female LS-DYNA FE model, B) LSTC Hybrid III 50th percentile male LS-DYNA FE model, C) LSTC Hybrid III 95th percentile male LS-DYNA FE model, D) MADYMO Hybrid III 50th percentile male ellipsoid model, E) Humanetics Hybrid III 50th percentile male LS-DYNA FE model, and F) National Highway Traffic Safety Administration (NHTSA) THOR-NT 50th percentile male LS-DYNA FE model.	84



Figure 62: Hybrid III ATD Finite Element Model. ....	85
Figure 63: THOR ATD Finite Element Model. ....	86
Figure 64: THUMS Model [240]. ....	87
Figure 65: GHBMC Human Model.....	88
Figure 66: ESI Human Models. ....	89
Figure 67: MADYMO Human Models. A) Active muscle control 50th percentile human model B) Passive muscle control 5th, 50th and 95th percentile human models. ....	89

## LIST OF TABLES

Table 1: Number of Known Injuries During Soyuz Abort and Landing. ....	23
Table 2: Incidence of Injury Related to Soyuz Landings.....	23
Table 3: Distribution of Motor Vehicle Injuries by Body Region [59]. ....	37
Table 4: Chest Injury Risk. ....	45
Table 5: Suit Effects on Neck Compression.....	46
Table 6: Comparison of Lumbar Failure Strength by Age - Values are compared to Age 30.....	49
Table 7: Deconditioning Factors. ....	54
Table 8: Chest Compression Injury Criteria [210, 211]. ....	63
Table 9. IARVs for the 5th percentile female Hybrid III ATD.....	77
Table 10. IARVs for the 50th percentile male Hybrid III ATD.....	77
Table 11. IARVs for the 95th percentile male Hybrid III ATD.....	77
Table 12: Proposed THOR IARVs [232].....	79
Table 13: Approximate Injury Risk. ....	82
Table 14: Relative Strengths and Weaknesses of Each Injury Assessment Method [223] <sup>1</sup> . ....	91

## ABBREVIATIONS

ACES	Advanced Crew Escape System
AFRL	Air Force Research Laboratory
AIS	Abbreviated Injury Scale
ARED	Advanced Resistive Exercise Device
ATD	Anthropomorphic Test Device
BDCR	Brinkley Dynamic Response Criteria
BDRM	Brinkley Dynamic Response Model
BRIC	Rotational Brain Injury Criterion
CG	Center-of-Gravity
DAI	Diffuse axonal injury
DR	Dynamic Response
DRI	Dynamic Response Index
DXA	Dual Energy X-Ray Absorptiometry
EuroSID	European Side Impact Dummy
ESI	Pacific Engineering Systems International
EVA	Extravehicular Activity
FAA	Federal Aviation Administration
FEM	Finite Element Model
GHMBC	Global Human Body Model Consortium
HHP	Human Health and Performance
HIC	Head Injury Criteria
IARV	Injury Assessment Reference Value
ISO	International Organization of Standardization
IVA	Intravehicular Activity
JPATS	Joint Primary Aircraft Training Systems
LNij	Lower Neck Injury Criteria
LOIS	Lightest Occupant in Service
LSTC	Livermore Software Technology Corporation
MADYMO	MAthematical DYnamic MOdel
MTBI	Mild traumatic brain injury
NASA	National Aeronautics and Space Administration
NCIS	Normalized Confidence Interval Size
NIC	Neck Injury Criteria
NHTSA	National Highway Traffic Safety Administration
OCSS	Orion Crew Survival System
ORIS	Operationally Relevant Injury Scale
Ph.D.	Doctor of Philosophy
SAE	Society for Automotive Engineers
SDH	Subdural Hematoma
PMHS	Post-Mortem Human Surrogates
SMC	Suit Mounted Connector
TBI	Traumatic brain injury
THOR	Test Device for Human Occupant Restraint
THUMS	Total HUMAN Model for Safety
TRL	Technology Readiness Level
U.S.	United States
USAF	United States Air Force
USOS	United States Operating Segment
USSR	Union of Soviet Socialist Republics
VC	Viscous Criterion
WISE	Vehicle Interface to Suit Equipment

## STATUS

Active: Work/research is currently being done towards this risk

### **RISK TITLE: Risk of Injury Due to Dynamic Loads**

Given the range of dynamic loads that can be transferred to the crew via the vehicle, there is a possibility of loss of crew or crew injury during launch, abort, and landing.

## EXECUTIVE SUMMARY

Crewmembers are at risk of injury from exposure to dynamic loads during the rapid acceleration and deceleration phases of a spaceflight. Dynamic loads are transient loads (lasting for less than 500 ms) that are most likely to occur during launch and landing, and during pad or launch abort, and parachute deployment.

Research on injury prevention and impact biomechanics is important for the aerospace and the automotive industries, and for athletics, and astronautics. Minimizing the risk of injury to a specific population involves assessing their environment. Although the probability of a high impact load is low when riding in a car (1 in 1.3 million miles traveled) or flying in a military aircraft (1 in 14,000 sorties), capsule-based spacecrafts expose crewmembers to dynamic loads during each flight [1, 2]. The National Aeronautics and Space Administration (NASA) takes a conservative approach to the low risk of injury during dynamic loads and incorporates adequate occupant protection standards into vehicle designs.

Several extrinsic factors affect the risk of injury from dynamic loads, including the profile of the vehicle, and the design of the seats, restraint systems, spacesuit, and helmet. Because each vehicle can have different launch, abort, and landing dynamics, the risk of injury is greatly influenced by the vehicle design. Vehicles that minimize crew exposure to dynamic loads will be inherently safer than vehicles that induce higher dynamic loads. The seat and restraint designs may either increase or mitigate risk of injury depending on how effectively they minimize movement of the body relative to the seat and other body regions. Finally, the spacesuit and helmet may contribute to the risk of injury if the design is not configured to protect the occupant during dynamic loads. For instance, the suit can hinder the effectiveness of the restraints, thus dynamic loads increase; rigid elements of the spacesuit can induce point loading; and the helmet can cause injury from blunt impact or it may overload the neck muscles if the neck is not properly supported.

In addition to the extrinsic factors described above, intrinsic factors such as age, sex, anthropometric measures, and physiological deconditioning due to spaceflight can contribute to the risk of injury. Age affects the risk of injury in other situations that are analogous to spaceflight-induced dynamic loads, such

as automobile collisions. Sex can influence the risk of injury from dynamic loads because men can have different body strength and have different geometry than woman. Anthropometric measures can affect injury risk because loads may not be proportional to the difference in anatomical structure and strength. For example, a one size fits all flight helmet will induce a larger burden for smaller necks than larger necks. Furthermore, after crewmembers have been exposed to microgravity, they may have a lower tolerance to dynamic loads than they did at the beginning of the mission due to the spaceflight-induced physiological deconditioning that degrades the structure and response of the musculoskeletal system.

Multiple methods are available to assess the risk of injury from dynamic loads, and each method has advantages and disadvantages. These methods can be grouped into 3 categories: humans, human surrogates, and numerical models. Tests on humans would seem ideal for assessing the risk of injury because humans can provide subjective feedback, but tests on humans must be limited to sub-injurious levels only. Injury metrics can be obtained from humans who have survived accidents; however, no prospective investigations of injury mechanisms are available in these types of situations, which typically limits inference from the data. Human surrogates include post-mortem human surrogates (PMHS), anthropomorphic test devices (ATD), and animal models. PMHS can be tested at injurious levels but cannot be used to investigate how living tissue responds to trauma, and they do not include active muscle tone. ATDs are manikins that vary in biofidelity depending on the design and the loading conditions. ATDs cannot be used to predict injury in all conditions; however, tests using ATD are easy to perform and the data is reproducible. Although animal models can be used to test injury to living tissue, animals are, of course, not anatomically identical to humans, making it difficult to translate results from animals to risk of injury for humans. Numerical models can be used to assess risk of injury, although the fidelity of a model depends on the quality and the quantity of the human and the human surrogate data used to validate the model. Dynamic response models are simple but have limited capabilities for predicting injury. ATD finite element models (FEMs) have similar limitations as the actual ATD tests but they can be used to assess cases that cannot be tested physically. Human FEMs have great potential for predicting injury but currently these models are not validated in all spaceflight loading conditions. Finally, regardless of the method used to assess the risk of injury from dynamic loads, adequate criteria for assessing low risk of injury (<5%) are needed.

Multiple knowledge gaps still exist in our understanding of the risk of injury from dynamic loads: the currently operating spacecraft has not been adequately characterized, insufficient injury metrics exist for all possible loading conditions including standing posture, no injury metrics exist that account for the differences between men and women, and the contribution of spaceflight-induced physiological deconditioning to injury risk has not been characterized. In addition, criteria must be validated to adequately assess low risks of injury, and adequate tools are required for assessing injury risk. These knowledge gaps highlight the areas of research that are needed to mitigate this risk.

# 1.0 EVIDENCE

## 1.1 INTRODUCTION

### 1.1.1 Context

It requires an extreme amount of kinetic energy to launch into space, and effective systems are required to dissipate energy during return to Earth. Although most of this energy is dissipated or absorbed by the vehicle, some of the kinetic energy will be transmitted to the occupants of the spacecraft. This energy, if not properly managed, may cause injury to the crewmembers.

After the Space Shuttle was retired, NASA began developing several vehicles with differing landing modes and conditions. If the vehicle's passengers are injured during the landing phase, this may impair or prevent them from evacuating the vehicle unassisted after the landing, or they may sustain an injury that would impede their ability to fly again. Unfortunately, the current NASA standards and requirements do not adequately address the risk of injury from many key factors. This was highlighted in the *Columbia* Crew Survival Investigation Report, which concluded that inadequate restraint and protection of the upper body could be lethal [3]. The NASA Columbia Crew Survival Investigation report recommended that future spacecraft suits and seat restraints use state-of-the-art technology as part of an integrated solution to minimize crew injury and maximize crew survival in off-nominal acceleration environments (Finding L2-4/L3-4). This report also recommended future vehicles incorporate conformal helmets and neck restraint designs similar to those used in professional auto racing, as outlined in L2-7 of the report [3].

NASA must develop human health and performance standards that adequately protect crewmembers from the effects of dynamic loads and must identify method(s) to meet those standards that will allow vehicle designers to mitigate the risk of injury in their designs.

### 1.1.2 Scope of Occupant Protection

Given the range of dynamic loads that could be transferred to the crew via the vehicle, there is a possibility of loss of crew or crew injury during launch, abort, and landing. This report provides evidence of this risk from spaceflight experience and from terrestrial data that is grouped into 2 major contributing factors—extrinsic and intrinsic factors. These factors influence the dynamic loads transmitted to the body, the body's inertial response, and human tolerance for dynamics load.

Currently NASA's Occupant Protection team is tasked with mitigating risk to the crewmember during transient accelerations, which are defined as accelerations lasting for less than 500ms. The Occupant Protection team assesses the risk of injury from elements that may come into forcible contact with the crewmember during dynamic phases of flight, such as the seat, restraint system, spacesuit, and helmet. It is presumed that the supporting structural elements of the vehicle, such as the walls, floor, struts, etc., will remain intact during all phases of the flight and will not impact the crewmembers. However, if these

structures impinge on the crewmember, they must also be considered when evaluating the risk of injury due to dynamic loads.

### 1.1.3 Definition of Dynamic Loading

The coordinate system shown in Figure 1 describes dynamic loading. Axes denote the direction of acceleration vector,  $G_i$  nomenclature represents the inertial responses of the body to the specific gravitational direction, and movements of the subject's eyeballs in response to the inertial response are given to assure the loading direction is understood.

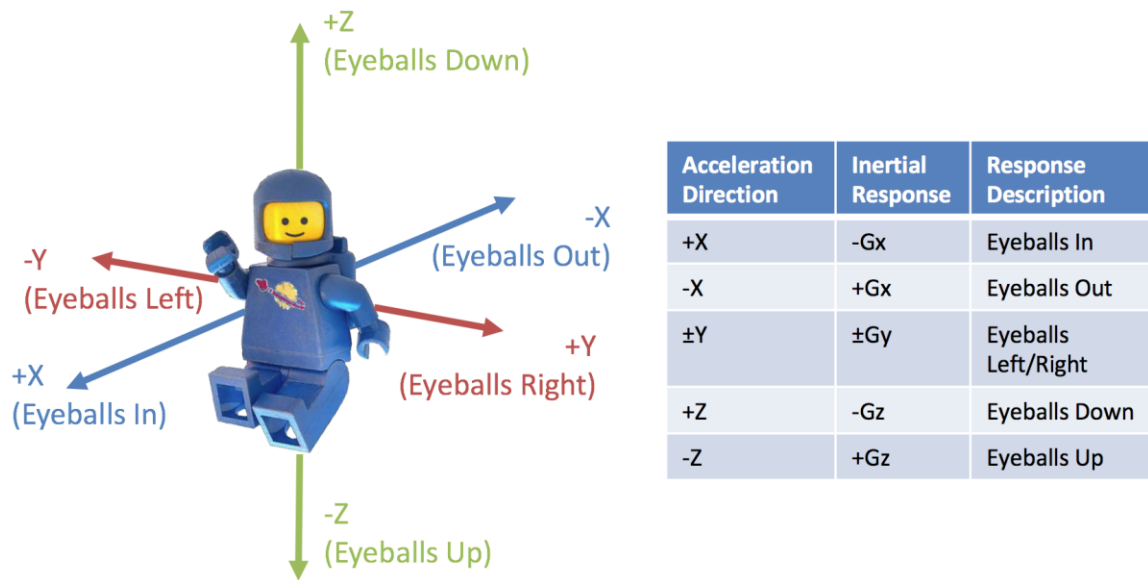


**Figure 1: Direction of Acceleration Relative to Body.**

It is important to note that the input acceleration is not the same as the acceleration response of the human (i.e., because the human is not tightly coupled to the seat an input of 10 g can result in a head acceleration of 30 g). Figure 2 illustrates acceleration versus time for a sled, "A," that was computed from displacement and velocity. Although the temporal pattern of the sled acceleration is trapezoid, the acceleration pattern on the torso of the sled's occupant, "B," resembles a half-sine wave. Furthermore, how the human body responds to acceleration will also depend on the direction of the applied acceleration. Therefore, fitting the trapezoidal acceleration-time histories to assess human response to complex multi-directional landing would be inadequate to predict risk of injury. Both the response of the human body and the dynamic loading measures are required to identify human tolerance levels.

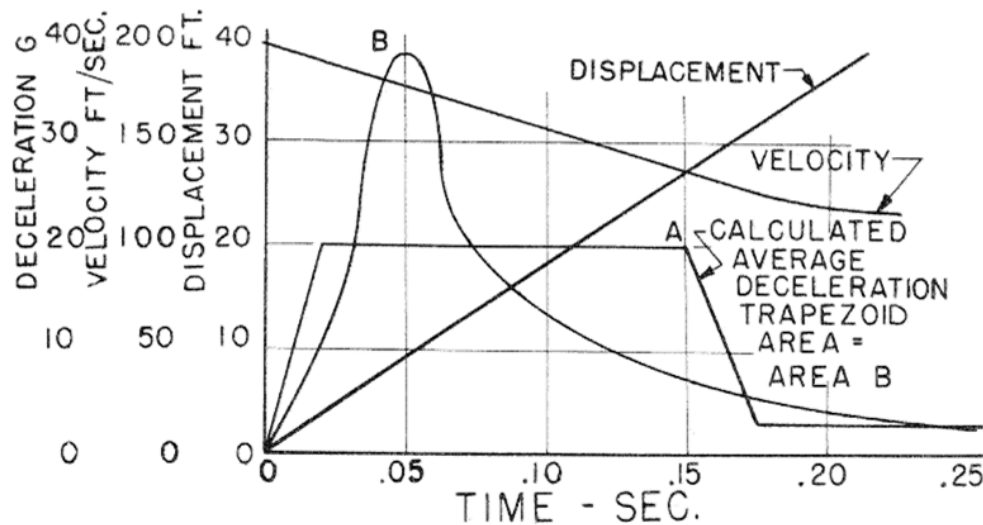


**Figure 2: Acceleration Input to the Sled versus Acceleration of the Body [4].**

#### 1.1.4 Standard Instruments and Methods to Measure Dynamic Loads

Historically, accelerometers were placed on the head and chest to determine a human's response to acceleration. Recent human tests have included additional accelerometers located on the thoracic spine (T1), and rotational velocity sensors located on the head, which allow reverse kinematic analysis to be performed to estimate neck loads [5].

Sensors can be placed throughout the inside of ATDs to extract specific desired measurements during testing. Typically, tri-axial accelerometers are used to measure accelerations in the center-of-gravity (CG) of the head, chest, and lumbar spine. Load cells, used to measure forces throughout the body, are usually placed in the shoulder, lap, upper and lower neck, and the lumbar spine. Angular velocity is also measured at the CG of the head.

Acceleration and force limits can also be analyzed on the vehicle itself. Accelerometers and load cells placed in the seat pan can measure the loads and forces the occupant will experience during flight or during impact. Forces on the restraints are often tested using specialized load cells during human or ATD tests.

#### 1.1.5 Definition of Injury

Although different types of injuries are possible during dynamic phases of flight, the current report addresses musculoskeletal and soft tissue injuries due to dynamic loads. Other controls are in place to address injuries such as burns, inhalation, and decompression sickness.

The severity of an injury is defined using the operational relevant injury scale (ORIS) [6, 7], a NASA developed injury scale that rates both the severity and the significance of the injury. Three elements are used to determine a composite score: the severity of the injury, the crewmember's ability egress the



vehicle unaided, and the crewmember's return to flight status. Injury severity is scored using an abbreviated injury scale (AIS) [8]. Because crewmembers may be required to egress the vehicle immediately, injuries could have operational consequences that are not captured in the AIS severity score. The return to flight status is a measure of the long-term consequences of the injury. For example, an injury that is classified as having no long-term consequence for an average civilian could possibly disqualify an astronaut from future flights.

When defining the consequences of an injury, it is important to also consider other spaceflight-induced conditions. Motion sickness or musculoskeletal deconditioning due to microgravity exposure may prevent an uninjured crewmember from egressing the vehicle unassisted. This degradation in performance is not included when defining the risk of injury from dynamic loads, however, any increase in injury risk due to these factors will be discussed below.

Occupant protection focuses on musculoskeletal injury based on biomechanics. Biomechanics is defined as "the science that examines forces acting upon and within a biological structure and the effects produced by such forces [9]." As a force makes contact with the body, it applies pressure over a given surface area, which is referred to as tissue stress. In turn, the tissue deforms resulting in tissue strain (deformation). The stress-strain relationship is characterized by dimension (uniaxial, biaxial, or triaxial) and direction (tension, compression, bending or torsion).

Every tissue in the body has a unique stress-strain characterization, similar to the one shown for bone in Figure 3 [10]. If the applied stress-strain is within the elastic range, the material returns to its original shape once the load is removed. If an exposure is applied beyond the tissue's yield point (outside the elastic region), the structure is compromised and will not return to its original shape. Depending on the type of tissue affected, this structural compromise may not constitute an injury and may induce sub-clinical changes instead. If the tissue is loaded to failure point (ultimate stress-strain), the tissue will tear or break. Moreover, many tissues in the body are rate-sensitive, i.e., the ultimate strength of the tissue is dependent on the rate of loading at onset, and tissues that respond primarily to higher onset rates typically have higher ultimate strength. Compromised tissue may, and damaged tissue will, result in injury, which could lead to loss of mission and/or crew.

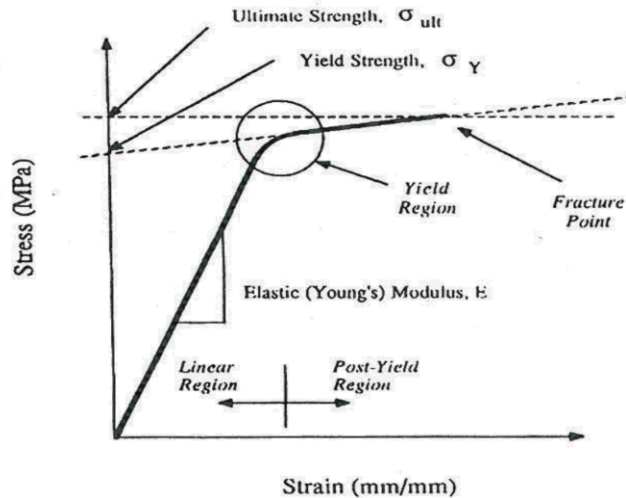


**Figure 3: Stress–Strain Properties of Bone in Tension [10].**

Dynamic loads may be transmitted from the vehicle to the occupant via several loading mechanisms, as identified by Wismans [11]. These loading mechanisms include elastic deformation, viscous deformation, and inertial deformation (Figure 4).

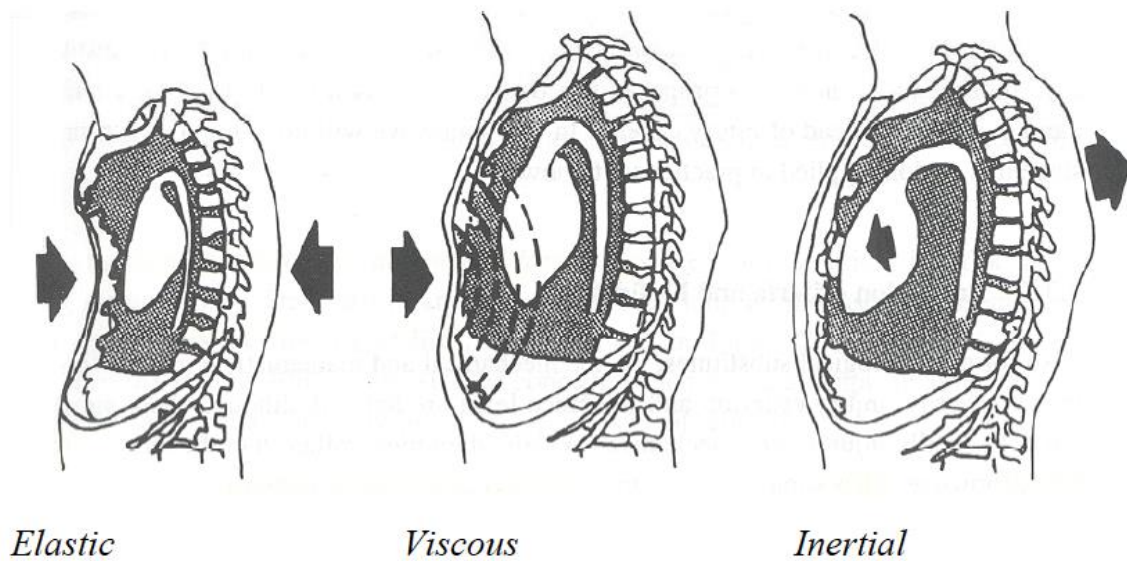


**Figure 4: Three Primary Injury Mechanisms [11].**

The risk of injury can be quantified using criteria that correlate with the severity of the injury to the body region under consideration. Typically, these criteria relate to physical quantities that can easily be

measured with human-like surrogates or models [11]. A range of surrogate response values for injury can be assessed, and an injury function relates a particular response (e.g. head acceleration) to an injury probability. The injury assessment reference value (IARV) provides a limit for a given risk of injury in a given design, and the risk is determined from the injury risk function. See section 1.4 for more information.

### 1.1.6 Unique Aspects of Spaceflight Injury Biomechanics

The biomechanics of spaceflight-induced injury include some unique aspects that are not necessarily considered in biomechanics of injury induced on the ground. These aspects include spaceflight-induced physiological deconditioning; multi-axial, complex loading; spacesuit components; egress needs; and impacts that occur during each and every flight.

### 1.1.7 Operationally Relevant Injury Scale

A new injury scale, the ORIS, was created to account for the unique operational environment of spaceflight. The ORIS was adapted from the AIS used to assess car accidents. The ORIS combines the AIS score, a measure of a crewmember's ability to self-egress the vehicle, and a measure that estimates the time to return to flight status (Figure 5). The equation for the calculation is shown below (Equation 1). As an example, clavicle fracture would score 2 on the AIS, but this injury could prevent a crewmember from egressing the vehicle, giving it a self-egress score of 3, and resulting in an ORIS score of 3.

***Equation 1: Operationally Relevant Injury Scale (ORIS) Score Calculation.***

$$Score = \sqrt{0.25 * (AIS)^2 + 0.5 * (SE)^2 + 0.25 * (FS)^2}$$

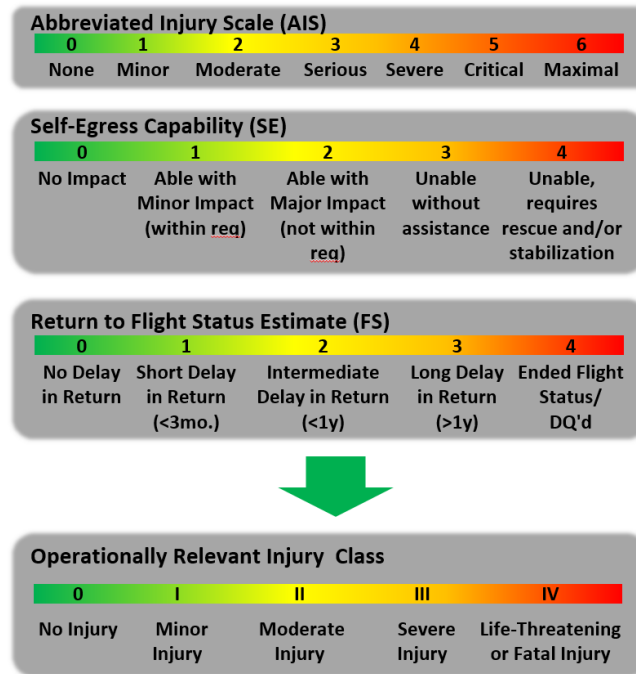


**Figure 5: ORIS and its Components.**

## 1.1.8 Standardized Testing

Currently, the National Highway Traffic Safety Administration (NHTSA) conducts multiple crash tests to rate the safety of a vehicle. These tests include a frontal crash test, a side barrier crash test, a side pole crash test, and a rollover resistance test ([nhtsa.gov/ratings](https://www.nhtsa.gov/ratings)). Similarly, multiple types of safety tests, specific to spaceflight, are required to evaluate up-coming spacecraft before all occupant protection concerns can be satisfied.

Additional aspects unique to spaceflight-induced injury are detailed in the following sections.

## 1.2 HISTORICAL SPACEFLIGHT EVIDENCE

### 1.2.1 U.S. Space Program

The U.S. space program has generated very little injury data that is attributable to landing. No injuries were reported during the Mercury and the Gemini programs. During the Apollo program, only one injury occurred during a 15 G landing when a loose item struck a crewmember resulting in a head injury [12]; however, this injury was not due to the dynamic loading on the crewmember or the interactions with the vehicle, so this injury does not meet the definition of injury above. One of the 3 parachutes failed during the Apollo 15 landing, resulting in a hard landing, primarily in the +X/+Z loading direction [13]. During the Apollo program, 12 men landed on the lunar surface in a standing posture, and no injuries were reported [14]. The highest acceleration for an Apollo lunar landing was about 0.55 g (Apollo 15), and the lowest

was around 0.1464 g (Apollo 17), as estimated using information about the landing conditions, assumptions, and simplified landing dynamics.

Because the Space Shuttle was designed to land on a runway, inducing similar levels of dynamic load as a commercial aircraft landing, no acute injuries would be expected from the dynamic loads during a nominal Space Shuttle landing. However, evidence suggests that injury can present well after landing: a 4.3 times greater incidence of herniated nucleus pulposus occurred in Space Shuttle crewmembers after landing than in control populations, which may have been caused by a variety of effects including landing impact [15].

The investigation of the Columbia Space Shuttle disaster revealed ineffective occupant protective measures. The *Columbia* Crew Survival Investigation Report concluded that inadequate restraint and protection of the upper body could be lethal, and stated that future spacecraft suits and seat restraints should include state-of-the-art technology as part of an integrated solution to minimize crew injury and maximize crew survival during off-nominal acceleration events (L2-4/L3-4), and that conformal helmets and neck restraints similar to those used in professional auto racing should be used in space vehicles (L2-7) [3].

Combined axial loading scenarios occur when capsule-type vehicles land. When capsules with roll control capability return to Earth, landing loads are expected to be primarily in the +X (eyeballs in) and +Z (eyeballs down) axes; however, capsules without roll control are expected to land with loads in the +X (eyeballs in) axis combined with loads in the  $\pm Z$  and the  $\pm Y$  axes.

### 1.2.2 USSR/Russian Space Program

In preparation for the Soyuz program, the former Union of Soviet Socialist Republics (USSR) conducted 130 landing tests using human volunteers (Figure 6). Landing orientations and impact velocities were varied to assess how these factors affect risk of injury [16].

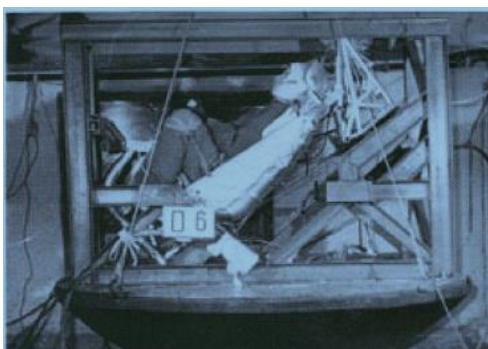


**Figure 6: Soyuz Drop Test Platform [16].**

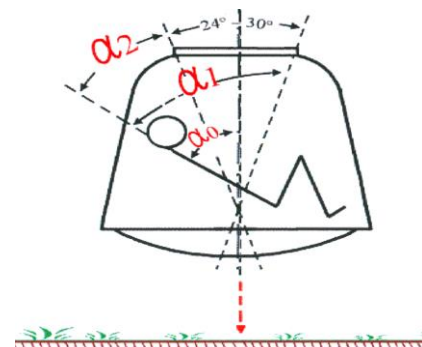


**Figure 7: Seat Testing at Various Angles [16].**

All high velocity impacts (5-6 m/s) resulted in pain in the head, abdomen, or hips. In some cases, blood was present in urine due to the impact. Landing tests were conducted at angles from  $36^\circ$  to  $82^\circ$  relative to the perpendicular vector from the ground (combined +X and +Z) (Figure 7). Results indicated that thoracic spine was at greater risk of injury from  $36^\circ$  landings (primarily +Z), whereas head and organs were at greater risk from  $82^\circ$  landings (primarily +X). One test of a  $36^\circ$  tilt landing at 4.5 m/s with no shock absorber resulted in spinal compression fractures in T4 to T5 region (Figure 8). Investigators later found the subject had scoliosis, which was overlooked in the physical.

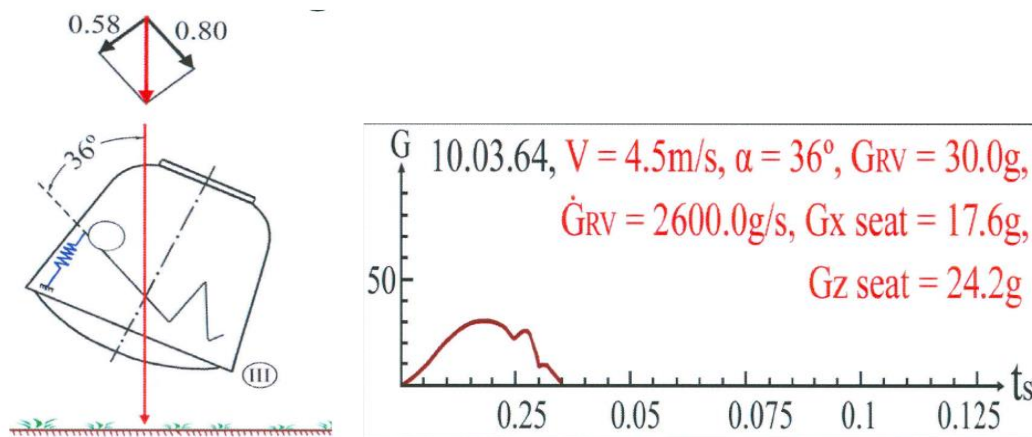


**Figure 8: Soyuz Test Condition Causing Spinal Injury [16].**

Operation of the Soyuz vehicle provides compelling evidence to inform the risk of injury due to vehicle dynamics for capsule-like landing vehicles. The Soyuz has been operating since 1967 and had completed 141 flights as of December 31<sup>st</sup>, 2019 and had carried a total of 286 crewmembers.

In 2003, the first United States Operating Segment (USOS) crewmembers returned from the ISS on the newly developed Soyuz-TMA variant. Since then, NASA began to systematically investigate and record landing-impact related injury outcomes in USOS crewmembers. The results of this effort as well as known injuries from previous USSR/Russian missions are shown in Table 1. As expected, increased rates of injury were recorded for the newer vehicle types; however, it is likely that minor injuries were underreported previously. This ongoing study has collected data from 70 USOS crewmembers.

During the Soyuz's 62-year history, 4 fatalities, 1 permanent disablement, 1 life-threatening injury, 7 moderate injuries, and 46 minor injuries are known to have occurred (see Table 1). Three of the fatalities did not result from inertial accelerations [17-19]. The number of minor and moderate injuries is suspected to be underreported, particularly for the earlier Soyuz missions.

**Table 1: Number of Known Injuries During Soyuz Abort and Landing.**

Soyuz Type	Number of Flights	Number of Crewmembers	Minor Injuries	Moderate Injuries	Severe Injuries	Life Threatening or Fatal Injuries
7K-OK	10	22	1	0	0	1*
7K-TM	29	56	3	0	0	1
T	15	38	2	2	0	0
TM	33	90	4	0	0	1
TMA/MS	54	159	36	5	0	0
Total	140	365	46	7	0	3*

\* Does not include Soyuz 11 Loss of Crew (3) because fatalities were not due to landing impact

The dynamics of the Soyuz's landings are variable, and several landings were reported to be hard (e.g. parachute failure, landing retrorocket failure, ballistic re-entry, etc.). Table 2 shows the injury rates during nominal, off-nominal, and hard landings [17-19]. As expected, more injuries occur during hard landings than nominal landings. Although these injuries have been documented, the landing dynamics that caused the injury are not currently available and records may no longer exist. Note that injury rates are calculated as percentage of total number of crewmembers. Some crewmembers may have experienced injuries that were not available to the authors. Also, some crewmembers experienced multiple injuries on a single mission.

**Table 2: Incidence of Injury Related to Soyuz Landings.**

Injury Rates*	Nominal	Off-nominal	Hard	Total
Minor	5.9%	8.8%	18.5%	12.6%
Moderate	1.0%	5.9%	3.7%	1.9%
Severe	0.0%	0.0%	0.0%	0.0%
Life Threatening / Fatal	0.0%	0.0%	7.4%	0.8%
Any Injury	6.9%	14.7%	29.6%	15.3%
Number of Crewmembers	304 (83%)	34 (9%)	27 (7%)	365
Number of Landings	114 (81%)	14 (10%)	12 (9%)	140

### 1.2.3 Chinese Space Program

The Chinese National Space Administration completed their first manned spaceflight mission in 2003 on their vehicle, Shenzhou. The Shenzhou is modeled after the Russian Soyuz and can accommodate 3 taikonauts (Figure 9). After the first manned mission, Shenzhou 5, the taikonaut reported discomfort due to low-frequency vibrations during launch [20], and he endured a minor cut on his lip during reentry,

descent, and landing [21]. Three astronauts flew on Shenzhou 6 and walked out of the capsule after re-entry, with assistance. No injuries were reported on any of the other Shenzhou missions (a total of 6 missions were completed with a total of 14 crewmembers).



**Figure 9: Photos of Shenzhou Missions.**

### 1.3 INJURY RISK FACTORS

Evidence of injury due to dynamic loading is grouped into 2 major contributing factors: extrinsic and intrinsic (Figure 10). Extrinsic factors are external environments and impacts with hardware that can injure the crew, and they include suit and helmet design, seat and restraint system, and vehicle dynamics. Intrinsic factors are individual physiological parameters that influence injury tolerance such as age, sex, anthropometric measures, and spaceflight-induced physiological deconditioning.

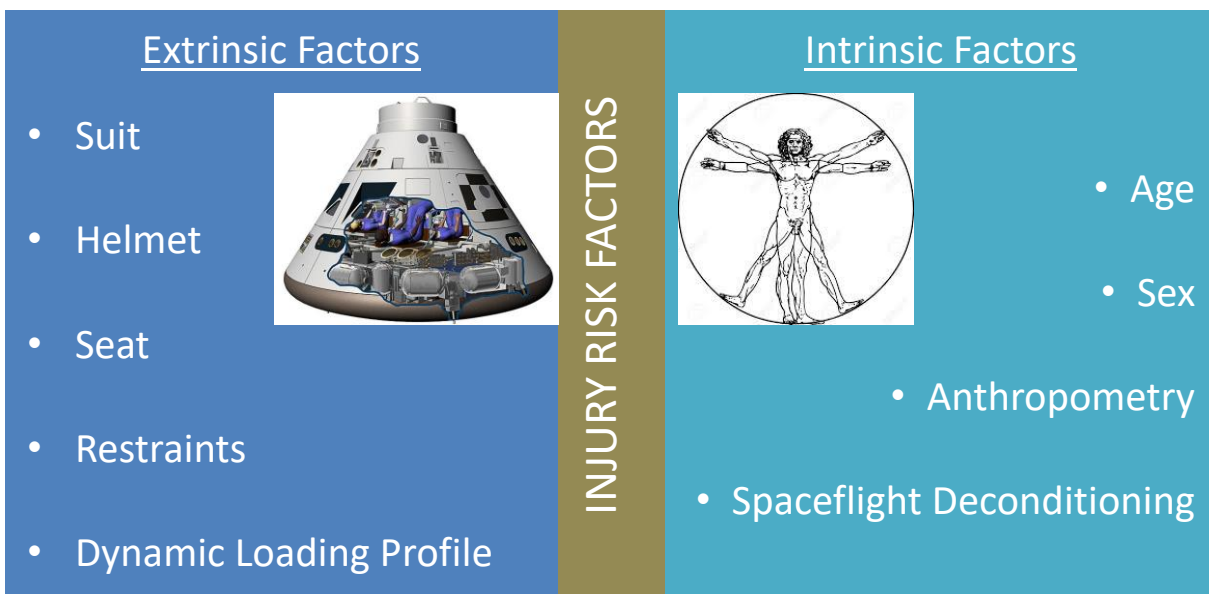


**Figure 10: Factors Affecting Risk of Injury from Dynamic Loads.**



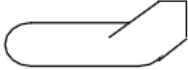




## 1.3.1 Extrinsic Injury Risk Factors

### 1.3.1.1 Vehicle Dynamic Profile

#### 1.3.1.1.1 Introduction

The dynamic profile of the vehicle is related to the vehicle's design, which is driven by the space mission. After the Space Shuttle was retired, NASA started developing several different vehicle designs. Figure 11 illustrates various designs for future space vehicles that NASA is considering. All current Earth-return vehicles under development are lifting ballistic designs.

Vehicle Category	Vehicle
Ballistic (Mercury)	
Lifting Ballistic (Gemini, Apollo)	
Lifting Body (ISS CRV)	
Winged (Space Shuttle)	
High-Fineness Lifting Body (X-43)	

**Figure 11: Vehicle Shapes [22].**

Whereas standard tests can be developed to assess the safety of all brands of automobiles, this is not the case for all spacecrafts because designs can be radically different from one another. Defining a standard test that all vehicles must pass could unintentionally allow vehicles with harder landing impacts to pass a less stringent test and could over-constrain designs with softer impacts by requiring designs for an impact that wouldn't be possible for that vehicle.

Each space vehicle will have unique dynamics depending on the design of the launch, abort, reentry, and landing systems; however, regardless of the vehicle type, spaceflight inevitably exposes crews to dynamic loading in various directions. Although each vehicle may have different inherent injury risk, dynamic loading can induce injury, and the injury threshold depends on the direction of the acceleration and is governed by musculoskeletal system. Figure 12 shows general occupant loading conditions in nominal and off-nominal landing scenarios along each axis.

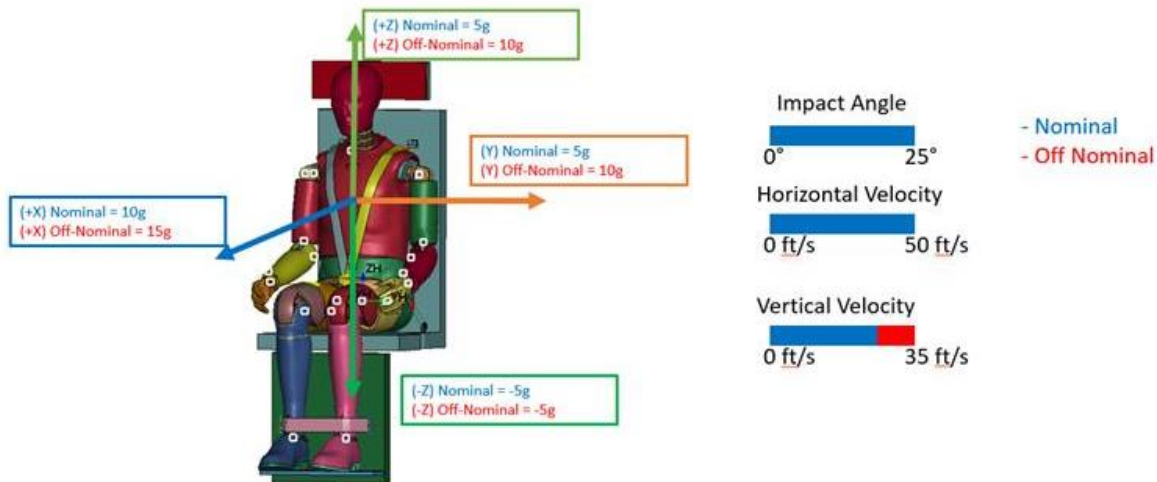


**Figure 12: General Occupant Loading Conditions in Capsule Landings.**

#### *1.3.1.1.2 Historical Background on Biomechanics Impacts from Spaceflight*

In the mid-1950s to early 1960s, aircraft designers developed enclosed escape systems such as the B-58 capsule, the XB-70 capsule, and the F/FB-111 crew escape cockpit, because these systems support escape at very high speeds and high altitudes. Each of these capsules was designed to land on the Earth's terrain or on water; however, they did not meet the acceleration limits due to the high rates of acceleration onset and the multi-directional nature of the landing impacts.

In the late 1950s, the United States Air Force (USAF) and NASA undertook the design of manned spacecraft. The USAF programs included Dyna-Soar and the Manned Orbiting Laboratory (1958 to 1967), and NASA successfully developed the Mercury, the Gemini, and the Apollo spaceflight programs [23]. The initial acceleration limits [24, 25] for rate of onset, amplitude, and duration were established for profiles known to be within voluntary tolerance and for profiles known to cause medium to severe injury. However, the trapezoidal acceleration-time histories were inadequate for predicting the injury risk due to the complex multi-directional landing impact scenarios of these vehicles.

These vehicles shared a common design constraint: the distance available for deceleration during landing was limited. For example, the B-58 capsule landed on the seatback bulkhead with only inches available for the stroke of its 4 metal cutting impact attenuation devices [4]. Under nominal recovery conditions, the Mercury capsule would land on water using an air bag skirt around its heat shield to attenuate impact; however, if the capsule was to be safely lifted away from the main launch rocket during an emergency abort on the launch pad, the skirt could not deploy and inflate quickly enough to protect the occupant during a land or water landing, and only a small column of crushable aluminum honeycomb under the astronaut's seatback would be available to attenuate the landing impact.

In contrast, ejection seats could be accelerated over a distance of about 3 feet; thereby permitting a more gradual rate of acceleration onset to meet the relatively low rate of onset limits enforced at that time by the USAF and the Navy.

The USAF and NASA began using analytical approaches, existing empirical data, and a mechanical dynamic systems approaches to study how the human body responds to the rapid rate of onset acceleration that would occur during escape capsule landings—extremely high rates of acceleration onset in the range of thousands of g/s [26]. In addition, Beeding and Mosely [27, 28] used a horizontal deceleration facility to study how volunteers wearing a lap belt and shoulder harness restraints respond to impact in forward-facing and rearward-facing seats, and in off-axis conditions [28]. The authors reported that the subjects sustained severe shock and repeated syncope with myalgia, requiring one volunteer to be hospitalized for 5 days after exposure to a 40-g sled deceleration with a rate of onset of 2,139 g/s and a velocity change of 48.5 ft/s in a rear-facing seat. The authors reported that the subject may not have survived without immediate medical care. Previous tests of volunteers in this position ranged from 25 to 40 g at onset rates from 1,034 to 2,139 g/s for durations of 50 to 190 ms, and impact velocities were below 50 ft/s. The acceleration-time histories could be defined in terms of the existing trapezoidal acceleration-time profile, although a half-sine pulse shape approximated the applied acceleration on the human body.

Efforts were soon expanded to investigate the effects of the multidirectional accelerations produced by the Apollo crew module. The initial multidirectional impact studies were conducted with volunteer military subjects, and used a vertical deceleration tower at Wright-Patterson Air Force Base to assess the safety of impact conditions expected during the Apollo crew module landings [29]. These were the first controlled multidirectional impact experiments to study the human response to impacts other than in the X axis and Z axis. Special concern was focused on the responses of the volunteers to sideward acceleration because the Apollo impact attenuation system was limited to a stroke distance of less than 8 inches in that direction. Before these studies, no volunteers had been exposed to sideward impact. The direction was incrementally changed, and impact levels were gradually raised until the Apollo impact levels were reached. Acceleration levels ranged from 3 to 26.6 g with rates of onset ranging from 300 to 2000 g/s and impact velocities up to 28 ft/s.

Tests conducted by the U.S. Navy using volunteers and a horizontal track at a Naval facility in Philadelphia provided the initial investigations of the effects of impacts in the -Z axis to support the Apollo program [30]. The USAF conducted tests using the horizontal deceleration facilities at Holloman Air Force Base (AFB) [31-33] to partially replicate the work of Weis et al. [29] and to include tests of -Z axis components that were not considered feasible using the vertical deceleration facility at Wright-Patterson AFB. More than 500 tests were performed at Wright-Patterson AFB and Holloman AFB to support the objectives of these multidirectional impact investigations.

Later, impact tests were conducted at Holloman AFB with volunteers to study the influence of developmental seats, restraints, and pressure suits, as shown in Figure 13 and Figure 14. Complete test plans, medical protocols, data recordings, and photogrammetric records of these tests have not been located. During these later impact tests of full pressure suit prototypes, one of 2 subjects exposed to +Z

axis impact conditions incurred a seventh thoracic vertebra fracture when the test was conducted with the pressure suit partly inflated [34]. The details of these tests remain unknown.

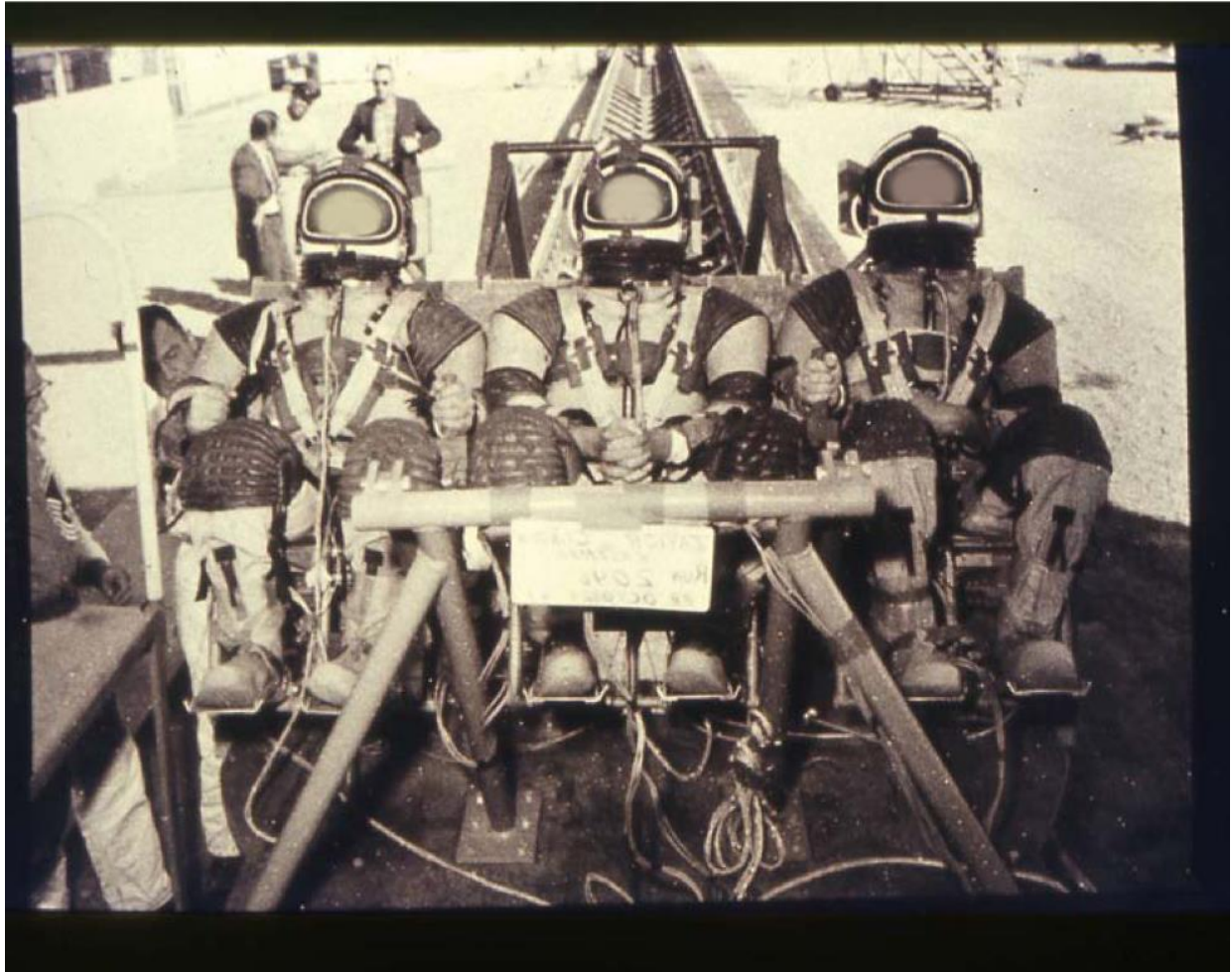


***Figure 13: Volunteers Undergoing an Impact Test in Developmental Pressure Suits, Lap Belts, Shoulder Harness, and Seating System (Credit: USAF).***



**Figure 14: A Volunteer Being Tested in a Developmental Pressure Suit While Wearing a Lap Belt, Shoulder Straps, and Inverted-V, Negative-G Straps (Credit: USAF).**

Payne [35] further developed numerical models of human body dynamics and used them to study the effects of body support and restraint systems during dynamic loading. Lumped parameter models of the human dynamic impact response demonstrated the influence of slack or preload in the restraint system. For example, slack in a restraint system will typically increase the injury risk of an occupant.

The results from the hundreds of impact tests using volunteer subjects, and results of the analytical modeling efforts were used to support the design and development the Apollo crew module and its occupant protection system. The module successfully transported all crewmembers without injury throughout the entire Apollo program. The final design of the body support and restraint system used in the Apollo crew module was simpler than the body support system initially used in the multidirectional impact tests with volunteers.

Since then, ATDs and FEMs have mostly replaced human test subjects. Investigators at the Medical College of Wisconsin used PMHS tests to correlate ATD head and neck injury responses in multiple loading scenarios [36]. FEMs can predict ATD responses to dynamic events. Investigators at Wake Forest University validated FEMs using tests on physically matched ATDs, and used the FEM to evaluate how seat designs for future vehicles affect injury risk during dynamic loads [37]. ATDs have been tested directly in a prototype Orion seat to validate the FEMs that will be used to assess occupant safety in possible landing

scenarios specific to the Orion spacecraft [38]. The validated ATD FEMs can be placed in models of the whole vehicle to assess all possible landing scenarios, which would not be possible using human subjects.

These various studies have identified that human tolerance is related to orientation of the body during impact. Spaceflight inherently exposes the crew to dynamic loading in various directions; therefore, it is important to understand tolerance and risk of injury associated with directional loading.

### **1.3.1.2 Directional Loading**

Human tolerance to acceleration is highly dependent on the direction of loading. Research conducted on individual loading directions is detailed below. In addition, loading in combined directions is briefly discussed. The acceleration of a reference point in the chest in a harnessed crewmember due to dynamic loading is referred to as the dynamic response (DR). This is often broken into x, y, and z components (i.e. noted as  $DR_x$ ,  $DR_y$ , and  $DR_z$ ). Initial work on ejection seats focused on predicting the  $DR_z$  and its resulting injury risk (referred to as dynamic response index [DRI]). This work was then extended to predict injury during loading along the other axes. This approach is referred to as the Brinkley Dynamic Response Model (BDRM), and the resulting injury criteria are the Brinkley Dynamic Response Criteria (BDRC) [39].

#### ***1.3.1.2.1 +X Axis Loading (Eyeballs In)***

Humans are most tolerant to acceleration in the +X axis if the body and head are well supported. Human volunteers tolerated accelerations from 10 to 45 g in the +X direction without injury [40]. However, neck injuries can occur if the neck extends during inertial loading, and the body can flail if the extremities are not well restrained.

NASCAR drivers can be exposed to +X accelerations if their vehicle spins and contacts the wall. These accelerations exceed 50 g in some cases, although most are more benign. Only one NASCAR injury has been attributed primarily +X acceleration [41].

IndyCar accidents routinely expose drivers to +X accelerations. Rear impacts in IndyCar crashes can result in accelerations up to 72 g, and with proper seat and restraint design these crashes can be tolerated without injury [42].

Neck injury, commonly referred to as whiplash, can occur if the head is not sufficiently supported during +X accelerations. High levels of +X impact loading can induce significant injury to the neck, and lower levels of +X loading can induce minor injuries to the neck resulting in chronic pain, although the mechanism isn't well understood. Each year more than 3 million Americans experience a cervical acceleration/deceleration-induced injury, with twice as many women as men experiencing this type of injury [43].

Suit-borne mass can induce an additional unique risk for +X axis loading during spaceflight. Some spacesuits are constructed with a significant mass attached to the suit that can impart loads on the body in addition to the inertial response of the body mass itself. For example, a suit umbilical connector

mounted on the chest may increase the risk of rib fracture in +X axis loading scenarios (see Section 1.3.1.5) [44].

#### *1.3.1.2.2 -X Axis Loading (Eyeballs Out)*

With proper restraint, -X axis loading is also well tolerated. In this loading direction, the occupant is propelled away from the seat back, so seat belts or some other restraint(s) are needed to restrain the occupant. The torso and pelvis must be restrained to reduce injury risk in these conditions. During extreme loading, such as conditions occurring during auto racing, head motion and neck forces must be restrained to prevent serious injuries.

Hundreds of human volunteers have been tested without incidence at accelerations in the -X axis ranging from 6 to 30 g [40]. The test subjects were restrained with both lap belts and torso restraints, preventing significant motion of the body relative to the seat, and the subjects were instructed to brace, thus minimizing head and neck motion. The Navy Biodynamics Laboratory conducted 1065 impact tests on 92 men at accelerations ranging from 2-16 g, and reported no injuries [45]. During these tests, the subjects' torso, pelvis, and extremities were restrained but their head and neck were unrestrained, and the subjects were not instructed to brace.

NASCAR drivers wearing 5-point harnesses can sustain clavicle fractures after frontal impacts, likely due to motion of the pelvis in the X direction causing the shoulder restraint to loosen. As the upper torso propels forward and contacts the now loose restraints, the closing velocity induces higher loads on the clavicle, which, during severe impact conditions, can result in a clavicle fracture [46] .

Most -X injuries to automobile occupants wearing 3-point belts can be attributed to contact with structures within the vehicle. If the occupant uses only a lap belt, their chance of sustaining a fracture of the lumbar spine increases. In these cases, the posterior vertebra is injured [47, 48].

#### *1.3.1.2.3 ±Y Axis Loading (Eyeballs Left/Right)*

Without proper restraint and seating support, lateral loading of the body can cause a variety of injuries. Viano et al. [49] report that 31.8% of car passenger fatalities occur after side impact. The aorta can sustain a traumatic rupture from side impacts during automotive accidents; however, the biomechanics resulting from automotive side impacts can vary significantly from the biomechanics resulting from lateral impacts in a spaceflight vehicle. The 3-point restraint used for front seat automobile occupants is less effective at arresting lateral motion of the torso than the 4- or 5-point harness used during spaceflight. In addition, automobile side impacts often include intrusion of the structure into the occupants' space that, in addition to the closing velocity between the occupant and the structure, may explain the high incidence of fatalities. Injury to the lower extremities are common due to contact between the occupant and structure. Approximately 70% of lower extremity injuries from lateral automotive near-side impacts that have an AIS of  $\geq 2$  are to the hip and pelvis. During spaceflight, the femoral head is particularly susceptible to strength loss due to microgravity exposure (see Section 1.3.2.4).

With proper support, the body can withstand high acceleration events that can occur during NASCAR automotive racing [41]: impacts at accelerations above 100g have occurred without serious injury. NASCAR drivers are protected by an elaborate system that minimizes relative lateral motion of the different body segments.

The USAF has conducted hundreds of side impact tests with human volunteers at various accelerations [40]. Subjects were restrained with various torso harnesses and one study included side supports for the shoulders and hips. Only one notable injury was reported, which was due to extreme leg flail resulting in a knee ligament tear [50]. The Navy Biodynamics Laboratory has also conducted hundreds of side impact tests. As with the X axis loading tests, the subjects were fully restrained except the head and neck, and all impacts were tolerated without injury [45].

#### *1.3.1.2.4 +Z Axis Loading (Eyeballs Down)*

Most injuries from +Z axis loading are due to compression of the spinal column. The location and nature of the injury is dependent on posture, spinal curvature, loading rate, and energy. For example, end plates can be disrupted at lower energy levels than typically required to induce vertebral fractures (Figure 15). The type and location of an injury depends on the curvature of the spine at the time of the acceleration event. If the occupant is in a slouched position, the spine will be preloaded in the area of curvature and +Z loading may overload the anterior portions of the vertebral bodies (Figure 16).



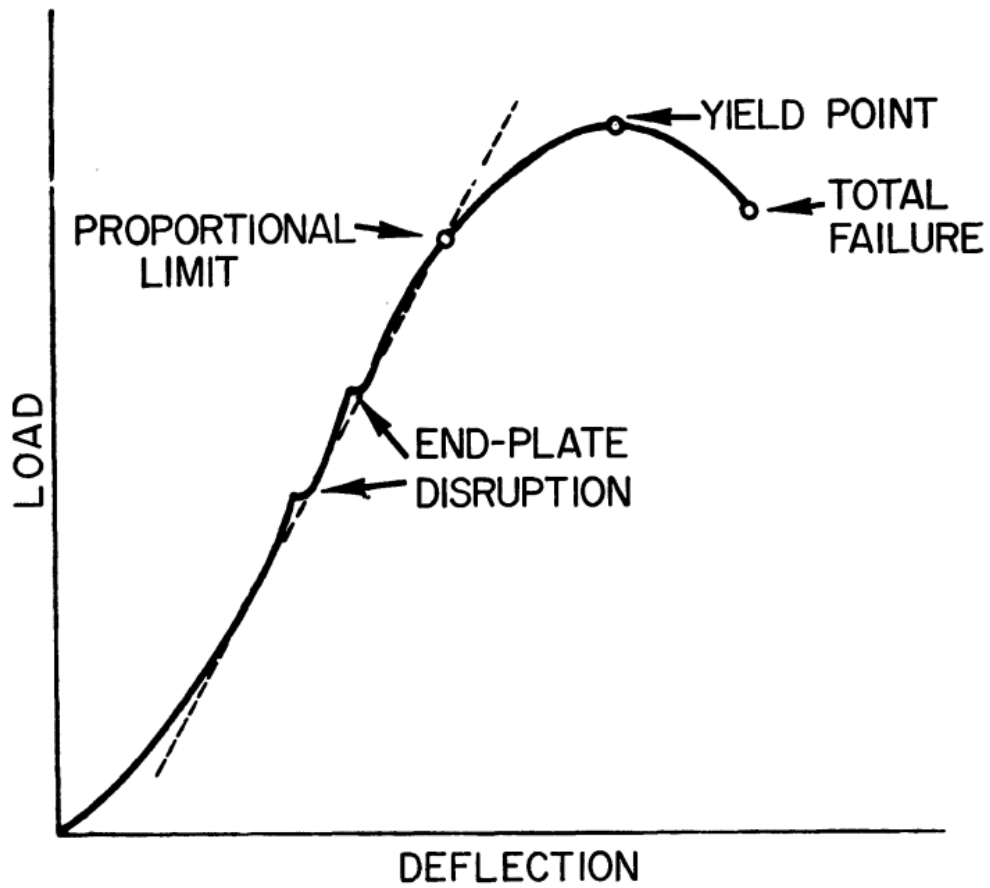


*Figure 15: Relationship Between End Point Disruption and Vertebral Fracture [51].*

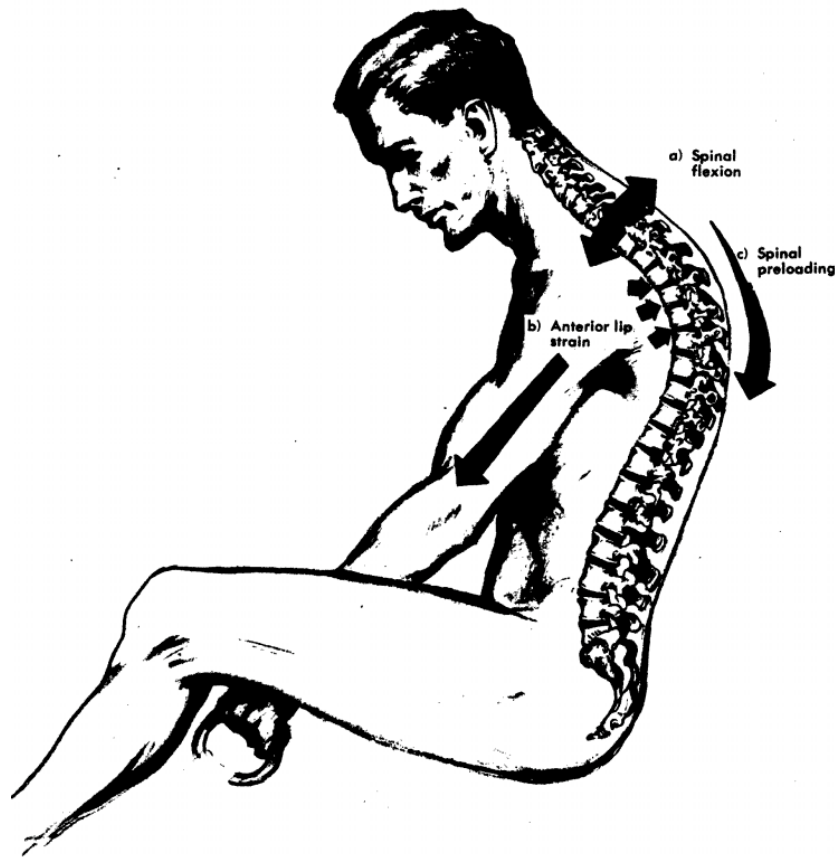


**Figure 16: Postural Effect on Spinal Injury during +Z Loading [51].**

Proper seat design is critical for reducing the risk of injury due to accelerations in the +Z axis. Controlling for posture and assuring correct alignment of the spine in the seat relative to the loading vector minimizes stress concentrations in the spine and distributes the load properly [51, 52]. Spaceflight causes the spine to straighten, reducing the natural lordosis of the cervical and lumbar spine and the kyphosis of the thoracic spine, which may increase the risk of spinal injuries after spaceflight (see Section 1.3.2.4). Seats or padding that allow significant motion of the pelvis in the Z direction can result in a closing velocity as the pelvis bottoms out and motion stops abruptly (see 1.3.1.3**Error! Reference source not found.**). Energy attenuators can be incorporated into a design to decrease peak acceleration and spread out the energy of the impact, thus lowering injury risk (see section 1.3.1.6).

Operational data from aircraft ejections shows injury rates between ~1% to over 40% depending on the aircraft type and associated seat design [52-54]. Only compression fractures (which have AIS scores of  $\geq 2$ ) attributable to the ejection acceleration were assessed in these studies, and data were only for male, military subjects with an average age of 28, which may not be indicative of the NASA astronaut population

#### *1.3.1.2.5 -Z Axis Loading (Eyeballs Up)*

Loading in the -Z direction is the least studied direction of loading. Downward ejection seats induce -Z transient accelerations. In this direction of loading, the occupant is pulled up away from the seat pan and is held in place by the seat belt restraints. Schulman et al. studied tolerance of 6 fully restrained subjects at varying levels of -Z acceleration, and reported varied discomfort and injury including headaches, throat pain, neck pain, and back pain. One subject was hospitalized after injury to his coccyx after rebounding back into the seat pan after the initial -Z acceleration [30].

IndyCar accidents can induce -Z acceleration during rear impact because the driver sits in a reclined position and during rear impacts with the wall the driver would ride up the seat back until the shoulder contacts the head surround, creating compression injuries to the spine [42]. This risk is reduced by allowing the seat back to crush during impact preventing the driver from riding up the seat back, and the impact is then primarily in the +X axis. Several aircraft have employed downward ejection seats, although the acceleration data and injury outcomes are no longer available [39, 55].

#### *1.3.1.2.6 Multiaxial Loading and Secondary Impacts*

The risk of injury from multiaxial loading can be complex to assess and is highly dependent on interactions with restraints and seat structure. For example, when a -X (eyeballs out) and a Y acceleration are combined, the head, neck and upper torso can be propelled forward in the seat and may not make contact with the side supports. Therefore, assessment of multiaxial loading is vehicle specific; not only specific to the seat and restraint design but also to the actual loading conditions possible for that vehicle.

Because regulation specifies the exact location of ATDs during automobile crash tests, a vehicle design could be optimized for that specific test condition but have poorer performance if occupants that aren't in that exact position. When developing the neck injury criteria, NHTSA conducted out-of-position tests with several different sized ATDs to assess a more realistic risk to occupants [56].

When Asiana Air Flight 214 crashed at the San Francisco International Airport in 2013, passengers were exposed to varying levels of multiaxial loading and were thrown forward in their seats while exposed to lateral accelerations. This resulted in a several serious injuries to the high thoracic spine (T1-8). This loading condition was well outside the certification tests conducted on the seats and restraints.

The F-4 ejection seat induced a higher rate of injury than other contemporary ejection seats [52] due to its design: the pilot was not aligned with the thrust vector of the seat and instead exceeded the recommend 5° range considered safe (Figure 17), which resulted in a perceived -X/+Z acceleration on the upper torso and head and increased incidence of thoracic spinal injuries.



***Figure 17: F-4 Ejection Seat Posture [52].***

### **1.3.1.3 Seat & Harness System**

When a vehicle transports an occupant, the occupant is moving at the same velocity as the vehicle. However, when an impact occurs, the vehicle quickly decelerates while the body continues to move in the same direction and velocity, and the body can make blunt contact with the vehicle. To prevent blunt contact, restraint systems are used to couple the occupant to the seat, which is coupled to the vehicle. Figure 18 shows how automotive restraints minimize displacement and acceleration of an occupant during impact and Figure 19 shows the displacement of an unrestrained occupant during the same crash conditions [57], highlighting that seat restraint systems are critical for occupant protection.

CRASH WITH RESTRAINED OCCUPANT

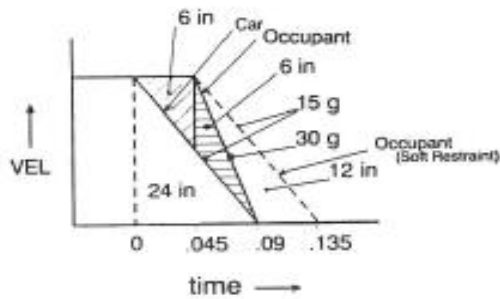


**Figure 18: Car Crash with Restrained Driver [57].**

CRASH WITH UNRESTRAINED OCCUPANT

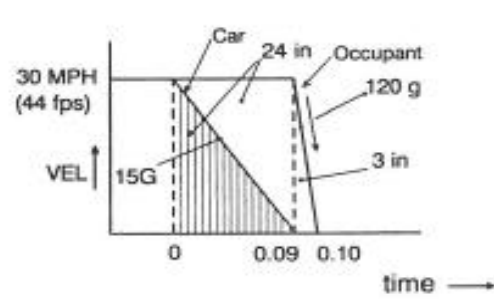


**Figure 19: Car Crash with Unrestrained Driver [57].**

In 2009, 33,808 Americans were killed and 2.2 million were injured during motor vehicle crashes. Of the fatalities, 10,591 were speeding related, and 4,885 occurred on roads with a posted speed limit of 55 mph or higher [58]. In Greece, compliance with wearing harnesses and helmets is low and motor vehicle accidents are one of the leading causes of death; Markogiannakis, et al. report that only 16.6 % of car occupants were using a seat belt and only 6.1% of motorcyclists were wearing a helmet during accidents. The anatomical distribution of injuries of these occupants is tabulated in Table 3 [59].

**Table 3: Distribution of Motor Vehicle Injuries by Body Region [59].**

Body Region	N	Percent
Head	365	50%
Thorax	222	30.4%
Abdomen	104	14.2%
Spinal Cord	70	9.6%
Pelvis	68	9.3%
Upper and Lower Extremity	265	36.3%
<b>Total</b>	<b>730</b>	<b>100%</b>

The overall risk of injury to a specific anatomical region and the severity of the injury may be determined by the tissue response from dynamic loads. For instance, the automotive industry uses the head injury criteria (HIC) to assess risk of injury to the head from acceleration. Figure 20 shows the National Highway Traffic Safety Administration injury risk curves for HIC 15 (a function of peak head acceleration for a duration up to 15 milliseconds) [60]. Further studies found improved harness restraint systems increased tolerance levels for the onset acceleration rate [25, 61].

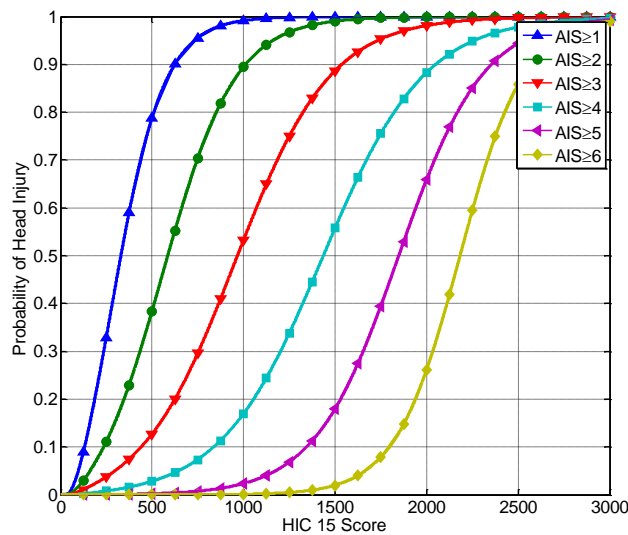


**Figure 20: Head Injury Criterion (HIC) 15 Injury Risk Functions [60].**

Automotive racing exposes drivers to extreme vehicle dynamics as seen in Figure 21**Error! Reference source not found.** [41]. When the risk of HIC-15 head injury was determined using data for the few incidents of head injury that have occurred during race car accidents (44 out of 4015 events resulting in injury to any part of the body), (Figure 22)**Error! Reference source not found.**, the risk was significantly lower than determined in previous research, suggesting that the seat and helmet played an important role in reducing the injury risk.

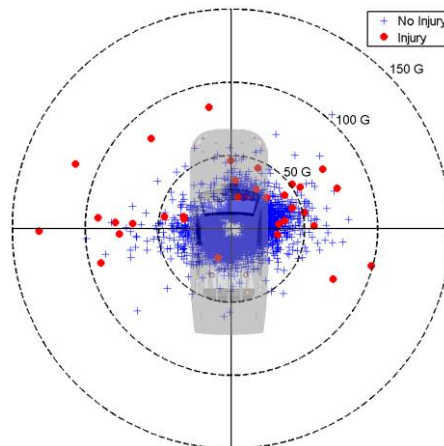


**Figure 21: NASCAR Injury Distribution [41].**

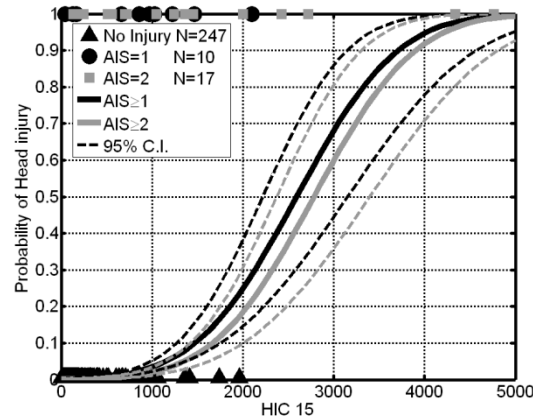


**Figure 22: NASCAR Head Injury Risk [41].**

The following studies provide evidence that dynamic loads can cause injury if restraint systems are not optimized. Eiband showed that an inadequate restraint and seat system magnified other acceleration parameters (onset, magnitude duration) of the human response, and stated that inadequate restraint systems would result in injury that could prevent a crewmember from egressing a spacecraft during an emergency [25].

In 1968, Snyder, et al. studied types and severity of injuries from crash impacts associated with the different restraint configurations shown in Figure 23 [62]. The Federal Aviation Administration (FAA) conducted 60 crash tests with Savannah baboons that were restrained with one of 5 different restraint systems. Although the tests using the simple lap belt were not all fatal, the tests of single diagonal belt tests were all fatal. Wearing only a lap belt during a crash can induce congestion and/or minimal hemorrhages in several organs such as the brain, spleen, heart, uterus and pancreas, and more severe injuries including ruptured bladders, pulmonary lacerations and interstitial pericapsular renal hemorrhages. The 3-point or double shoulder harness offered more protection than single belts, however, the occupant could slip out of the belt during side impact, and the 3-point or double shoulder harness offers no protection for the cervical spine, risking injury to the neck. During high G impacts, scapula fracture and partial dislocation of humerus occurred while wearing the Y-yoke restraint. The conclusion of this study states that the Y-yoke (with inertia reel) and especially with the airbag provided more protection than the other restraint options [62].

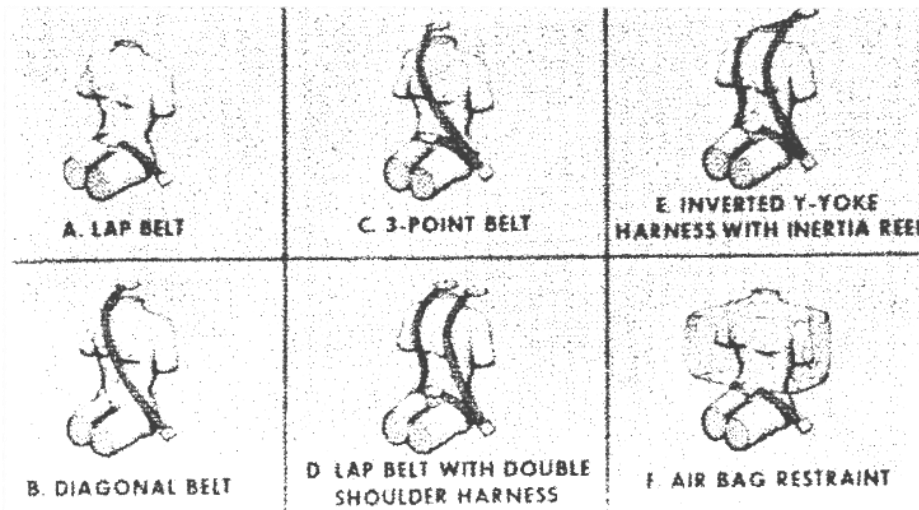


**Figure 23: Harness Configurations [62].**

Zaborowski tested 52 human volunteers wearing a combination of restraint systems during deceleration and lateral impact [33], and determined that the restraint system allowed a minimum deflection of 5° during testing. While no permanent damage was observed, minor complaints of sore neck muscles were reported for more than 60% of the exposures above 8 G. One subject fainted in the seat, their blood pressure could not be detected by the sphygmomanometer, and their heart rate slowed to 20-30 beats/minute; they recovered within 5 minutes once posed in supine position [33].

No matter the restraint system used, to reduce risk of injury it must fit appropriately to the body to ensure that there is minimal slack in the system [63]. Without proper fit of the restraint system, the human response relative to the vehicle will be amplified. The Space Shuttle *Columbia* accident investigation determined lethal effects occurred due to the lack of proper restraint because the inertial reel did not engage during the off-nominal loading. This resulted in inadequate upper body support and allowed the body to swing with only the lower body restrained, resulting in trauma [3].

Optimized restraint systems restrain the occupant during onset of impact, distributing loads over the body and minimizing body movement relative to the seat [57]. Seat design is also an important aspect of occupant protection. Early impact studies identified the benefits of individually contoured body support that could be formed to fit the occupant by evacuating air from the liner, which was filled with small plastic spheres (Figure 24) [64]. The contoured seat was used as an additional restraint system in combination with the harness (Figure 25).



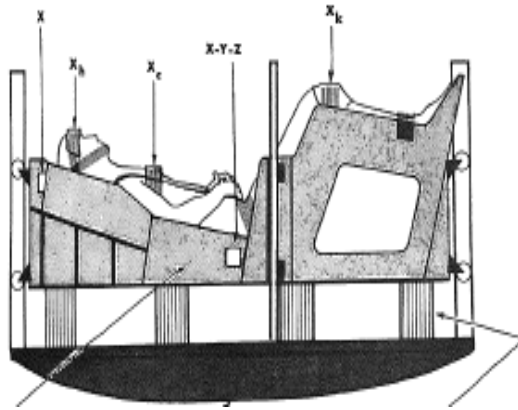


**Figure 24: Impact Vehicle Test Apparatus [64].**



**Figure 25: Contour Body Support Seat [64].**

USSR engineers used a similar contoured seat design to provide “uniform pressure distribution for the human body [61].” From 1963-1967 the USSR performed over 130 drop tests with human volunteers at varying angles of impact and velocity using a shock absorbing actuator (Figure 26). Testing concluded this design feature of the seat was critical for supporting the occupant, and a conformed liner for every occupant aboard the Soyuz is required to this day.



**Figure 26: Kazbek Seat for Soyuz Vehicle [61].**

Further human testing was conducted to characterize the effect of body weight on the shock absorbers, the effects of the headrest recline angle, the mitigation of suit and helmet effects using a conformal seat, and the efficacy of limb restraints to prevent flail. Modifications were aimed at reducing acceleration onset rate and decreasing flexion of the spinal column and neck [61].

The Air Force Research Laboratory (AFRL) has conducted numerous experiments to evaluate how factors such as seat geometry, restraint system design features (including attachment position), and seat cushion properties influence the likelihood of injury during vertical and horizontal impacts. The cushion properties for example may amplify the impact response by storing up the energy in the seat and releasing elastic recoil during impact. Caldwell et al. found significant differences ( $P < .1$ ) in the chest z-displacement of human volunteers during testing of the Vertical Impact Protection seat and the Advanced Crew Escape Suit (ACES) II F-16 seat [65]. The chest z-displacement has been demonstrated by computational models and empirical human testing to be a risk for spinal injury [66]. Other studies have assessed the effects of seat back angle on impact response [67], and the use of a negative-G strap for mitigating risk of injury [68].

Eliminating slack is important for proper restraint. Payne [35] notes that “a slack of only half an inch in the spinal mode would increase the DRI of a continuous 20-G acceleration pulse (with zero rise time) by as much as 100%.” Such a pulse is used for analytical purposes but is not feasible using any impact test facility. Payne also notes that additional preloading, beyond that required to eliminate restraint slack, is of little value.

The position of the restraint system with respect to the body is critically important. Incorrect placement of restraints has been shown to dramatically increase injury risk, and this increased risk is not reflected in the BDRC discussed later in this report [69, 70].

Proper restraint of the pelvis is necessary to protect spaceflight crews. Because the pelvis provides a large contact area on bony structures, it is an ideal location for restraints; however, improper placement can cause injury to the abdomen [69, 70], and lap belts must ride within the curvature of the pelvic bone preferably just below the iliac crest. The harness buckle must be centered on the body 25 to 50 mm (1 to 2 inches) below the belly button when all belts are tensioned [71]. If movement of the torso is minimized, this not only protects the ribs and internal organs, but also protects the spine from induced forces and moments [72].

The negative-G strap provides 2 critical functions. First, by tethering the negative-G strap to the forward part of the seat, it prevents the lap belt from moving up and over the anterior superior iliac spines of the pelvis, and pressing into the abdomen, which can cause serious internal injuries [68]. Complete transection of the rectus abdominal muscles and hepatic lacerations have occurred in anesthetized baboon subjects as a result of seatbelt submarining during high -Z-axis impacts [73]. Stapp [74] also reported that “the forward motion of the shoulders during impact applies traction to the shoulder straps, raising the lap belt, permitting the lower half of the body to begin bending around it. The upper edge of the belt lodges against the lower margin of the ribs and against the upper abdomen.” Second, the negative-G strap prevents the pelvis from moving upward during -Z-axis acceleration. Schall [75] reported that a USAF RF-4 aircraft pilot suffered a cervical vertebrae fracture and transient paralysis as a result of -Z-axis aircraft acceleration that caused canopy contact, and induced cervical flexion during a subsequent +Z-axis acceleration.

During the dynamic phases of spaceflight injuries can be caused by extremity flail if the crewmembers' limbs make forcible contact with the surface of the vehicle or objects, or if they hyper-extend, hyper-flex, hyper-rotate, fracture, or dislocate. Features such as harnesses, form-fitting seats, hand holds, foot holds, and tethers may help maintain the proper position of the crewmember's body and limbs and reduce movement or contact with vehicle surfaces. In addition, the design of the suit may help reduce flail injury if it prevents the inadvertent contact of extremities with vehicular structure or interior components. Extremity guards, tethers, garters, and hand holds have been used in spacecraft, aircraft, and automobiles to reduce flailing of extremities. Limiting limb motion to within the seat envelop reduces the likelihood that the limbs will hyperextend, hyperflex, or hyper-rotate. Limiting and preventing contact with surrounding structure reduces the likelihood of blunt trauma injuries to the limbs.

Aligning the spine within 5° of the Z-axis acceleration vector can minimize the risk of injury to the spinal column because thoracic spinal injury can be induced if the head is bent forward during Z axis (eyeballs down) dynamics [52].

The seat back and seat pan must support the body with no gaps. Gaps can contribute to amplification of the dynamics, which may lead to a higher probability of injury. Gaps between the lateral seating surfaces and the occupant must also be minimized.

An angle of >90° between the seat pan and seatback may cause the pelvic seatbelt to submarine, increasing the risk of injury. A seat reclined 2° forward with respect to the impact vector would have no effect on injury risk, a seat reclined 20° with respect to the impact vector decreases risk of spine and neck injury by 5-10%, and a seat back perpendicular to the impact vector (crewmember in recumbent position) substantially decreases the risk of spine and neck injury [63, 67, 76, 77].

The seating system used in the development of the ±Y DR limits (eyeballs left and right) had minimal gap between the subject and the seat support surfaces. The gaps between the occupant and side panels should be as small as possible to prevent injury due to closing velocity impacts.

Seat padding, cushion design, and non-rigid seat components can amplify the transient accelerations to the occupant due to dynamic overshoot effects, and this can increase the risk of injury. Cushioning that can store energy and can quickly restore that energy back to the occupant should be avoided. Crushable foam or rate sensitive foam are recommended for lateral supports, seatbacks, and headrests. Amplification of +Z axis accelerations are of primary concern because energy absorption is the only strategy to mitigate spinal injury in this axis. In previous vehicles, rate-sensitive foam has helped protect the crew [78]. Perry compared 2 ejection seat cushions: the original B-2 ejection seat cushion made of a 0.63" Confor® foam layer covering a 0.375" layer of polyethylene foam, and a thicker comfort cushion composed of a 0.5" C-45 Confor® foam in the contoured buttock contact area covering a 1.0" thick layer of C47 Confor® foam (Figure 27), which also had a raised area at the back, sides, and thigh with an additional 1.0" layer of C-45 Confor® foam between the top and bottom layers. The raised layers were credited with providing additional comfort.

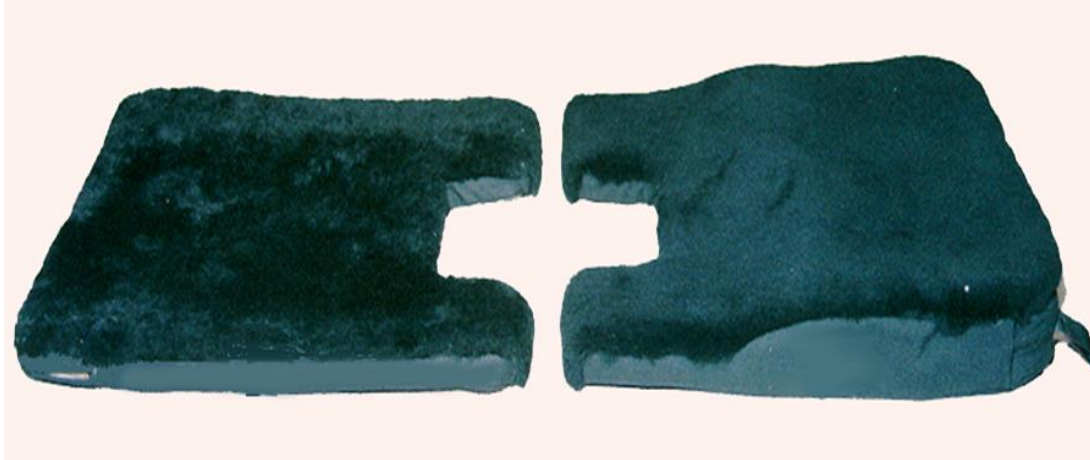


**Figure 27: Comparison of B-2 Ejection Seat Cushions. Original Cushion (left) and Proposed cushion (right) [78].**

Hearon and Brinkley [66] also showed that rate-dependent foam resulted in more benign effects from impacts in +Z axis. Cheng and Pellettiere [79] report data from test of a broader set of cushions using the mid-size male Hybrid III. Although differences were observed (presumably due to the shape as well as material properties), the authors concluded that lumbar spinal force is a better measure to ensure system performance than specifying a specific type of foam. Finally, Miller and Morelli [80] compared several additional cushion configurations, including a 2 in (51 mm) C-47 Confor® foam cushion, using small female and large male ATDs, and concluded that it is safe to include 1 or 2 in (25 or 51 mm) Confor® foam in ejection seats.

The primary strategy for preventing spinal injury is to minimize loads to the lumbar spine, thus the use of rate-dependent foam in seat cushions is recommended because it reduces +Z axis loads transmitted to the lower spine. However, foam in the seat pan should not exceed 51 mm (2").

Planetary lander vehicles will likely use a powered descent approach to land because there is no atmosphere on the Moon and insufficient atmosphere on Mars to adequately decelerate the vehicle either for reentry or under parachutes. Because powered descent results in a much lower impact acceleration, a standing posture may be considered, as was the case for the Apollo lunar module [81]. In the Apollo lunar module, the commander and pilot stood for the entire descent and landing procedure and were restrained by a cable and pulley system providing positive force to the floor. For this scenario, the discussion above about improper restraint doesn't apply; however, it is unclear where the boundary between standing tolerance and the need for a seat occurs.

#### **1.3.1.4 Spacesuit and Helmet**

One of the unique aspects of spaceflight is the use of a pressurized suit, or spacesuit. This suit is designed to protect the crew from the vacuum of space by providing them with a pressurized environment around the body, a breathable atmosphere, thermal protection, and micrometeorite protection. In addition to these basic functions, other factors are considered in suit design including mobility, suits must fit a wide range of crewmembers, and must support contingency Extravehicular Activity (EVA). Because the suit

must provide all of these functions, it may not be optimized from an occupant protection standpoint. The following studies provide evidence the design of the suit and helmet could induce injury during dynamic loading [44, 82-84].

Several factors related to the suit design should be considered to protect the occupant during abort and landings. First, the suit, unlike most clothing, may contain rigid elements, which, depending on their placement, could induce point-loads or blunt trauma resulting in crew injury. For instance, PMHS studies conducted by NASA at Ohio State University investigated the effect of rigid suit elements during landing impacts [82]. Although an insufficient number of PMHSs were tested, the results clearly indicated that the rate of injury from poorly placed suit elements, such as ring placement, drastically increases the risk of injury [83].

Another rigid section on the suit is the suit mounted connector (SMC), which includes supply and return lines for air, cooling water, power, and communications. Wake Forest University conducted impact simulations of a model to investigate the human response to the mass, shape, and placement of the SMC [44]. The design locations were evaluated using the test matrix shown in Table 4. Figure 28 shows the 2 proposed mounting locations, the chest and the thigh. The analysis found that the thigh location had a negligible effect on the risk of injury; however, simulations of the chest mounted connector showed the potential for severe injury, as summarized in Table 4 [44, 85]. Minimizing chest compression not only reduces risk of fracture, but reduces the risk of commotio cordis, which is a circulatory arrest due to a non-penetrating impact to the chest that could result in sudden death [86]. Therefore, the placement and design of suit components is critical for protecting the crew during dynamic loading.

**Table 4: Chest Injury Risk.**

Simulation	V*C (m/s)	Deflection (%)
No Umbilical	0.3635	-20.71%
5 lb, 1 mm	0.7476	-29.87%
5 lb, 15 mm	1.0785	-30.43%
5 lb, 30 mm	1.2240	-30.30%
7 lb, 1 mm	0.8575	-34.78%
7 lb, 15 mm	1.0126	-35.72%
7 lb, 30 mm	1.2614	-36.14%

If  $V \cdot C > 1$ , >25% risk of AIS 4+ injury

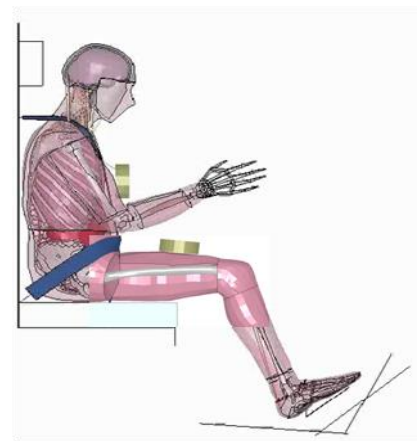


**Figure 28: SMC Mounting Locations.**

Another rigid element of the suit that poses a risk is the non-conformal helmets, which are unique to the spaceflight industry. Other industries (automobile racing, military, sports) design their helmets to mitigate

energy transferred to the neck and spine, however, the spaceflight helmet has several functions. As a result, design of spaceflight helmets may not be optimized for occupant protection.

Radford et al. conducted a study of the suit as a whole during +Z accelerations and with a hybrid III FE model (see Figure 29) [84] and concluded that the head mounted mass was a concern because the helmet approximately doubled the neck compression force compared to neck compression force in the unsuited case as shown in Table 5.

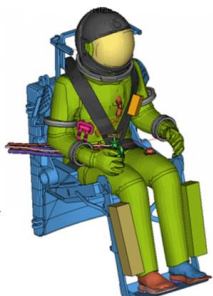


**Figure 29: Suited Model [84].**

**Table 5: Suit Effects on Neck Compression.**

Load Condition	Probability of Occurance	Peak Neck Compression Unsuited [N]	Peak Neck Compression Suited [N]
Nominal	92.9%	690	1,400
Nominal	92.9%	500	1,300
Off-Nominal	6.7%	800	1,900
Off-Nominal	6.7%	1,200	2,100
Off-Nominal	0.2%	960	2,200

Yoganandan et al. report that 700 N of compressive axial force induces a 5% rate of neck injury [87]. If the spine is not aligned the risk of injury increases considerably [88, 89]. This was determined operationally on the F-4 ejection seat, where a misaligned spine resulted in a 34% rate of injury versus predicted 5% injury rate if the spine was aligned [19, 52, 54]. ILC Dover, NASA, Gentex Corporation, and Hamilton Sundstrand Helmet researched design considerations for a spacesuit helmet that maintained visibility inside and outside the vehicle and protected the crewmember during landing. Recommendations were to reduce the mass of the helmet, secure the helmet to remove the helmet load from the neck, and provide a foam collar for the neck. Another possible design is a conformal helmet. [90]. These recommendations are consistent with the *Columbia* Crew Survival Investigation Report, which cited several potentially lethal events and recommended countermeasures to improve survivability in the future. One of the 5 potentially lethal events identified was the nonconformal ACES helmets that do not provide adequate head protection or neck restraint during dynamic loading. Recommendation L2-7 from the report states: “Design suit helmets with head protection as a functional requirement, not just as a portion of the pressure garment [3]”. The *Columbia* Crew Survival Investigation Report also stated “Suits should incorporate conformal helmets with head and neck restraint devices, similar to helmet and head restraint techniques used in professional automobile racing [3].”

An additional challenge of occupant protection is restraining the body while wearing a pressurized suit. When landing with the suit inflated, the body may move around inside the suit during impact. In this case, the vehicle restraint system is no longer restraining the crewmember, but is instead restraining the suit allowing the occupant to move freely inside the suit [57]. Kornhauser reported one case of a fracture in the seventh thoracic vertebra, which occurred during impact testing with the pressurized suit partly

inflated [91]. This could be analogous to a loose restraint system. In other studies, subjects experienced severe and persistent pain as a result of a loose restraint system [31, 92].

During future planetary landings, the suit used for surface EVAs may be worn during descent and landing, as occurred during the Apollo program. This is desirable because mass is a key driver in mission architecture, so not having to land with an additional pressure suit is ideal for minimizing overall vehicle mass; however, a suit optimized for surface EVA activities is likely not well suited to protect the occupant during a landing. NASA's next generation EVA suit, the Exploration Extravehicular Mobility Unit (xEMU), will likely weigh significantly more than the Apollo pressure garment, and could even exceed the weight of the smallest occupant. In addition, the suit features a hard, upper torso that does not conform to the crewmember, allowing movement of the body inside of the suit. This could result in injuries caused by closing velocities between the crewmember and suit, which would invalidate many of the assumptions made about proper restraint, because restraining the suit would be inadequate to prevent motion of the crewmember.

#### **1.3.1.5 Rigid Suit Elements**

Rigid suit components or seat and cockpit hardware that may impinge on the occupant are not explicitly considered in the BDRC [82, 84]. Components that impinge on the torso and or the head and neck during transient loading create the highest potential for model invalidation, and these components must be inspected and/or analyzed to ensure that no blunt trauma effects are induced. Rigid components on extremities must also be inspected and/or analyzed as required to ensure they do not cause fracture, immobilization, or overall compromise of occupant restraint during exposure to acceleration. Chest mounted equipment have been shown to increase injury risk [44].

#### **1.3.1.6 Energy Attenuation**

The basic principle of energy attenuators is to dissipate energy over a longer distance, thus reducing the peak acceleration experienced by the occupant, and reducing injury risk. In theory, energy attenuators can be used to dissipate energy in any loading direction. This was the case for the Apollo command module. The crew couch was suspended from the capsule via a series of struts that could attenuate energy during hard landings. During the Apollo 15 landing, one parachute failed, and the system stroked 0.1". Energy attenuators are employed in modern rotorcraft seat designs to reduce the risk of spinal injury during +Z acceleration impacts during emergency landings that exceed the capabilities of the landing gear, resulting in a large +Z load on the occupants.

### **1.3.2 Intrinsic Injury Risk Factors**

Currently, NASA vehicles must accommodate 1<sup>st</sup> percentile females to 99<sup>th</sup> percentile males [93]. No limit exists for age. Protecting such a wide population is challenging because most occupant protection and dynamic load data is derived either from young, male military subjects or from elderly male PMHS—subjects that can differ in sex, anthropometric measures, and age from astronauts.



### 1.3.2.1 Age

As the human body ages, tissue properties change, e.g., the yield point, Young's Modulus, and human tolerance during dynamic loading are lowered. Evidence that age changes tissue properties is well documented. Figure 30 illustrates that bone strength begins to degrade after the age of 39 years. Other anatomy, such as the intervertebral disc, degenerates after the age of 25 [57]. Pintar et. al found that the Young's Modulus of the anterior cruciate ligament of young specimens (16-26 years) was markedly higher (111+/- 26MPa) than that of older (48-86 years) specimens (65+/-24MPa) [94]. Muscle is another tissue that changes with respect to age. Foust et al. studied cervical spines of 180 volunteers ranging in age from 18-74 years old. Older volunteers had up to 40% less range of motion, 23% less muscle reflex, and 25% less strength than younger volunteers [95]. The same concept applies to other sections of the body such as thoracic, abdominal, pelvis, cervical and extremities [57, 96, 97]. Figure 31 illustrates the probability of cervical spine failure with respect to age of the spine at a loading rate of 2.2 m/s.

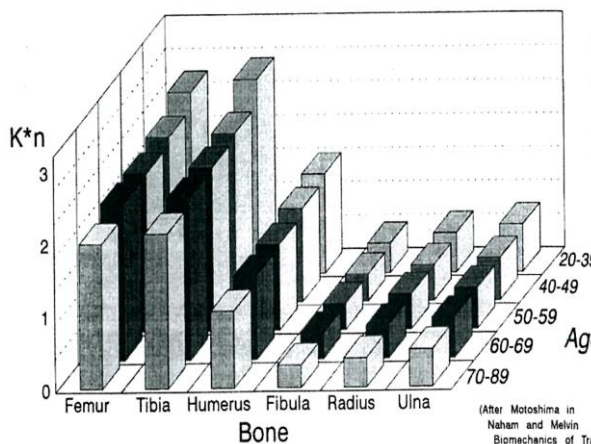


**Figure 30: Bone Strength Decreases with Age [57].**

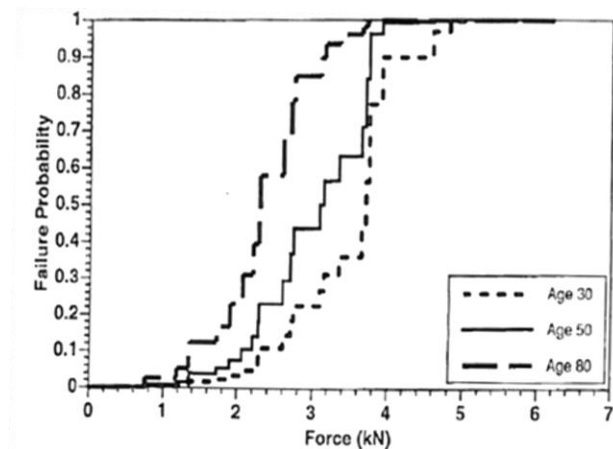


**Figure 31: Failure of Male Cervical Spine [98].**

Further evidence exists showing that the risk of injury due to dynamic loading increases with age. Fatality Analysis Reporting System analyzed data from the NHTSA regarding accidents that occurred from 1975-1998. Conclusions state the risk of death due the same type of blunt trauma increases 2.52% per year for males and 2.16% per year for females after the age of 20 [99]. Little information from the automotive industry is available regarding age and injury, and even less is known in the spaceflight industry. Therefore, gaps of knowledge remain regarding the risk attributed to age during dynamic loading with spaceflight profiles.

The aging processes induces physical changes that affect a person's tolerance to loading. Published literature shows injury risk increases with age, due to effects such as disc degeneration, and decreases in bone strength, ligament strength, and muscle strength and reaction [57, 94, 95].

Table 6 shows how breaking strength of lumbar vertebra relates to age 30 [100-103]. These age-related changes in strength are related to decrements in bone density in the vertebra, and do not include any changes or loss of vertebral strength due to spaceflight. These studies were based on a general population



as compared to the astronaut corps, who must maintain adequate bone mineral density (BMD) to be selected for flight, which may influence extrapolation of these results to astronauts [104].

**Table 6: Comparison of Lumbar Failure Strength by Age - Values are compared to Age 30.**

	Age 40	Age 50	Age 60
<b>Lumbar Failure Force [100, 101]</b>	-11%	-22%	-35%

Evidence also indicates that age affects the cervical spine. Figure 32 shows the probability of injury from axial compressions of the head and neck for a 62-year-old and a 45-year-old. Data, which were obtained from a study using PMHS, indicate that increased age is associated with higher risk of injury. At 45 years of age, forces of 2.0 kN and 4.4 kN were associated with a 5% and a 50% probability of injury, respectively (Figure 32). Not all the injuries in this study were sustained by compression-related mechanisms, but further analysis concluded that age was also a significant covariate when the dataset excluded specimens with pure ligamentous damage [87].

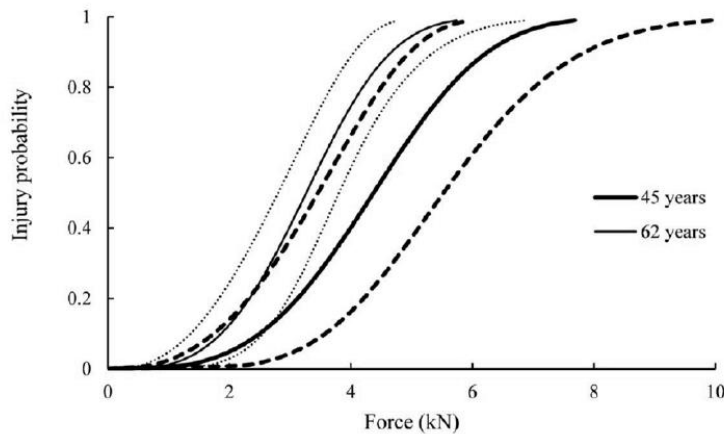


**Figure 32: Comparison of Probability Curves and  $\pm$  95% Confidence Intervals for Upright Tests [87].**

The same study by Yoganandan et al. [87] determined that age was not a covariate in distraction- or extension-related injuries. Comparison of the forces at all risk levels indicated a greater magnitude of force with the first part of the study than the second, reflecting the differences between compressive loading (borne primarily by bone) in the former, versus distractive and extensive loading (borne primarily by soft tissues) sustained in the latter set up. The bending moment may be a better risk metric than the axial force when assessing extension-types of injuries [87].

The structure of the human vertebrae and their mechanical properties deteriorate with age. Increased age is associated with increased risk of compression and fracture injuries of the vertebrae; however, this phenomenon has not been investigated for soft tissues. Ligament, disc, and joint injuries were common

in the inverted drop tests mentioned above. Age was not a significant covariate for soft tissue injury in that study. Tests of one-day-old to 67-year-old PMHS lumbar spine ligaments [94, 105, 106] indicate that during quasi-static loading of the lumbar anterior and posterior longitudinal ligaments (ALL and PLL) the rate of decrease in the dissipation of energy decreases considerably after 40 years [16]. Although another study tested ALL and PLL, supra- and inter-spinal ligaments, and inter-transverse ligaments, and ligamentum flavum (LF) from 30- to 80-year-old PMHS, only 4 (from one 50-year-old and three 60-year-old PMHS) ligament specimens were tested from the cervical spine [16]. A recent study tested cervical spine ALL, PLL, and LF (23-year-old to 84-year-old PMHS) at 0.002 m/s [17]. Although the failure load was significantly ( $P < .05$ ) greater between the youngest (23 years) and oldest (61 to 84 years) PMHS in the 3 ligaments, no significant difference was detected in load failure ( $P > .05$ ) between the medium age (42-46 years) and older PMHS for ALL and LF. Studies using PMHS cervical ligaments from different vertebra levels and types have been tested at wider loading rates ranging from 0.09 to 2.5 m/s, however, data delineating age dependency in the DR of cervical ligaments are not conclusive [16-21]. Overall, PMHS studies seem to indicate that age-associated levels of ligament deterioration are lower than age-associated rates of bone deterioration.

The tensile strength of discs in the human cervical intervertebral of 20 to 39-year-olds was  $330 \pm 20$  MPa, whereas values were  $290 \pm 30$  MPa for 40 to 79-year-olds. No change in tensile and torsional strengths and deformation properties of the discs were detected in the 40- to 80-year-old group [22]. The mechanical properties of these soft tissues are likely to be less sensitive to increasing age than bony tissues are [87]. However, because crew selection criteria controls for age-related BMD loss, the NASA Human System Risk Board accepted the risk associated with age-related BMD loss for astronaut populations [107].

### **1.3.2.2 Sex**

Sex is a significant factor for the risk of injury during dynamic loading. Epidemiology studies conducted by the automotive industry use information from accidents to improve countermeasures. For the same automobile accident conditions, the fatalities for women were 22%-25% greater than for men [108, 109]. Women have a 20% greater risk of injury to the thoracic spine than men.

Allnutt reviewed medical and safety literature and reported that women's bone has differences in density, structure, size, and strength than bone from a well-matched control cohort of males of the same age, height and weight. This is in part due to the female bone structure, which has a thinner cortical layer relative to the trabecular section of the bone in men [110]. Another study that compared tomography scans of cervical spine at C4 from matched sized volunteers found significant differences in geometry through analysis of variance [111]. Gallagher et. al. reported levels of stress in the cervical spine during a dynamic loading condition were 14-18% greater in woman than in men [112]. Sex differences should be further investigated to fully understand the risk of injury due to dynamic loading and to better protect female astronauts.

Women have an increased risk of neck injury during loading [98, 111-113]. Pintar et al. report that women's tolerance to neck compression loading was 600 N less than men's tolerance [98]. Neck failure loads in PMHS due to pure compression were  $1.2 \pm 0.5$  kN for females and  $2.5 \pm 0.9$  kN for males [114].

Tolerance of neck bending moment is also lower in women than in men: failure moments were  $23.7 \pm 3.4$  Nm for flexion and  $43.3 \pm 9.3$  Nm for extension in women [115], and the failure moments were  $29.0 \pm 6.3$  Nm for flexion and  $49.5 \pm 17.6$  Nm for extension in men [116], i.e. women had 12% to 18% less tolerance.

In contrast, isolated tests of PMHS head and neck in a superior-inferior direction indicate that force and moment risk curves for women are similar to those for men and woman combined (Figure 33). The force value of 330 N for the women and 341 N for the men and women combined are associated with a 50% probability of injury. Failure moments are 99 Nm for the women and 95 Nm for the women and men combined, and the lower neck injury criteria are 1.29 and 1.41, respectively. The mean force of 214 N, moment of 54 Nm, and lower neck injury criteria ( $LN_{ij}$ ) of 0.89 were associated with 5% injury probability. The normalized confidence interval size (NCIS) for these metrics were 0.90, 0.95, and 0.89. These results can be used as criteria for lower-neck injury for women under postero-anterior accelerative loading for evaluating the effects of vehicle crashes [117].

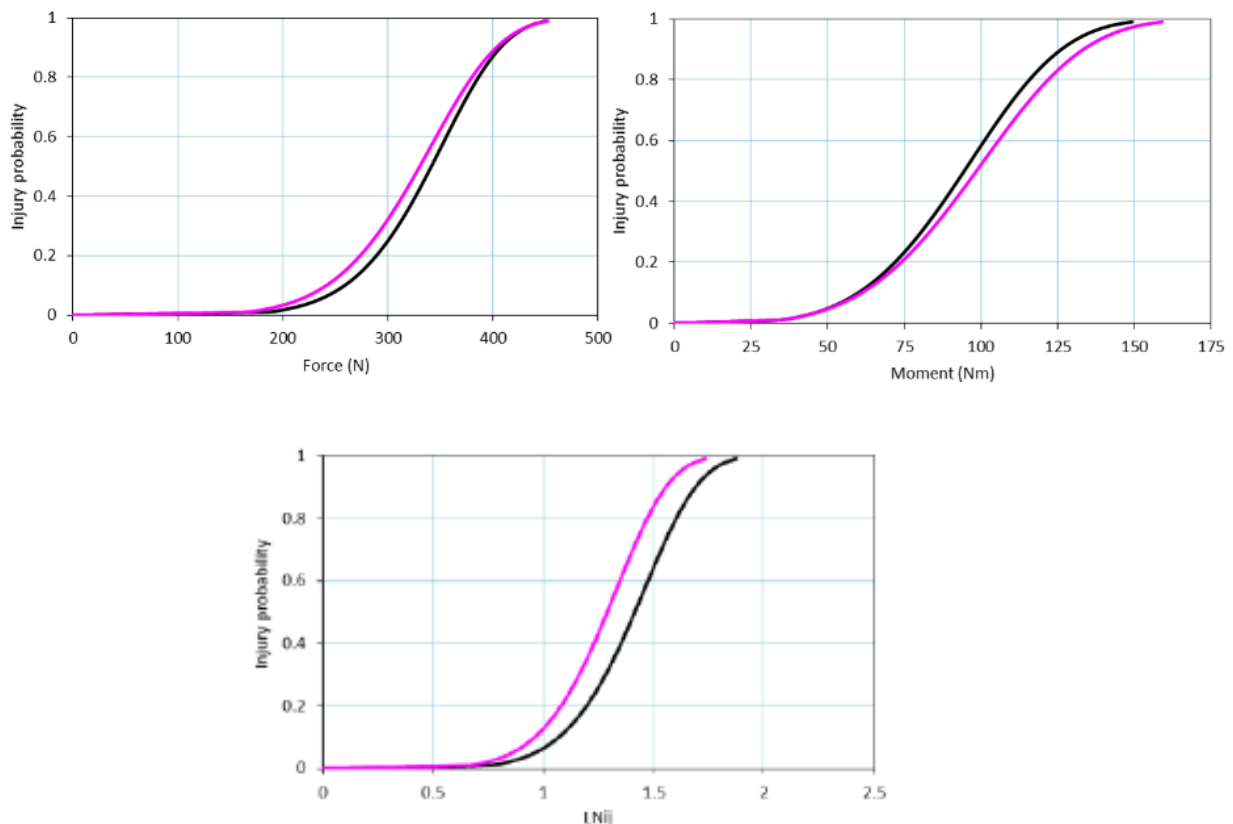


**Figure 33: Force, Moment, and Lower Neck Injury Criteria Risk Curves for Combined (black) and Female-Only (pink) Datasets.**

Finally, tolerance to lateral neck bending is lower for women than for men. Perry et al. report that peak neck moments were 29% higher in female subjects than male subjects during the same loading conditions (25.2 Nm versus 19.3 Nm) [118].

Although healthy men and women have the same levels of BMD in cervical and lumbar regions [101, 112], when normalized for weight, stress in the lumbar and cervical spine is 15% greater in women [113]. The effect of an increase in cervical stress on the DRI probability of injury curve has not yet been established, but is expected to lead to a slight increase in risk of neck injury for women [113].

### **1.3.2.3 Anthropometry**

It is critical that individual anthropometric measures be considered then fitting the occupant to the seat with the restraint system. If the configuration of the restraint, seat, suit, and helmet is not optimized for the occupant, the risk of injury increases [63]. The length of the spine is altered due to gravitational changes and fluid shift during spaceflight [119]. A crewmember's body height can increase 4-6 cm [120-122], and their seated height can increase up to 6% [123] during spaceflight. During bed rest, lumbar spinal length increases up to 3.7+/-0.5mm and spinal curvature decreases. It has been recommended that the seats allow for height adjustment based on this research [123]. Research of the cause of spinal lengthening is ongoing. An additional spaceflight study found no significant change in intervertebral disc height before, during, and after 117-213 day missions [124], suggesting that the spinal lengthening is due to the decrease in spinal curvature, rather than the swelling of intervertebral discs. Another short duration spaceflight study of an 8-day shuttle mission confirmed these results [125]. In contrast, many reports suggest that intervertebral discs do swell in microgravity, although these conclusions are based on bed rest studies [15, 125, 126]. Ongoing research to characterize spinal changes during spaceflight will be critical for developing occupant protection countermeasures.

Anthropometric measures affect injury risk during dynamic events. Although they have less mass, smaller crewmembers are at a greater risk of neck injury because the cross-sectional area of their cervical vertebra is smaller, causing significantly higher vertebral stress. No significant correlation was found between lumbar stress and height or sitting height for either males or females [113]. In addition, because different size crewmembers interact with the seat, suit, and restraints differently, a small and a large ATD must be tested to assess unique design specific interactions.

### **1.3.2.4 Spaceflight-Induced Physiological Deconditioning**

During spaceflight, the structure and function of the musculoskeletal system changes over time due to unloading of the body in microgravity environment. During prolonged spaceflight, the density of the skeleton changes, primarily in the lower extremities and spinal elements [127]. Studies using dual energy X-ray absorptiometry (DXA) have determined average decreases of 1-1.6% in the spine, femoral neck, trochanter, and pelvis, and an average decrease of 1.7% in the tibia after only one month in microgravity [128, 129]. Bone changes in combination with physiological deconditioning could increase injury risk. For example, increasing the time in space increases the risk of herniated nucleus pulposus (HNP), especially during the early periods after return from spaceflight [130].

Because skeletal deconditioning is time dependent, any method for mitigating the losses (e.g. exercise or supplements) will be specific to the mission length. NASA is funding research to further understand the risk of fracture for astronauts. BMD decreases between 1-1.5% per month [131]. Although BMD is often used to assess bone strength, BMD does not provide information on the structural properties of the bone. The size and geometry of bone are good predictors of the compressive and bending strength of bones [131]. Figure 34 shows that the larger diameter bone has greater compressive and bending strength than a smaller diameter bone with the same areal BMD. However, decreased bone mass is a predictor of increased fracture risk. Areal BMD, as assessed by DXA and biomarkers for bone turnover, are monitored in astronauts after their return from space to assess skeletal changes; however, DXA cannot be used to measure volumetric parameters of bone, which could be useful in determining bone quality. Other measures such as high resolution computed tomography and magnetic resonance imaging provide microarchitectural insight but expose the human to higher doses of radiation [132]. Ground studies of deconditioned bone continue to assess effective countermeasures for bone loss, but ground studies can not reproduce the unique architectural changes to the bone that are induced in microgravity.

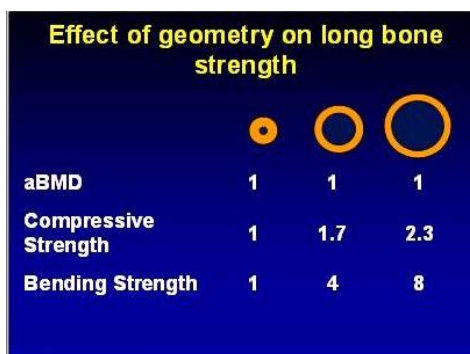


**Figure 34: Bone Strength is Dependent on BMD and Geometry [131].**

Before missions, crewmembers have set physical training requirements that consist of cardiovascular training, resistance exercises, and weight training personalized to each individual. Crewmembers are also scheduled for 2.5 hours of exercise 6 days a week during the mission [133]. Even with consistent training before and during a mission, crewmembers experience varying levels of physiological deconditioning related to exposure to microgravity, including changes to the musculoskeletal system [128, 129, 134-141]. Figure 35Error! Reference source not found. shows example of BMD losses after long-duration spaceflight. Data were collected on crewmembers before the use of the advanced resistive exercise device (ARED) and may be conservative compared to today's crewmember losses.

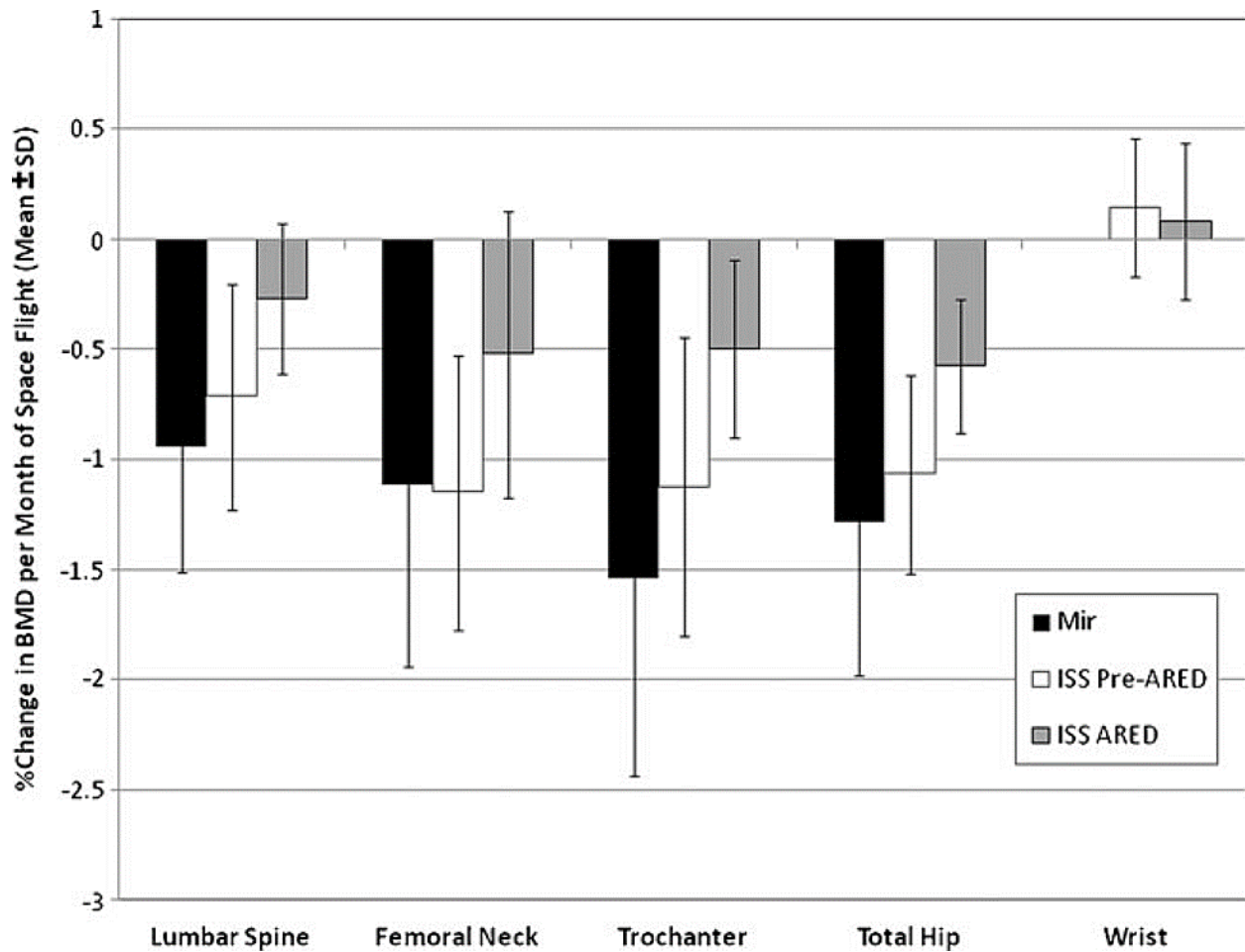


**Figure 35: Changes in BMD after Long-Duration Spaceflight [142].**

To account for changes in injury risk due to microgravity exposure, scaling factors have been developed to reduce the BDRC limits for specific regions of the body. Additional information can be found in Lewndowski et al. and the Human System Integration Requirements Document [127, 143].

Table 7 shows the deconditioning factors for regions of the body. These factors are considered when assessing any dynamic event that occurs after 1 month of reduced gravity exposure (e.g. entry, descent, and landing). These limits estimate the reduction in human tolerance and are used to protect deconditioned crewmembers after up to 6 months in space. Physiological deconditioning limits for longer missions should be discussed and agreed to by a panel of medical experts.

**Table 7: Deconditioning Factors.**

Anatomical Region	Deconditioning Factor
Spine	0.86
Lower Extremities (including hip)	0.75
All Other Regions	1.0

To account for the effects of spaceflight-induced physiological deconditioning, the deconditioning factor for the spine is applied to the appropriate injury metrics. Because the pelvic restraint designs may not contact the iliac crest and could concentrate the load on the femoral head and neck, increasing the risk of fracture after spaceflight, the deconditioning factor for the lower extremities is applied to the DR<sub>v</sub> limits to protect the femoral head and neck during lateral impacts [144]. These values are used after crewmembers have been exposed to reduced gravity for more than 1 month.

Figure 36 illustrates compressive strength of trabecular bone from the lumbar spine is almost twice the strength along z-axis (inferior to superior) versus strength in the x-axis (anterior to posterior) or y-axis (medial to lateral).

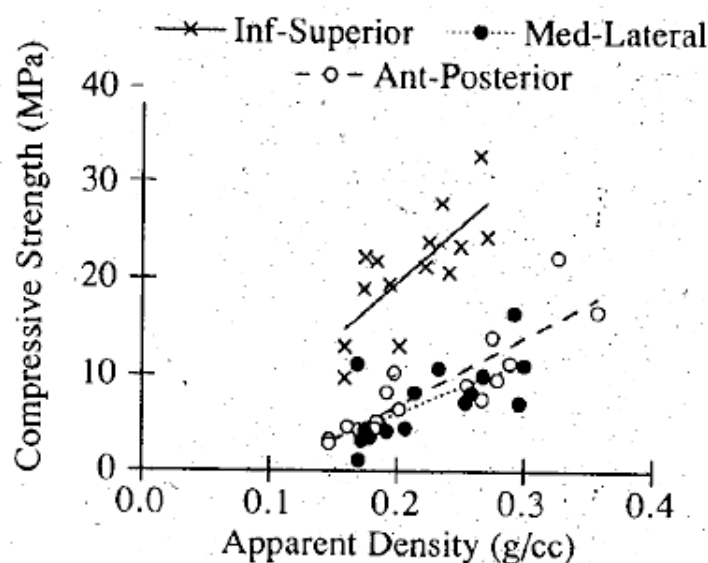


**Figure 36: Compression Strength of Trabecular Bone from Lumbar Spine Correlates with Loading Direction and with Bone Mineral Density [145].**

Muscle mass, endurance, and strength also degrade during spaceflight. Bed rest studies show that muscle will start to atrophy within 7-14 days of disuse [146]. Leg volume decreased by 7-10% [136] during Skylab missions, and decreased as much as 19% in during missions on board the MIR space station [137, 138]. The muscle loss experienced by crewmembers is also selective; the size of the different types of muscle fiber in the vastus lateralis decreased at different rates after 5-11 days in flight. Edgerton et al. report decreases of 16% in Type I, 23% in Type IIa, and 36% in Type IIb fibers [139, 140]. During missions lasting 117-213 days, the functional cross-sectional area of lumbar paraspinal muscles decreased and the lumbar lean muscle mass decreased as a percentage of total lumbar cross sectional area [124]. Rodents that flew for 15 days in space had more disc degeneration than an earth-based control population [147]. No direct correlation has been found between the duration of the space mission and disc degeneration, so continued research is needed to assess the effect of time in space on disc degeneration [148]. Exercise

devices, such as the ARED (Figure 37), are used on the ISS to mitigate the effects of physiological deconditioning during long-duration missions, and have shown to be successful [131] . Astronauts who used the ARED during a 6 month mission on ISS experienced a loss of fat mass and an increase in muscle mass [146].

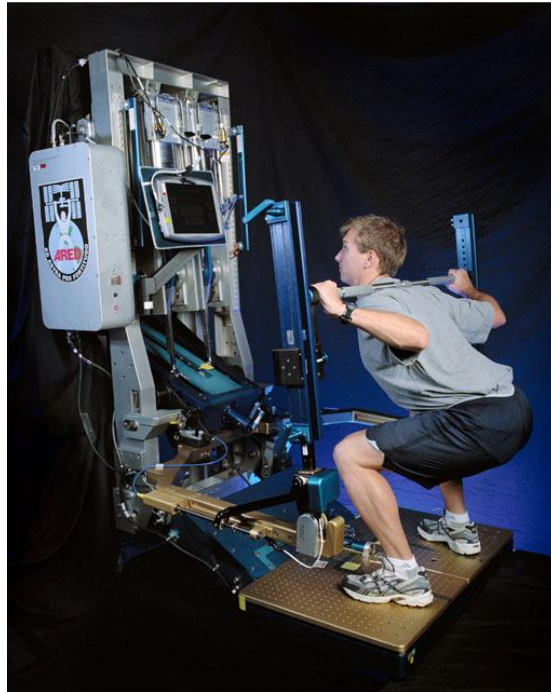


***Figure 37: Ground Version of the Advanced Resistive Exercise Device (ARED) [146].***

When tendon tissue, which attaches the muscle to the bone, was studied using unloading models (unilateral lower limb suspension and bed rest), an increase of Young's Modulus in the tendon resulted in muscle shortening, which negatively affects muscle function and performance [141]. Mertz et al, conducted impact testing with human volunteers and measured the effects of muscle tension and kinematics of the head. Figure 38 illustrates that a subject in a relaxed posture during various impacts had greater magnitudes of torque and angular displacement about the occipital condyles than the subject who tensed their muscles before impact (Figure 39). The relaxed testing technique testing was halted by the volunteer but the volunteer could tolerate higher loads when the neck muscles were tensed (the voluntary limit was higher with a pre-tensed neck) [149].



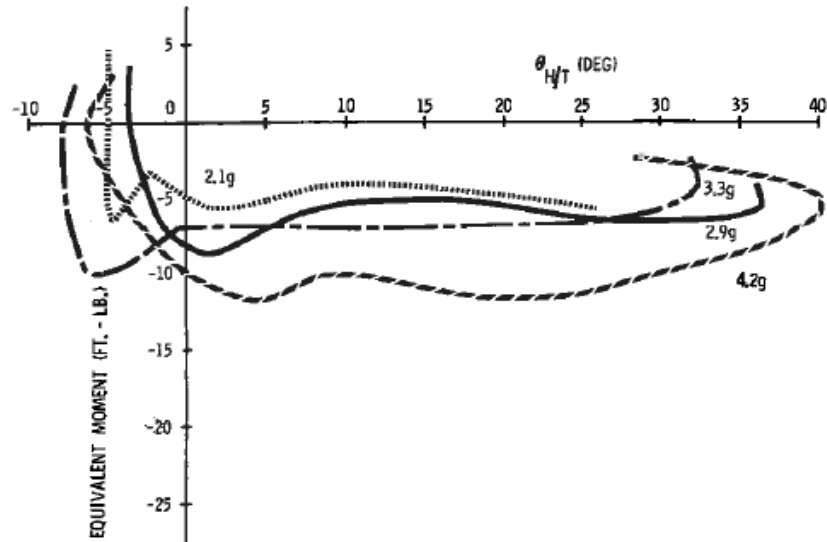


**Figure 38: Relaxed Posture During Impact [149].**

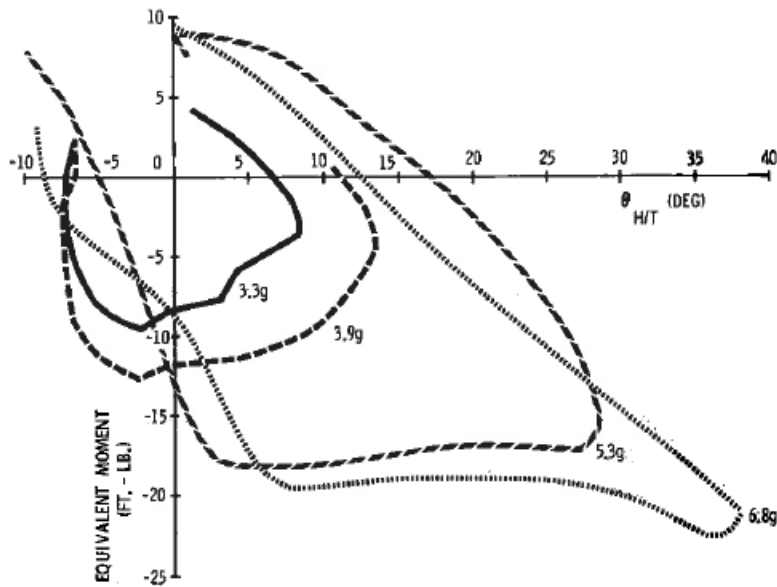


**Figure 39: Tense Posture During Impact [149].**

Exposure to microgravity can change cross-sectional area of intervertebral discs and change the overall shape of the spine [15]. Reduced compression on the spine causes spine lengthening. Astronauts have reported generalized back pain due to spaceflight, which is likely due to spine lengthening or muscle weakness. It is thought that the intervertebral discs adapt to microgravity by changing osmotic pressure within the disc, making them more susceptible to injury when exposed to higher G levels [150]. Studies are further investigating intervertebral discs during spaceflight; however, no research currently addresses the risk of injury during dynamic loading for a deconditioned spine.

Townsend created a finite element model of the whole spine [148], and used the model to predict potential injury sites in the spine during a 9-day mission. The author found that risk of spine injury increased due to microgravity-induced swelling.

## **1.4 Injury Criteria Definition**

Regardless of which method is chosen, injury criteria are needed. These criteria can be tolerance limits, defined by results of non-injurious tests, or can be IARVs that relate a particular response to injury risk. Either way, these tolerance limits or IARVs must predict injury in a range that is appropriate for the application. NASA currently defines injury risks to be <0.5% for nominal landings and 5% for off nominal landings (based on the BDRM). Most current injury risk functions for ATDs or numerical models are not validated to assess a 5% risk of injury: most are validated for serious injury ( $AIS \geq 3$  or  $AIS \geq 4$ ), and a higher risk of injury (15-50% risk).

### **1.4.1 Head Injury**

#### **1.4.1.1 Traumatic Brain Injury**

Traumatic brain injury (TBI) is defined as brain damage that “results from external forces, as a consequence of direct impact, rapid acceleration or deceleration, a penetrating object (e.g. gunshot), or blast waves from an explosion” [151]. Although TBI can include both closed and penetrating injury modes, the most common types of TBI in environments analogous to spaceflight are closed brain injuries.

Mild traumatic brain injury (MTBI) is diagnosed based on the severity of a patient’s symptoms. These symptoms are transient confusion, disorientation, impaired consciousness, dysfunction of memory (around the event), or loss of consciousness lasting less than 30 minutes. In addition, the following signs of neurologic dysfunction may also be present: seizures, headache, dizziness, irritability, fatigue, or poor concentration [152]. MTBI has been of interest recently in relation to concussion effects in American Football players [153-162]. MTBI is of particular interest to NASA due to the low-risk posture needed for capsule landings (which occur on each flight).

Diffuse axonal injury (DAI) is a more severe injury causing structural damage to the brain tissues, typically distributed throughout the brain. DAI is caused by shear forces induced in the brain tissues during rapid acceleration. These shear forces cause damage to the neural cells, disrupting normal brain function and often resulting in coma.

Acute subdural hematoma (SDH) is a severe condition characterized by blood collecting between the dura mater and brain surface that is most often caused by tears in bridging veins in the subdural space. These veins are strain-rate sensitive and tear under rapid acceleration [163]. Symptoms of acute SDH include loss of consciousness, coma, and severe headache.

### 1.4.1.2 Skull Fracture

A skull fracture occurs when an impact to the head causes a break or crack in the cranial bone, or skull. Skull fractures can have varying severities, and some do not break the skin or even need medical treatment. The severity depends on the force of the impact, location on the skull, and the object of impact. Types of fractures include open, closed, depressed, and basal fractures. Open fractures occur when the skin breaks and the bone protrudes. In a closed fracture, skin isn't broken. If the skull collapses into the brain cavity, it is characterized as a depressed fracture.

### 1.4.1.3 Head Injury Mechanisms

Linear acceleration has been studied at great length and is well correlated with skull and brain injury [164]. The exact injury process varies depending on the circumstances of the loading, for instance contrecoup brain injuries are due to inertia movement of the brain within the skull.

Rotational acceleration has been researched extensively over the years [157, 165-171], and with the recently renewed interest in MTBI, researchers are showing correlation between rotational acceleration and diffuse brain injuries. Rotational acceleration is believed to contribute to strain in brain tissue, causing diffuse disruptions of function, beginning with MTBI [172].

Blunt trauma to the head is common in vehicles crashes when inertia of the head causes the head to impact surfaces inside a vehicle causing a secondary collision. Blunt trauma is often associated with skull fracture and focal brain injuries.

### 1.4.1.4 Head Injury Metrics

Several injury metrics have been proposed to predict the risk of head and brain injury. The most common translational dynamic metric is the HIC (Equation 2), which is calculated from the resultant head acceleration,  $a(t)$  over time ( $t$ ) [173-175]. In addition, metrics based on rotational dynamics of the head have been proposed, including rotational acceleration of the head [155], rotational velocity of the head, cumulative strain damage measure [176, 177], and Kinematic Rotational Brain Injury Criterion (BrIC) (Equation 3) [178, 179].

#### ***Equation 2: Head Injury Criterion (HIC).***

$$HIC = \max_{t_1, t_2} \left\{ \left[ \frac{1}{t_2 - t_1} \int_{t_1}^{t_2} a(t) dt \right]^{2.5} (t_2 - t_1) \right\}$$

**Equation 3: Kinematic Rotational Brain Injury Criterion (BrIC): where  $\omega_{x,y,z}$  are the maximum angular velocities about each representative axis, and  $\omega_{xc,yc,zc}$  are the critical angular velocities about each respective axis [179].**

$$BrIC = \sqrt{\left(\frac{\omega_x}{\omega_{xc}}\right)^2 + \left(\frac{\omega_y}{\omega_{yc}}\right)^2 + \left(\frac{\omega_z}{\omega_{zc}}\right)^2}$$

## 1.4.2 Spinal Injury

Although the cervical, thoracic, and lumbar spine are investigated separately and have different metrics to predict injury, the types of injuries and mechanisms are similar, so both are discussed here.

Injuries of the spine can be classified into one of 3 categories: vertebral fractures, disc injury, or ligament damage. Fractures of the vertebra vary depending on the injury mechanism, and can include Jefferson, hangman, atlas, odontoid, wedge, and burst fractures [180]. Disc injury is primarily caused by disc rupture. Ligament damage is also observed in neck injuries and can include damage to the anterior longitudinal, and transverse ligaments [181].

### 1.4.2.1 Spinal Injury Mechanisms

#### 1.4.2.1.1 Neck

Because the response of, and injury risk to, the cervical spine is dependent on load rate [182], loading rate is key to whether an injury will occur. Axial compression has been studied at length, and although pure compression of the neck is not necessarily a good indicator of injury, combined compression and bending moments can greatly reduce human tolerance to neck injury [183-185]. In most cases, injury is a result of vertebral fracture or ligament damage. Axial tension has not been as extensively studied [149, 186, 187]; however, axial tension can cause vertebral fracture typically in the lower cervical spine [186]. As with axial compression, tolerance to axial tension decreases when combined with extension moments [188]. Other injury mechanisms are bending moments and shear forces [149]. In addition, research has suggested that the lower neck is more likely to be injured if the head is supporting extra mass (i.e. helmet) [189].

#### 1.4.2.1.2 Thoraco-Lumbar Spine

Similar to the neck, the thoraco-lumbar spine shows a rate-dependent response to loads [190]. Higher loading rates cause more severe fracture than lower loading rates of the same magnitude [191]. A study of blunt trauma cases involving the spine determined that compression fractures occurred most commonly in the thoracic spine, and transverse process fractures occurred most commonly in the lumbar spine. The most common vertebrae injured were L1 and L2 [192].

### 1.4.2.2 Spinal Injury Metrics

$N_{ij}$  is an interaction-based force and moment injury criteria created to evaluate severe neck injury from a frontal impact. The formulation is given in Equation 4, where  $F_z$  is the axial force,  $F_{crit}$  is critical force intercept,  $M_y$  is the flexion-extension moment and  $M_{crit}$  is its critical intercept. All these quantities are time

dependent. Respective critical values were obtained from risk curves corresponding to 90% mean values, and they are dependent on sign (i.e. there are separate limits for compression vs. tension and extension vs. flexion).

**Equation 4: Neck Injury Criterion ( $N_{ij}$ ).**

$$N_{ij} = \frac{F_z}{F_{crit}} + \frac{M_y}{M_{crit}}$$

$N_{ij}$  is not used to evaluate low speed rear-end impacts. Therefore,  $N_{km}$  (Equation 5) was created.  $N_{ij}$  analyzes axial forces, whereas  $N_{km}$  is calculated using shear forces, which are the critical values in rear-end impacts [193].

**Equation 5:  $N_{km}$ , where  $F_x(t)$  is the shear force,  $M_y(t)$  is the flexion/extension bending moment, both acquired from load cells on the upper neck.  $F_{int}$  and  $M_{int}$  are intercept values used for normalization.**

$$N_{km} = \frac{F_x}{F_{int}} + \frac{M_y}{M_{int}}$$

Neck injury criteria (NIC) is also used to evaluate low-intensity injury from rear-end impacts (Equation 6). The NIC is based on the acceleration and velocity of the top of the cervical spine relative to the bottom [194]. However, the NIC can only be used to evaluate the first 150ms of an impact [193].

**Equation 6: Neck Injury Criterion (NIC), where  $a_{rel}$  and  $v_{rel}$  are the relative acceleration and velocity between the top and bottom of the spine, respectively.**

$$NIC = a_{rel} * 0.2 + v_{rel}^2$$

Recently, NASA developed a new injury metric to assess the risk of neck injury from rearward (eyeballs in) loading. This new injury metric, called the  $LN_{ij}$ , uses rear shear force in the lower neck load cell combined with the neck extension moment in the sagittal plane (Equation 7). This new injury metric is based on impact testing of the Hybrid III 50<sup>th</sup> percentile male ATD and PMHS matched-pair tests [195].

**Equation 7: Lower Neck Injury Criteria ( $LN_{ij}$ ), where  $F_{crit}$  and  $M_{crit}$  are critical values obtained from risk curves corresponding to 90% mean values.**

$$LN_{ij} = \frac{F_x}{F_{crit}} + \frac{M_y}{M_{crit}}$$

Peak thoraco-lumbar forces predict injury and thoraco-lumbar bending moments are also be involved in injury. These 2 parameters are used in the lumbar spine index calculation (Equation 88) [196]. When adjusted for age, lumbar spine index was a good predictor of thoracolumbar fracture (90% correct) for 11 motor vehicle crashes. The same study found age-adjusted principle stress in the trabecular bone can predict injury. Spinal axial compression force is also used to predict injury [197].

**Equation 8: The Lumbar Spine Index as Proposed by Ye [196]; where  $F_z$  is the axial force,  $M_r$  is the resultant bending moment, and  $F_c$  and  $M_c$  are the critical values.**

$$\text{Lumbar Spine Index} = \frac{F_z}{F_c} + \frac{M_r}{M_c}$$

### 1.4.3 Upper and Lower Extremity Injury

Upper extremities include the hand, elbow, arm, and shoulder, and the lower extremities include the hip, thigh, knee, lower leg, ankle, foot, and toes. Any injury to these body parts is classified as an upper or lower extremity injury. These injuries could include muscle strains, ligament sprains, contusions, fractures, and lacerations [198, 199].

#### 1.4.3.1 Upper and Lower Extremity Injury Mechanisms

Hyperextension of the joints could occur when bending moments exceed the strength of the joints in the upper and lower extremities. Injuries from hyperextension include cartilage damage, joint dislocations, muscle strains, and transverse fractures [200]. Also, bending or torsional moments imparted on bones could cause fracture [201]. Ligament injuries can occur when bones, such as the femur and tibia, are excessively translated or rotated relative to each other [202]. Axial loading through the plantar surface of the foot has been shown to cause calcaneal, talus, midfoot, and various ankle fracture [203]. Blunt trauma is also a mechanism for fractures, contusions, and lacerations. The severity of injury depends on the geometry and material properties of the object, the location of impact, and the force of impact.

#### 1.4.3.2 Upper and Lower Extremity Injury Metrics

Peak elbow bending moment is used to predict risk of elbow dislocation and elbow injury [200]. Bending moment is also used to predict fracture in the humerus and forearm [201]. Many injury metrics in the lower extremities induce peak loads, and some include load duration. Kuppala et. al proposed that femur axial force is a good predictor of knee-thigh-hip injuries [202].

Relative displacement of bones as has been proposed to predict ligament injuries in the knee. Axial compression tests have been proposed to predict bone fracture limits. Tibia axial force and mass of the subject can be used to predict tibial axial injury.

The tibia index calculation uses combined bending and axial compressive loads to predict fractures to the tibia shaft (Equation 9) [204]. After further research, the tibia index was revised using different critical values [202, 205, 206].

**Equation 9: Tibia Index; where  $F$  is the measured compressive force,  $M$  is the measured bending moment, and  $M_c$  and  $F_c$  are the critical values for force and moment in the tibia.**

$$TI = \frac{F}{F_c} + \frac{M}{M_c} < 1$$

Axial force in the lower tibia is a good predictor of foot and ankle injuries [96, 207, 208]. Rotation of the foot can cause ankle ligament injuries and malleolar/talus fractures, but compressive axial forces can also be involved in these injuries. These injuries can be predicted with ankle joint bending moment [202]. Inversion and eversion of the foot has also been studied to predict ligament injuries and ankle bone fracture [202, 209].

#### 1.4.4 Thorax Injury

The thorax includes the ribs, sternum, clavicle, and the internal organs in the thoracic cavity, including the heart and lungs. A rib fracture can occur when any of the 24 ribs in the body become cracked or broken. A depression fracture in the ribs can also cause a hemothorax or pneumothorax in the pleural cavity or lung. Flail chest is a severe condition that occurs if a rib breaks and separates from the chest wall, which could cause pain and shortness of breath. A clavicle or sternum fracture is also possible.

Trauma can also cause many soft tissue injuries in the thorax. Contusions or lacerations involving major internal organs including the heart and lungs are possible. Injuries such as bilateral lung laceration, major aortic laceration, and major heart contusion are severe and potentially life threatening. High magnitude blunt impacts, such as those experienced in automotive crashes, can fracture the ribs and the sternum, rupture main arteries, and injure the walls of the heart. Because the tissues in the thorax are viscoelastic, the type of injury is related to loading rate [210].

##### 1.4.4.1 Thorax Injury Mechanisms

A major mechanism in the thorax injury is chest compression, which can fracture ribs and lead to a punctured lung or organ contusions. Compressive forces can be imparted on the chest by restraint systems and other blunt objects, such as a steering wheel. Chest compression in combination with a bending load can lead to wedge fractures. Pilots who eject from aircraft, and restrained occupants in severe frontal automobile crashes, often sustain wedge fractures [210].

##### 1.4.4.2 Thorax Injury Metrics

Neathery et al. report that a 50<sup>th</sup> percentile male would sustain an AIS 3 injury as a result of a chest compression of 76 mm [211]. Table 8 shows chest compression injury criteria of a 50<sup>th</sup> percentile male, based on data from frontal impacts.

**Table 8: Chest Compression Injury Criteria [210, 211].**

Chest Compression (%)	50 <sup>th</sup> percentile male chest compression (mm)	Abbreviated Injury Scale (AIS)
30	69	2
33	76	3
40	92	4

Another criterion for chest injury from frontal impacts is the viscous criterion (VC) (Equation 1010) [212].

**Equation 10: The Viscous Criterion (VC); where  $V$  is the chest wall velocity and  $C$  is the chest compression in percent of chest depth.**

$$\text{Viscous Criterion} = V * C$$

The VC and chest compression are both reasonable predictors of injury from lateral impacts [49, 213]. Based on data from tests conducted by Cavanaugh (1990), a VC higher than 1 m/s would result in thoracic injuries of AIS 4 or 5. The Thoracic Trauma Index was also developed as a chest injury criterion based on accelerations (Equation 1111) [214].

**Equation 11: The Thoracic Trauma Index (TTI); where  $T12_y$  is the peak T12 lateral spinal acceleration,  $Rib_y$  is the peak rib 4 acceleration,  $Mass$  is mass of the subject, and  $Mass_{50}$  is mass of a 50<sup>th</sup> percentile male [210, 214].**

$$TTI = 1.4 * Age + 0.5 * (T12_y + Rib_y) * Mass / Mass_{50}$$

### 1.4.5 Abdominal and Pelvic Injury

Trauma-induced organ damage is more common in some organs based on their location in the abdomen. The most commonly injured organs in blunt abdominal trauma are the spleen and liver [215].

Pelvic fractures can be severe, and potentially life-threatening injuries. Fractures involving the pelvic ring are typically serious because they can lead to hemorrhage, which increases mortality rates. If the presacral venous plexus blood vessel in the pelvis is ruptured it can cause extensive loss of blood [216]. Minor fractures require rest and medication.

#### 1.4.5.1 Abdominal and Pelvic Injury Mechanisms

Research has been conducted to assess abdominal injury from compressive or blunt impact forces. Abdominal injury from seatbelt loading has been investigated extensively. If a seatbelt is positioned improperly, a crash can cause the lap-belt to impart compressive forces in the abdomen, potentially harming internal organs and soft tissue [69, 217, 218]. Abdominal injury can also occur from blunt trauma/contact forces, such as during car crashes when the occupant contacts armrests, the steering wheel, or other interior surfaces of a vehicle [217].

Pelvic fractures are far more common in the elderly than in younger people. Pelvic fractures in young people are most likely to occur from severe falls or automotive accidents, whereas older patients can sustain fracture from a fall from standing height. Furthermore, falling has been identified as one of the most reported causes of pelvic fracture [219].



### 1.4.5.2 Abdominal and Pelvic Injury Metrics

Peak abdominal compression and rate of abdominal compression both contribute to risk of abdominal injury [220]; these injuries are often seen in car crashes if the occupant impacts the steering wheel. Compressive forces can induce hematoma and lacerations of abdominal organs, such as the liver and spleen. Also, deceleration forces can cause injury involving interaction between stable (e.g. bones) and moveable (e.g. organs) objects in the abdomen resulting in stretches or tears (e.g. the inertia of the kidneys can pull on the renal arteries) [221].

A combination of metrics can be used to predict acetabular fracture, including the location of the femoral head in relation to the hip. In addition, the magnitude and direction of forces to the acetabulum correlate with type and severity of injury [219]. Other pelvic injuries are the result of iliac wing forces and pelvic symphysis forces.

## 1.5 INJURY RISK ASSESSMENT METHODS

Three main categories of methods are used for assessing injury risk due to dynamic loads. The categories are humans, human surrogates, and numerical models. As seen in Figure 40, each category (indicated by color) has several possible methods of assessment. Regardless of the method chosen to assess injury, criteria must be defined to relate responses to injury risk.

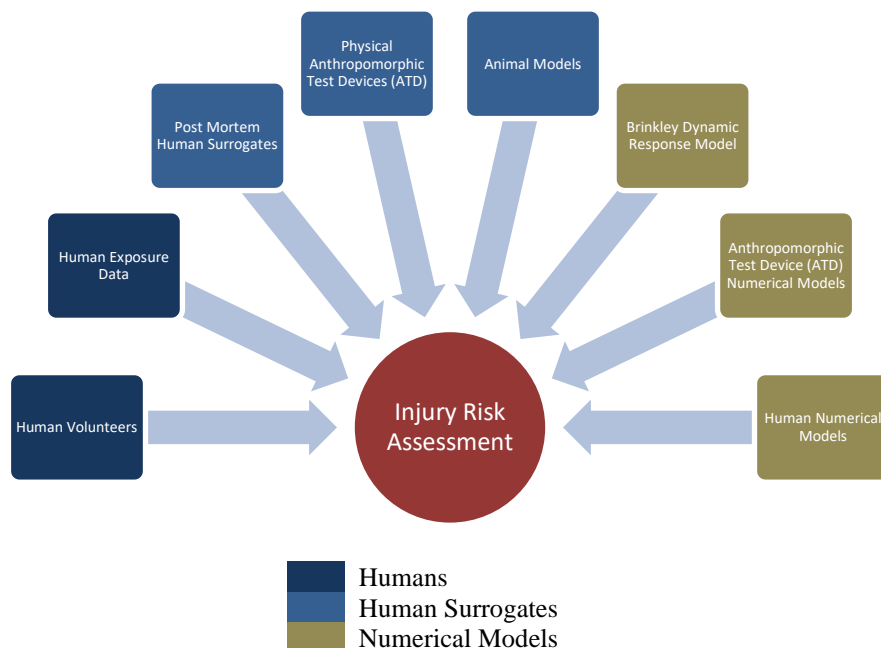


**Figure 40: Available Injury Assessment Methods.**

## **1.5.1 Humans**

### **1.5.1.1 Human Volunteers**

To understand injury tolerance levels for crewmembers, the obvious choice would be to test the crewmembers after the spaceflight mission when tolerance is lowest. However, injuring the crewmembers would be unreasonable. Tests of dynamic loads in healthy human volunteers would provide whole body human tolerance curves, but tests on humans must be limited to sub-injurious levels because it would be unethical to purposefully test for minor injury [222]. In addition, human volunteer testing is very time consuming and expensive, and testing facilities in the U.S., and expertise to conduct these studies, are limited.

### **1.5.1.2 Post Mortem Human Surrogates**

PMHS or cadavers are another option for assessing injury risk. Because PHMS are humans, their anatomy and anthropometries are human, and PMHS can be used to more accurately pinpoint the threshold at which a human injury would occur. Sensors can be imbedded into the body to directly measure forces, accelerations, and moments, and a post-test autopsy can be conducted. These data can be used to determine risk of injury to specific anatomical regions. PMHS are also a valuable tool to devise ATDs and computational models [222].

Although there are many advantages of using PMHS for testing dynamic loads, availability of PHMS are limited and subjects may not represent the age and fitness level of the astronaut corps. In addition, positioning of PMHS for testing can be difficult because PHMS do not have active muscles to maintain an upright posture in a seat. A lack of active muscle contractions, differences in tissue properties, and differences in tissue responses may affect the measured responses, thus affecting the assessment of injury risk for a live human. Finally, limited facilities are available to test PMHS, and equipment use is complicated (i.e., suits that cannot be reused after testing) [223].

### **1.5.1.3 Human Exposure Data**

Injury metrics can be obtained from humans who have inadvertently sustained injury during accidents. Some examples are automotive crash data, automotive racing impacts, and military aircraft mishaps. Although these types of events are undesirable, and every effort is made to prevent them, they still occur, and some are well documented.

Human exposure data can provide information that is unattainable in laboratory setting, such as intrinsic comparison (age, sex, anthropometrics) and multidirectional dynamic loads [99, 108, 109, 224, 225]. However, details of the incidents are critical to evaluate if the data is applicable to spaceflight conditions. For instance, neck injury can occur during an emergency ejections from an aircraft, but the loads to neck would likely be greater in these situations than neck loads induced during nominal spaceflight conditions [65], so this data would be useless for predicting risk for injury during spaceflight scenarios.

### 1.5.1.4 Injury Risk Curves

#### 1.5.1.4.1 Head Injury Risk Curves

Interest in populations that are susceptible to low-magnitude head impacts has increased because these subjects can be used to assess the effects of concussions. Funk and colleagues developed a risk curve for brain injury based on HIC and using on-field data from American Football (Figure 41) [160]. In addition, Rowson and Duma used data collected from collegiate football players to create a risk curve for concussion based on data for combined rotational and linear acceleration of the head (Figure 42 [171]).

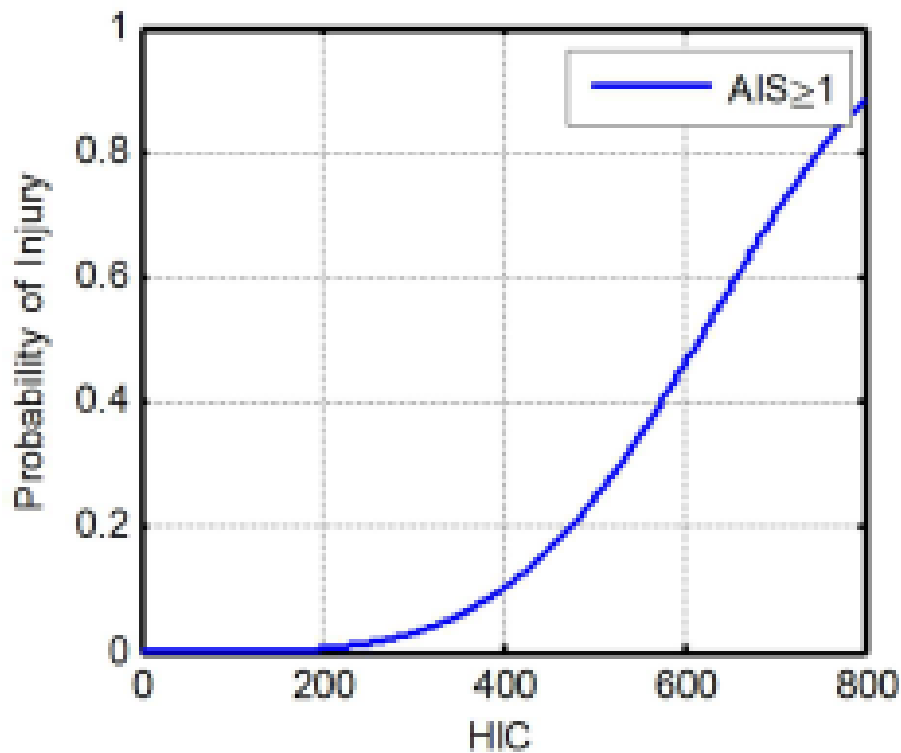


**Figure 41: Probability of Human Head Injury Based on Head Injury Criterion (HIC) [226].**

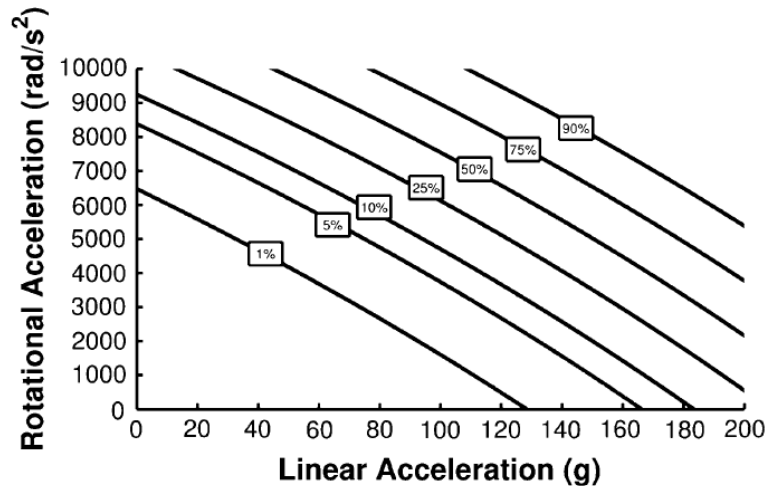


**Figure 42: Risk of Concussion Based on Combined Rotational and Linear Accelerations of the Head [171].**

#### 1.5.1.4.2 Neck Injury Risk Curves

Risk curves for neck injury that were generated using the shear force and sagittal bending moment derived from rear-impact tests on PMHS are shown in Figure 43. Both metrics are significant ( $P < .01$ ) injury predictors. The mean force of 233 N and mean moment of 50 Nm were associated with a 5% probability of injury, and a NCIS of 0.68 and 0.97, respectively. Critical intercepts at 90% risk for force and moment were 407 N and 126 Nm, respectively [195].

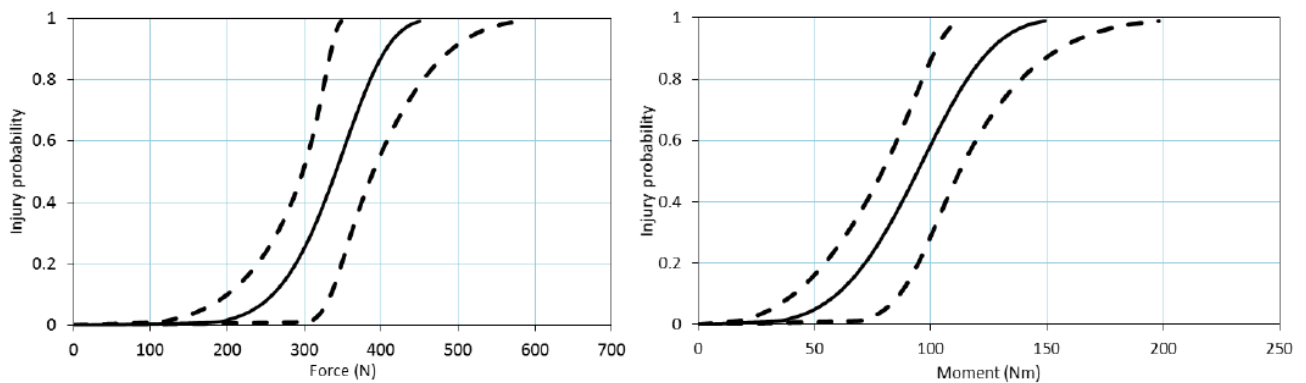


**Figure 43: Risk of Neck Injury From Force (left) and Moment (right) Derived using PMHS [195].**

The mean risk of  $LN_{ij}$  and the 95% CIs for the PMHS data in rear-impact tests referenced above are shown (Figure 44). The combined values for force and moment predicted injury. The mean  $LN_{ij}$  of 0.96 was associated with a 5% probability of injury. Figure 45 shows the probability of neck injury due to neck axial compression.

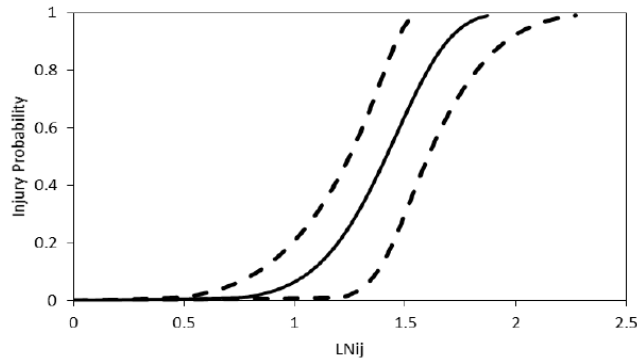


**Figure 44: Lower Neck Injury Criteria and Injury Probability Derived from Rear-Impact Tests on PMHS [195].**

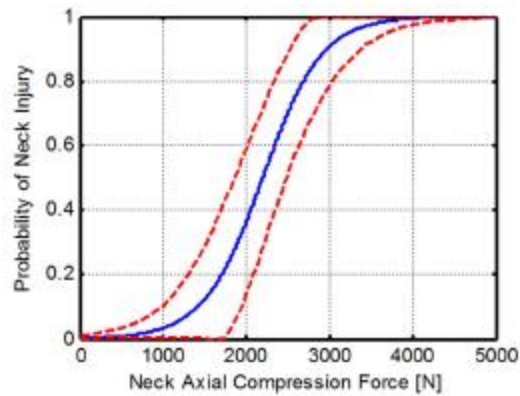


**Figure 45: Probability of Neck Injury due to Neck Axial Compression [227].**

#### 1.5.1.4.3 Thoracic Injury Risk Curves

Impact tests conducted with PMHS subjects were used to develop a curve representing the probability of chest injury based on sternal compression (Figure 46).

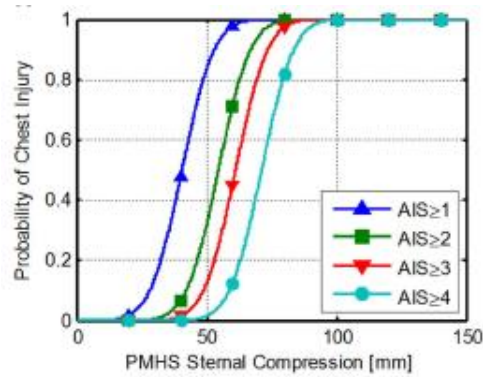


**Figure 46: Injury Risk Function for PMHS Sternal Compression [228].**

#### 1.5.1.4.4 Lumbar Spine Injury Risk Curves

Figure 47 shows the fracture probability curve in the thoracic spine region based on spine axial force, and the probability of fracture of thoracic and lumbar spine regions. These tests were conducted on spinal columns specimens from PMHS; on either the thoracic spine alone or thoracic and lumbar spine specimens. The curve shows a higher probability of fracture in the thoracic spine alone, indicating that the lumbar spine may be more tolerant to fracture than the lumbar spine.

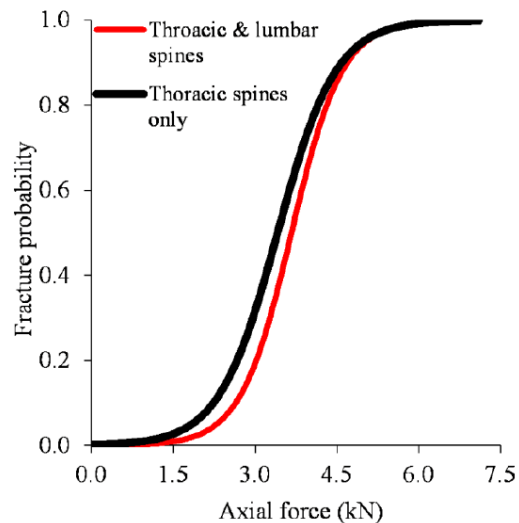


**Figure 47: Injury Probability as a Function of Axial Force to the Thoracic and Lumbar Spine Regions [197].**

#### 1.5.1.4.5 Lower Extremity Injury Risk Curves

The following risk curves for lower extremity injury were created using human exposure data from automotive crashes. Analyses indicated that femur axial force is a good predictor of injury to the knee, thigh, and/or hip (Figure 48) [202]. Figure 49 shows injury to the tibia as a function of tibia axial force. Figure 50 shows injury to the tibia as a function of tibia axial force and bending moment. Figure 51

shows foot and ankle injuries as a function of axial force in the lower tibia [96, 207, 208]. Malleolus and surrounding ligament injury can be predicted with foot dorsiflexion moment and inversion/eversion moment (Figure 52).

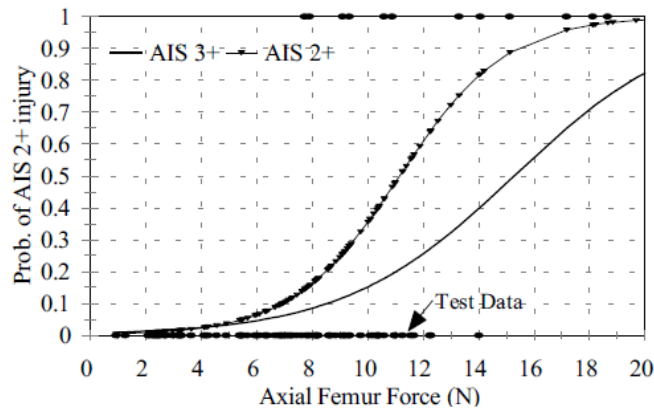


**Figure 48: Probability of AIS 2+ and 3+ Knee, Thigh, or Hip Injuries as a Function of Axial Femur Force [202].**

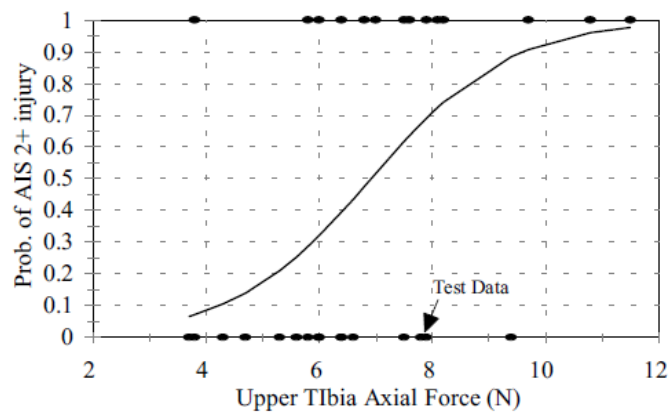


**Figure 49: Risk of AIS 2+ Tibial Plateau or Condyle Injury as a Function of Upper Tibia Axial Force for a 50th Percentile Male [202].**

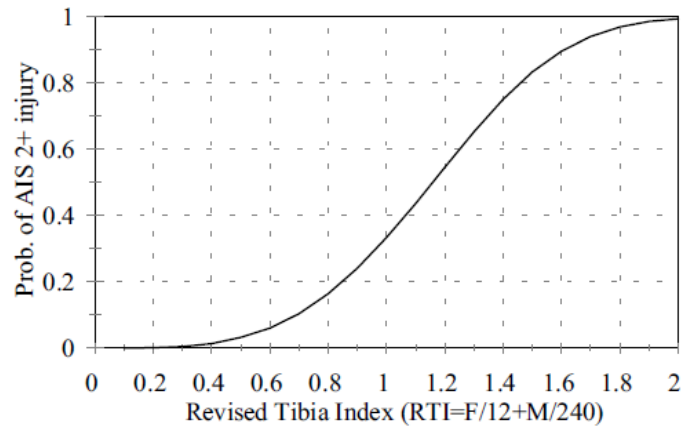


**Figure 50: Risk of AIS 2+ Injury as a Function of Revised Tibia Index [202].**

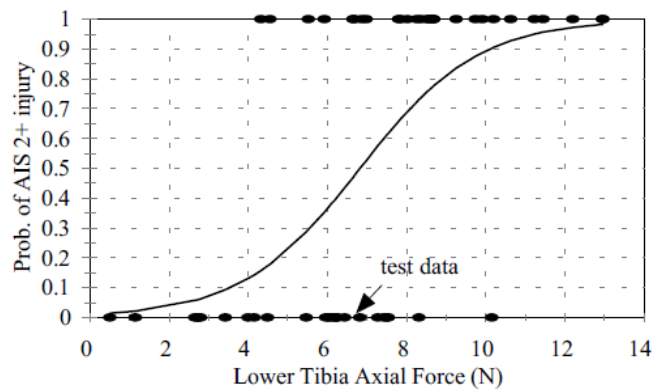


**Figure 51: Risk of AIS 2+ Injury in Calcaneus, Talus, Ankle, and Midfoot as a Function of Lower Tibia Axial Force [202].**

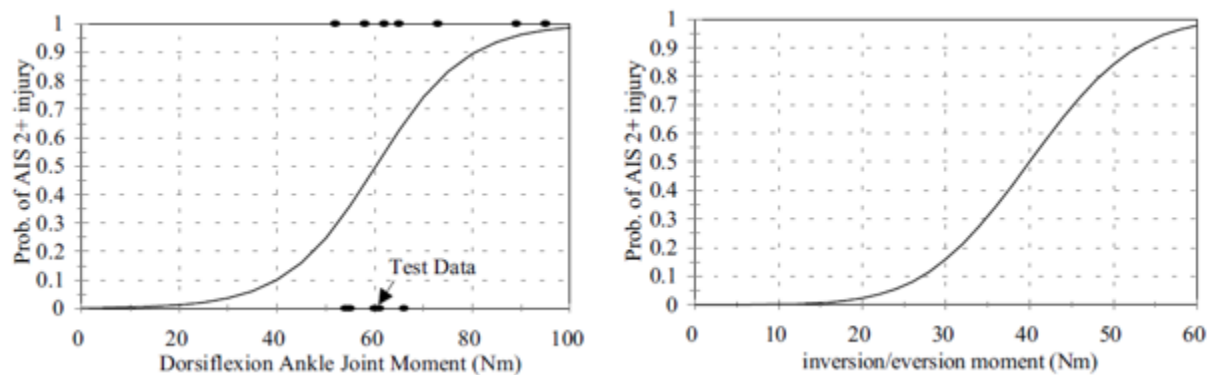


**Figure 52: AIS2+ Injury of Malleolus and Surrounding Ligaments as a Function of Foot Dorsiflexion Moment (left) Inversion/Eversion (right) [202].**



## 1.5.2 Human Surrogates

### 1.5.2.1 Physical ATDs

ATDs, also known as crash test dummies or manikins, have been used for decades to assess injury risk to humans during specific impact scenarios. Originally, ATDs were used to mitigate military aircraft injury, and are now commonly used to develop and verify safety measures for a variety of transportation systems. ATDs replicate human responses to particular impact situations and the ATD responses are highly repeatable, which is a significant advantage over previously discussed assessment methods, which are prone to significant inter-individual variability.

Some factors prevent the ATD from responding in the same manner as a human. First, ATDs are designed to withstand higher forces than a human so that they can be reused. In addition, many simplifications are necessary in the anatomy of the ATD to allow cost-effective design and construction. Because ATDs do not always respond as humans would, injury risk functions are used to relate the ATD responses to actual human injury, and this process is not optimized to detect minor injuries or human tolerance because an ATD cannot provide feedback regarding discomfort and pain. In addition, ATDs are not designed to predict the low injury risk that is relevant to spaceflight because they are designed to assess severe automobile crashes. The automotive industry is focused on preventing severe injuries during very low probability events. NASA vehicles, such as the Orion, involve a low risk of injury during dynamic phases of flight but the occupants will experience dynamic loading during every flight.

ATDs span a wide range of purposes, sizes, and applications. The automotive industry has a large variety of ATDs that are available to assess different impact directions and occupant sizes. Figure 53 shows a variety of different sized ATDs developed for different uses.

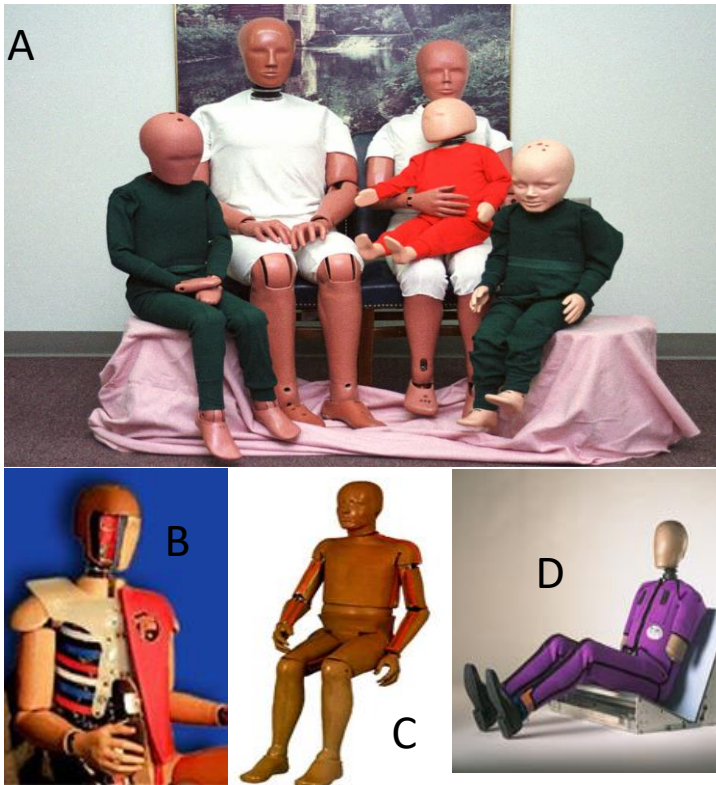


**Figure 53: Anthropomorphic Test Devices (ATD) A) Hybrid III Frontal Impact Family (L to R: 10-year-old, 50th percentile male adult, 5<sup>th</sup> percentile female adult, 3-year-old, 6-year-old), B) THOR 50<sup>th</sup> percentile Frontal Impact ATD, C) ADAM 95<sup>th</sup> percentile Military Vertical Impact ATD, and D) WorldSID 50<sup>th</sup> percentile Side Impact Dummy.**

#### *1.5.2.1.1 Hybrid III ATD*

The Hybrid III ATD was developed in the 1970s initially to test frontal automotive impacts and was designed to assess vehicle designs for safety without the use of seatbelts. It was later adapted for assessing the safety of airbag systems. The military has developed aerospace versions of the ATD for assessing the performance of ejection seats, and the FAA has created a version for assessing aircraft seats in crash scenarios.

#### *1.5.2.1.2 Automotive ATD*

The original ATD was a mid-size male version developed for the automotive industry. In the 1990s, the Centers for Disease Control sponsored development of a small female and large male version of the ATD by scaling the mid-size male [57]. Most of the data available for the Hybrid III has been collected using the mid-size male automotive version.

In addition to the actual ATDs, several FEMs exist of the ATDs that can be used to simulate impact conditions. These tools can be used to evaluate impact conditions that are not easily recreated in a test and can evaluate large numbers of impact cases, beyond what is feasible for testing.

#### *1.5.2.1.3 Aerospace and Military ATD*

The aerospace version of the ATD was developed to assess the risk of injury during ejection, particularly the initial +Z axis acceleration used to propel the seat and occupant from the aircraft. Recently, the USAF

has been using the aerospace Hybrid III ATD to assess the effects of the heavy, unbalanced helmet designs used in modern aircraft (night vision goggles, heads-up display, and other helmet mounted technologies that add to the mass of the helmet and move the CG of the helmet and head to a suboptimal position, increasing injury risk). Similar to the automotive versions, 3 adult sized Hybrid III ATD are used for aerospace tests: small female, mid-size male, and large male. In the 1990s, the military developed several additional sized ATDs to better capture the risk to a range of occupants as part of the Joint Primary Aircraft Training Systems (JPATS) program. A total of 7 difference sizes were specified (referred to as case 1-7) that included varied anthropometric measures to better reflect the range of anthropometries in the military flying population. The lightest occupant in service (LOIS) is the most used version of the JPATS ATDs and has a mass of 46.7 kg (103 lbs) including a 3.7 kg (8.1 lb) head.

The aerospace version of the ATD retains most of the same components as the automotive version including the head, neck, ribs, arms and legs, in addition to unique components: an articulating pelvis, a straight lumbar spine, and a reinforced chest [229].

There are no FEMs of aerospace ATDs.

#### *1.5.2.1.4 FAA Hybrid III ATD*

The FAA dummy (Figure 54) is the Hybrid III 50<sup>th</sup> Male ATD with modifications in the lower torso and legs that are necessary for the dummy to be valid for testing dynamic emergency landing conditions. The dummy is designed to be seated in an aircraft seat in the fuselage and belted in. Testing of the FAA dummy entails swinging and dropping the fuselage to simulate a crash landing. Instrumentation is included to measure the head injury criteria, spine vertical loading, and axial loads in the femurs. The FAA dummy is designed with a straight spine, in contrast to the slouch of the automotive dummy, and has a fixed pelvis.



***Figure 54: Federal Aviation Administration (FAA) Hybrid III 50th Male ATD.***

#### *1.5.2.1.5 Pedestrian ATD*

The first pedestrian dummy was developed in the 1970s to assess injury to pedestrians who are struck by vehicles; the present-day version is shown in Figure 55. Vehicle manufacturers use the data from tests to design vehicles that will mitigate injury to a pedestrian. The pedestrian ATD is a version of the automotive

Hybrid III ATD with modifications to the lower torso and knees, including modified knee joints that rotate, a straight spine instead of a curved one, a modified pelvis that allows the legs to rotate in a standing position, and modified ankle that allows the ATD to stand. The pedestrian dummies are able to stand on their own, with up to 80% of their weight on one leg and are made in the same sizes as the automotive Hybrid III ATDs: 5<sup>th</sup> percentile female, 50<sup>th</sup> percentile male, and 95<sup>th</sup> percentile male.



**Figure 55: Hybrid III 50th Percentile Male Pedestrian ATD.**

#### *1.5.2.1.6 Various Size ATDs*

Many different sized ATDs have been created to assess safety of all subjects. The aerospace industry and the military have the lightest version of the Hybrid III ATD in service (LOIS) and they have large anthropomorphic research dummy sizes, along with the 5<sup>th</sup> female, 50<sup>th</sup> male, and 95<sup>th</sup> male. Child ATDs have also been created: the Hybrid III 3-year, 6 year, and 10-year-old.

Many FEMs of ATDs are also available to better evaluate risk of injury. The Hybrid III 5<sup>th</sup>, 50<sup>th</sup>, 95<sup>th</sup>, and the 50<sup>th</sup> FAA Hybrid III all have FEMs available. Child FEMs are also available for the Hybrid III 3-year, 6 year, and 10-year-old.

#### *1.5.2.1.7 Spaceflight Application ATDs*

The Hybrid III manikin is not validated for dynamic multi-axial impacts, nor is it designed to predict injury risk in loading conditions outside of purely frontal impact (eyeballs out) or spinal impacts (eyeballs down). The Orion landings will produce primarily rear and spinal direction loading, although landing conditions, particularly when vehicle roll is prevalent, could produce a multi-axial (including lateral impact loading) impact loading, which the ATD is not validated to assess. The occupant protection standards currently specify the use of the Hybrid III ATD as a supplement to the BDRC for risk of injury to the head and neck. In this limited application, the Hybrid III is validated for limited off axis loading of the head and neck, so it can be used to predict injury risk, but these predictions may be inaccurate. The current crewed spacecraft is certified by analysis using FEMs of the Hybrid III ATD of various anthropometric sizes [226].

Additional research is needed to further characterize Hybrid III ATD injury metrics for spaceflight loading conditions. Current studies are evaluating new injury risk functions for the Hybrid III for the low probability of minor injuries that could occur during spaceflight.

#### 1.5.2.1.8 Injury Assessment Reference Values (IARVs)

To correlate ATD response to acceptable injury risk to humans, IARVs were defined for all 3 sizes of the Hybrid III ATD (Table 9, Table 10, Table 11). These values represent metrics for the allowable limits of injury during dynamic events in spaceflight for both nominal and off-nominal cases, and for both conditioned and deconditioned crewmembers.

**Table 9. IARVs for the 5th percentile female Hybrid III ATD.**

	Conditioned		Deconditioned	
	Nominal	Off-nominal	Nominal	Off-nominal
HIC15	375	525	375	525
Head rotational acceleration (rad/s <sup>2</sup> )	2500	4200	2500	4200
Neck injury criteria	0.5	0.5	0.4	0.4
Neck axial tensile force (N)	4287	4287	4287	4287
Neck axial compression force (N)	3880	3880	3880	3880
VC (mm)	187	187	187	187
Lumbar axial compressive loads (N)	3500	4200	3000	3600
Extremity flail (N)	490	490	490	490

**Table 10. IARVs for the 50th percentile male Hybrid III ATD.**

	Conditioned		Deconditioned	
	Nominal	Off-nominal	Nominal	Off-nominal
HIC15	340	470	340	470
Head rotational acceleration (rad/s <sup>2</sup> )	2200	3800	2200	3800
Neck injury criteria	0.5	0.5	0.4	0.4
Neck axial tensile force (N)	6806	6806	6806	6806
Neck axial compression force (N)	6160	6160	6160	6160
VC (mm)	229	229	229	229
Lumbar axial compressive loads (N)	5300	4600	6200	5300
Extremity flail (N)	780	780	780	780

**Table 11. IARVs for the 95th percentile male Hybrid III ATD.**

	Conditioned		Deconditioned	
	Nominal	Off-nominal	Nominal	Off-nominal
HIC15	325	450	352	450
Head rotational acceleration (rad/s <sup>2</sup> )	2100	3600	2100	3600
Neck injury criteria	0.5	0.5	0.4	0.4
Neck axial tensile force (N)	8216	8216	8216	8216
Neck axial compression force (N)	7440	7440	7440	7440

VC (mm)	254	254	254	254
Lumbar axial compressive loads (N)	5800	6500	5000	5600
Extremity flail (N)	980	980	980	980

#### 1.5.2.1.9 THOR ATD

The test device for human occupant restraint (THOR), shown in Figure 56, is a frontal impact dummy developed in 1995 and modelled after the 50<sup>th</sup> percentile adult male. The THOR ATD includes more biofidelic features and instrumentation than the original Hybrid III ATD. In 2010, the next version, THOR-K, was developed by the Society for Automotive Engineers (SAE), and further enhancements led to the THOR-50M in 2011. The THOR-50M has improved biofidelity: occipital condyle and muscle representation in the neck, thorax and shoulder improvements to assess interaction with restraints, enhanced joints in the spine and pelvis, and improved axial load response in the femur. A THOR-5F was also developed to represent a 5<sup>th</sup> percentile female. Humanetics Innovative Solutions offers FEMs of both the THOR-50M and the THOR-5F.



**Figure 56: THOR-50M.**

NASA and AFRL recently completed a collaborative evaluation of the THOR-K version of the impact test manikin for use in developing advanced occupant seating systems [230, 231]. The biodynamic response of the THOR-K spine to restraint harness loading was measured for various impact orientations and loading conditions. The data for select test configurations were compared to the response of the Hybrid III 50th aerospace manikin. Testing was conducted in 3 impact orientations: +z-axis, +y-axis, and -x-axis, and with input accelerations at various impact G levels that ranged from 8 to 20 G. Testing also determined the frequency response of the THOR-K manikin by varying the time-to-peak G of the applied input acceleration from 30 ms to 100 ms. In general, the THOR-K provided good linear response across the various test conditions out to a 20 G input acceleration for the measured test parameters evaluated. The maximum THOR-K response was recorded at the 30 ms time-to-peak input condition. The THOR-K responded in a similar fashion to the Hybrid III manikin in terms of peak values; however, the head and

neck responses were consistently lower in the THOR-k regardless of peak input acceleration or the input acceleration's time-to-peak value.

#### 1.5.2.1.10 THOR Injury Assessment Reference Values (IARVs)

The following table of IARVs for use with the THOR ATD were proposed by Somers et al. [232] for use in regard to spaceflight (Table 12).

**Table 12: Proposed THOR IARVs [232].**

	Conditioned		Deconditioned		IARV confidence level (0-5)
	Nominal	Off-nominal	Nominal	Off-nominal	
HIC15	340	470	340	470	4
BrIC	0.04	0.07	0.04	0.07	2
Neck axial tension force (N)	880	1000	760	860	2
Neck axial compression force (N)	580	1100	500	950	3
Max chest deflection (mm)	25	32	25	32	2
Lateral shoulder force (N)	2700	3300	2700	3300	4
Acetabular resultant force (N)	1600	2900	1200	2200	3
Thoracic spine axial compression force(N)	5800	6500	5000	5600	3
Ankle dorsiflexion moment (Nm)	18	31	14	23	3
Ankle inversion/eversion moment (Nm)	17	22	13	17	3
Average distal forearm speed (m/s)	8.1	10	801	10	3

#### 1.5.2.1.11 EuroSID ATD

The European side impact dummy (EuroSID) is a side-impact dummy developed in Europe in the 1980's. This dummy is used in regulatory testing in Europe. Two more versions of this dummy now exist, the ES-2 and the ES-2re (rib extensions). The addition of the ES-2re to testing specified in the U.S. Federal Code of Regulation is being considered. The ES-2re is modeled after a 50<sup>th</sup> percentile male, with the lower arms removed, and incorporates rear rib extension brackets to more accurately analyze interactions with a seatback.

The EuroSID dummy can be used to evaluate the sideward impact forces occurring at the crewmembers' shoulder and hip while seated. However, although a side impact dummy such as the EuroSID is useful for assessing pure lateral loading, the Orion produces multi-axial loading and the EuroSID would not be amenable for use in the finite element modeling approach described above (simulating multi-axial loading). In addition, the slouched posture of the EuroSID precludes using it in spaceflight seats [233].

#### *1.5.2.1.12 WorldSID ATD*

The worldwide harmonized side impact dummy (WorldSID) was also created to assess lateral impacts (Figure 57). The International Organization of Standardization (ISO), automotive manufacturers, and government organizations, in coordination with the International Harmonized Research Activity collaborated with the goal of creating a dummy that was acceptable all over the world or assessing the effects of side impacts. Anthropometries were chosen to reflect the world population of vehicle occupants. The WorldSID was designed to be tested in a seated posture. Instrumentation allows injury and restraint systems to be assessed ([worldsid.org](http://worldsid.org)). As with the EuroSID, this ATD does not fit properly in spaceflight seats because of its slouched posture.



***Figure 57: The Worldwide Harmonized Side Impact Dummy (WorldSID) ([humaneticsatd.com](http://humaneticsatd.com)).***

#### *1.5.2.1.13 BioRID ATD*

The BioRID was designed as a rear impact dummy to evaluate seat restraints (Figure 58). It has a unique vertebral column of 24 individual vertebra made of torsion washers, urethane bumpers, and muscle-simulating springs to increase biofidelity [234]. The BioRID has seen very little use, is not readily available for use, and insufficient data is available to develop appropriate injury risk functions.





*Figure 58: BioRID-II (humaneticsatd.com).*

### 1.5.3 Animal Models

Animal models have been used extensively in the past and have several advantages and limitations. Clearly, animals offer the unique advantage of studying the response of living tissue. In some cases, a combination of surrogates are required to determine countermeasures. Although PHMS data may be used to determine brain motion and deformation, PHMS do not provide information on live physiological response such as minor traumatic brain injury, which takes time to develop after impact [222]. Animal test data may be further used to develop mathematical models specific to research needs. Because animals are not anthropometrically similar to humans, only trends may be identified relative to human response [235].

### 1.5.4 Numerical Models

#### 1.5.4.1 Brinkley Dynamic Response Model

The acceleration of a reference point in the chest of a harnessed crewmember due to dynamic loading is referred to as the DR. This was initially used to predict injury during the +z loading experienced during ejection from an aircraft. Human volunteers were used to predict the DR due to +z loading (referred to as DRz) and predict injury due to this DR (referred to as the DRI). This same approach was later applied in all three axes, and referred to as the BDRM. The BDRM was developed to define the human DR and risk of injury during multi-axial impacts. The BDRM is a set of 3 simple, lumped parameter, single degree of freedom models, which are intended to predict the whole body response to acceleration as shown in **Error! Reference source not found.** The response of the body is calculated using the input of acceleration at the seat [54].

Once the DR on each axis is calculated, the BDRM is used to calculate  $\beta_{max}$ , which predicts approximate injury risk, as shown in Table 13 for each risk level.

Because the BDRM is a simple, lumped-parameter, single degree of freedom model, it only predicts the range of injury risk for any injury, and cannot provide information as to the severity or anatomical location of an injury.

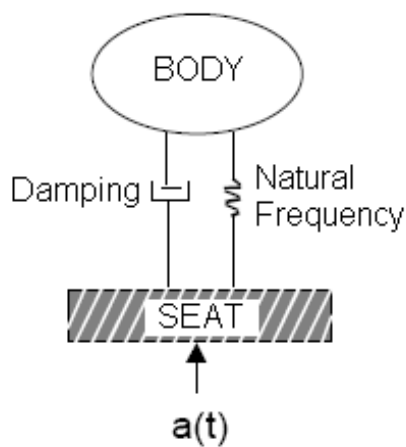


**Figure 59: Lumped Mass Diagram of the Brinkley Dynamic Response Criteria Model.**

**Table 13: Approximate Injury Risk.**

Risk Level	Approximate Risk
Low	0.5%
Moderate	5%
High	50%

A second limitation stems from the assumption that the spine is in alignment with the acceleration vector  $G_z$ . If the spine is  $5^\circ$  out of alignment relative to the load vector, the risk of injury increases dramatically. This was determined operationally on the F-4 ejection seat: when the spine was misaligned it resulted in a 34% rate of injury (the BDRC predicted a 5% risk of injury) [52, 54].

The BDRC for +Z axis acceleration is anchored on operational ejection data based on injuries sustained in the thoracolumbar spine; however, no statistically based methods were used to assign BDRC injury levels for the other axes ( $\pm X$ ,  $\pm Y$ , and  $-Z$ ) [54, 236]. Mr. Brinkley has also expressed concern regarding the Y-axis model and warns that the Y-axis model for unsupported lateral loads is not correct [237]. Because the BDRM was developed based on simple acceleration profiles, it may not be appropriate to use this model alone to assess the complex loads expected for the Multi-Purpose Crewed Vehicle (Orion) and other future spacecraft.

Brinkley [236] expected that different dynamic models/model parameters would be necessary for changes in the seat and restraint configuration. The BDRM was developed with minimal gaps between the supporting seat surfaces and the test subjects. Additional gaps can allow increased contact forces and increased risk of injury. Because the model treats the whole body as a lumped mass, the seat geometry and restraints used during the test data collection are critical to achieve the same injury risk prediction. The implications of these limitations are twofold. First, the BDRM does not account for the significant improvement in restraint systems over the last 25 years. The consequence is either an overly conservative design, or a design that is not as protective as possible, because no seat design improvements are reflected in the BDRM results. This consequence was shown operationally when the Royal Air Force rates

of injury during airplane ejection were not predicted by the DRI [225, 238]. In addition, with the seat and restraint system the BDRM has no way of accounting for the current spacesuit and helmet donned by the crew. The original BDRM was developed with minimal head supported mass (helmets which weighed less than 5 pounds). Additional helmeted mass (which is probable given NASA's current designs) may cause the natural frequency and damping parameters of the human to change, invalidating the model. In addition, increased head supported mass poses a real risk to the neck due to compressive loading during +Z accelerations, which are not accounted for in the BDRM [84]. Furthermore, rigid elements on the suit must be accounted for in the model to accurately predict injury. Suit testing performed by NASA at Ohio State University found that poorly placed suit elements drastically increase the risk of injury, which the BDR model did not predict [82].

Finally, the BDRM also lacks fidelity regarding variation in sex, anthropometrics, and age. The BDRM represents the response of young, healthy military personnel, which is not representative of the astronaut corps, and does not factor in the microgravity-induced physiological deconditioning status of the crew's health. A detailed evaluation of the model is documented in Somers, et al 2013 [39] .

#### **1.5.4.2 ATD Numerical Models**

As discussed previously, ATDs have several advantages and disadvantages, as do numerical models of ATDs. Numerical models allow tests of various configurations, loads, and responses that are not easily tested with the physical ATD. Thus, numerical models of ATDs offer the advantage of simulating complex testing and assessing hardware without the need to fabricate prototypes. However, numerical models of ATDs are sensitive to initial conditions such as the initial position of the ATD in the seat, initial tension in the restraints, friction coefficients between the seat and ATD, pre-deformation of the ATD into the seat, and gaps between the ATD body regions and seating surfaces. Studies are needed to understand how sensitive the responses are to these variations in these initial conditions

Several popular numerical solvers are currently available. The majority of solvers are Finite Element solvers, and popular software packages include LS-DYNA®, RADIOSS®, and PAM-CRASH®. Each solver has different behavior, but with some work, FEMs can be ported between environments. Within these environments, FEMs of various ATDs are available with varying degrees of fidelity and performance. Mathematical DYnamic MOdel (MADYMO®) is another solver that uses ellipsoid representations of physical structures to estimate responses. In addition, MADYMO offers the ability to interface with FEMs, which allows co-simulation with more complex structures. A range of models for many different ATDs are available within MADYMO. Several popular ATD numerical models are shown in Figure 60.

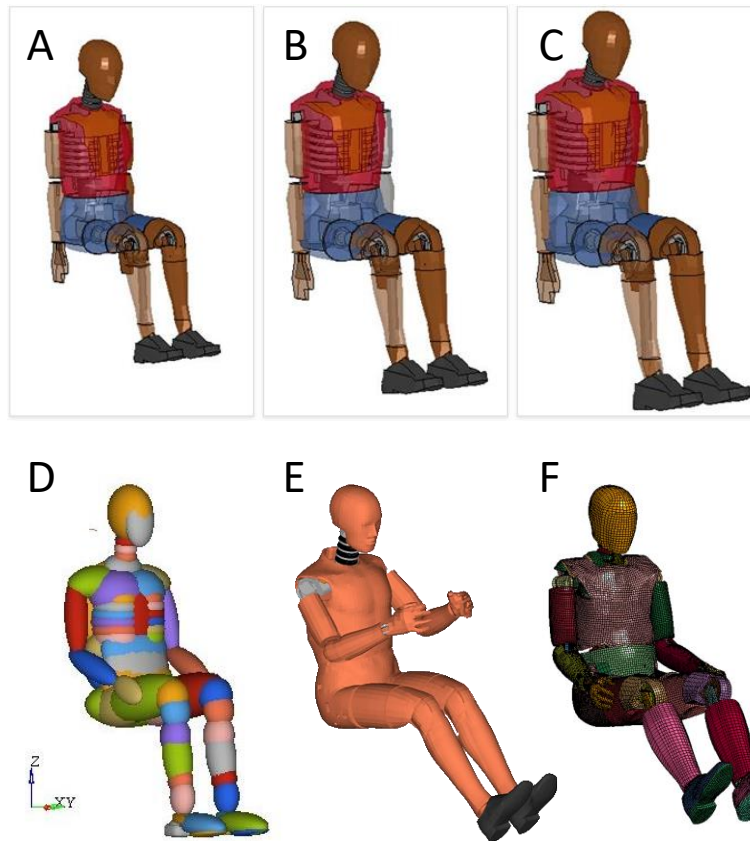


**Figure 60: Various Anthropomorphic Test Device (ATD) Models. Shown are A) Livermore Software Technology Corporation (LSTC) Hybrid III 5th percentile female LS-DYNA FE model, B) LSTC Hybrid III 50th percentile male LS-DYNA FE model, C) LSTC Hybrid III 95th percentile male LS-DYNA FE model, D) MADYMO Hybrid III 50th percentile male ellipsoid model, E) Humanetics Hybrid III 50th percentile male LS-DYNA FE model, and F) National Highway Traffic Safety Administration (NHTSA) THOR-NT 50th percentile male LS-DYNA FE model.**

#### 1.5.4.3 Hybrid III ATD FEM

The response of the Hybrid III FEM (Figure 61: Hybrid III ATD Finite Element Model.) has been validated using tests of matched physical ATD, and model predictions are highly correlated with ATD responses. When the variance of the model sensitivity and response was evaluated, it was determined that the loading condition variables for each region were generally more predictive of injury metric outcome than the environmental variables were. Loading condition parameters included acceleration pulse shape, relative magnitude, and peak resultant acceleration. Environmental variables included belt forces, seat orientation with respect to gravity at impact time, and initial positioning on the model with respect to the seat vertex [37].



**Figure 61: Hybrid III ATD Finite Element Model.**

In additional testing, the response of the Hybrid III head and neck were isolated for the 50<sup>th</sup> percentile male, 5<sup>th</sup> percentile female, and 95<sup>th</sup> percentile male, and the physical response was compared to the Hybrid III ATD model of each respective size. The response of the Livermore Software Technology Corporation (LSTC) FEM for the 50<sup>th</sup> and 5<sup>th</sup> Hybrid III ATD correlated well with the response of their respective physical counterparts, however, the FEM of the 95<sup>th</sup> percentile male did not correlate well with the physical ATD.

The geometry of the neck in the large male ATD FEM was updated to match the actual ATD. The geometry of each part was resized in the FEM, spacer parts were added to match the neck parts used in the ATD, and mass was added to the FEM head-form to match the ATD design specifications. Geometry of the updated head and neck FEM was verified against measurements taken on the actual ATD. After updating the FEM geometry and mass, a material calibration was performed to improve the FEM prediction of the physical ATD test data. Three optimizations were performed to calibrate the parameters used to define the shear modulus of the neck puck material in the FEM. After calibration, the updated head and neck FEM was assessed against head and neck test data through qualitative evaluation and the quantitative curve correlation metrics. The updated large male head and neck FEM closely predicted the response of the physical ATD in all test conditions evaluated. Significant improvement was shown, as quantified using the ISO/TR 16250 Road Vehicles—Objective Rating Metrics for Dynamic Systems curve rating system [38].

#### **1.5.4.4 THOR ATD FEM**

The THOR ATD FEM (Figure 62) was also evaluated against responses in actual THOR ATD. The model was highly correlated with physical response of the THOR ATD, however responses to acceleration in +X-direction were not evaluated. It also showed more sensitivity to loading condition variables and less to environmental variables (seat and restraints) [37].



**Figure 62: THOR ATD Finite Element Model.**

The responses of the calibrated THOR FEM were very similar to the response of the THOR ATD during all validation tests. In addition, the THOR FEM showed good agreement to human-volunteer data under spinal loading, but limited biofidelity under frontal loading. This may suggest a need for further improvements in both the THOR ATD and FEM [239].

#### **1.5.4.5 Other FEM ATDs**

Several other ATD models have associated FEMs; however, they have not been assessed for use in spaceflight loading conditions because of the constraints of their corresponding physical ATDs.

### **1.5.5 Human Numerical Models**

#### **1.5.5.1 Total Human Model for Safety (THUMS®)**

THUMS® is a group of FEMs developed by Toyota, as shown in Figure 63, which represent a total human including a biofidelic skeleton, muscle and ligament tissues, and internal organs. Currently, several models of interest for spaceflight applications exist including an American mid-sized (50<sup>th</sup> percentile) male, an American small (5<sup>th</sup> percentile) female, and an American large (95<sup>th</sup> percentile) male.

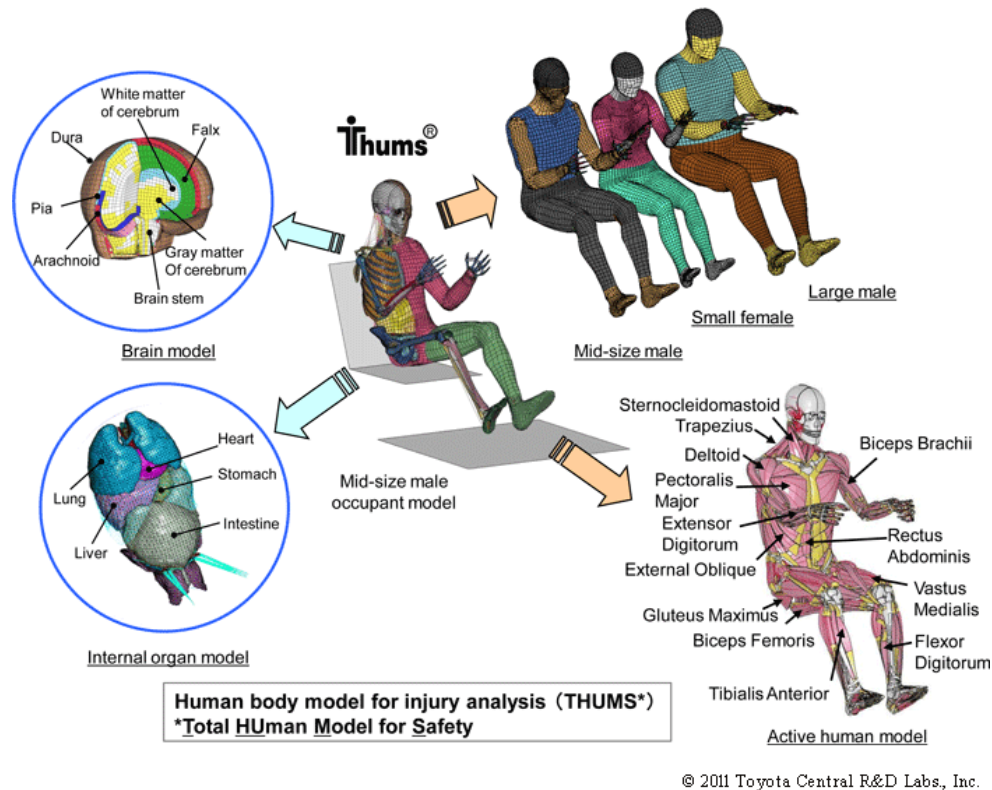


**Figure 63: THUMS Model [240].**

### 1.5.5.2 Global Human Body Model Consortium (GHBMC)

The Global Human Body Model Consortium (GHBMC) is a consortium of auto makers, suppliers, universities, and governments that are collaborating to create a single human body model for advancing crash research technology. In 2011, the GHBMC released a 50<sup>th</sup> percentile male model and has since developed a 5<sup>th</sup> percentile female and 95<sup>th</sup> percentile male model in the pedestrian and occupant configurations. The models include detailed anatomical features as shown in Figure 64.

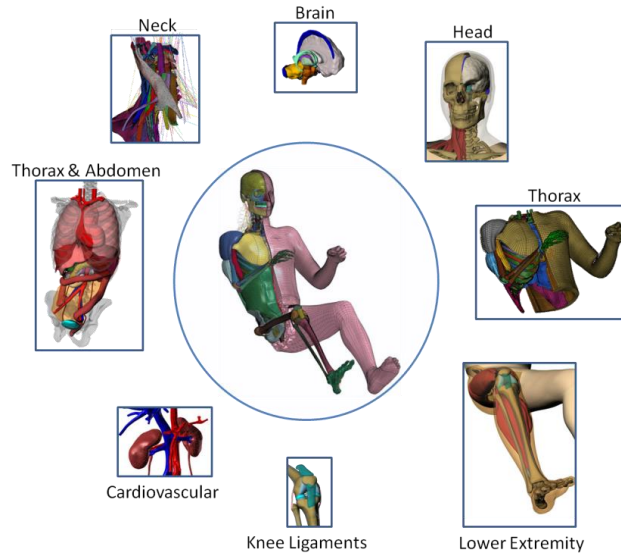


**Figure 64: GHBM Human Model.**

The GHBM model was validated using human volunteer impact data, and model predictions were highly correlated with human responses to accelerations in the +Z-direction. However, the GHBM model did not correspond well with human responses to impacts on other axes accelerations, possibly because the human volunteers braced before the impact. When the GHBM predictions were compared to the predictions from other models; in some regions, including the neck, lumbar spine, and lower extremities, the GHBM predictions more closely resembled those of the THOR; however, in the head, thorax, and pelvis, the results of the GHBM were closer to those of the Hybrid III [37].

The predictions of the GHBM simplified 50<sup>th</sup> percentile male occupant was compared to responses of human volunteers tested in forward, rearward, lateral, and vertical orientations. Overall, the model closely replicated the results of the experimental tests. More specifically, the head and neck responses of the model are highly biofidelic [241].

### **1.5.5.3 ESI Human Model**

Pacific Engineering Systems International (ESI) has a line of 4 human models of a 50<sup>th</sup> percentile American male, each representing varying levels of fidelity (Figure 65). The AM50a model has rigid body segments and articulated joints. The AM50s has deformable ribs, simplified organs, and flesh, and it is available in both sitting and standing postures. The AM50d, which is still under development, will be a full deformable human model with modular segments.



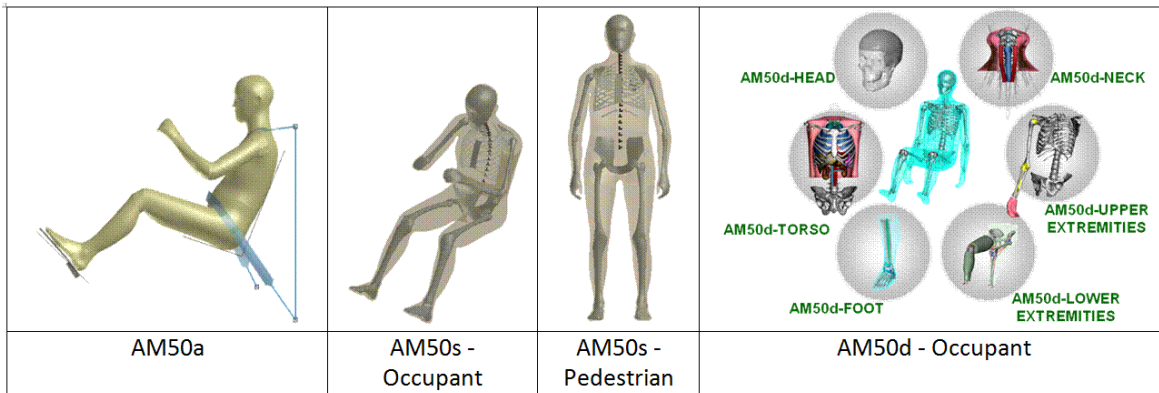


**Figure 65: ESI Human Models.**

#### 1.5.5.4 MADYMO Human Model

MADYMO human models (Figure 66) are available with active muscle control (in the 50<sup>th</sup> percentile male model) and with passive musculature (5<sup>th</sup> percentile female, 50<sup>th</sup> percentile male, and 95<sup>th</sup> percentile male).

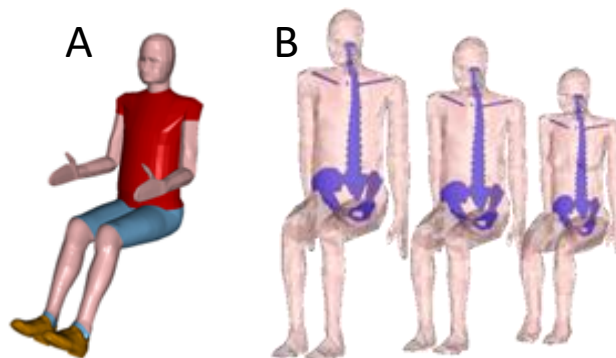


**Figure 66: MADYMO Human Models. A) Active muscle control 50<sup>th</sup> percentile human model B) Passive muscle control 5<sup>th</sup>, 50<sup>th</sup> and 95<sup>th</sup> percentile human models.**

#### 1.5.5.5 Advantages and Limitations

Computational models of humans are a developing field of research that offers great potential for addressing many of the limitations of other methods used to assess the impacts of dynamic loads. Human models can be developed to simulate a variety of intrinsic factors, i.e., they can be developed, through material property modifications, to account for differences in anthropometric measures, sex, and age, and possibly even spaceflight-induced physiological deconditioning in the future. In addition, human models can have realistic soft tissue, internal organs, and the skeletal system, allowing detailed investigations of injury potential to these areas. Because they are anatomically and anthropometrically

correct, these models can be positioned just as a human would be positioned in a restraint system. Finally, unlike human volunteers, human models can be subjected to injurious conditions, and can even be used to simulate tissue failures (e.g., bone fractures).

Although human models may one day eliminate the need for other methods of assessment, currently, the technical readiness level is low. Current human models are being developed to assess automobile impacts and are not validated for assessing dynamic multi-axial impacts. In addition, human volunteer, PMHS, and animal data are needed to inform the accurate simulation of these models. Much more data is needed before these human models can be used to accurately predict injury.

### **1.5.6 Summary**

Human testing provides quantitative values in parallel with perception of tolerance for actual human exposure, but testing can only be conducted at sub-injurious levels. PMHS do not provide perception of tolerance but can provide direct measures of tissue responses during dynamic loading. Human surrogates and numerical models can provide valuable information concerning risk of injury due to dynamic loading.

Human surrogates predict injury risk based on correlated human responses. ATDs, for instance, can provide mechanical measures during different loading conditions, but they lack the physiological and biofidelic responses of a human. One limitation of ATDs is the lack of local injury prediction from point loads or blunt trauma during impact. Animal models provide valuable data on physiological trends in different testing configurations, but results must be scaled to represent human response.

Numerical models are developed using data derived from tests of humans and human surrogates, therefore, these models are only as accurate as the data that was used to develop the model. Models vary in their level of fidelity (anatomy, physiologic response, direct observation of injury) and technology readiness level (TRL). Some better validated models have a high TRL, whereas models with lower TRLs are not as well validated and may not accurately represent human responses in all conditions. In addition, models with higher fidelity can be used to predict injury risk from more factors. Technological advances in computational simulation software and testing instrumentation are used to develop high-fidelity transfer functions that further enhance these models. Because each method for assessing injury has distinct limitations (Table 14), a combination of models may be required to assess injury risk to crewmembers.

Finally, injury criteria must be validated for the desired level of injury risk and severity. Only IARVs or tolerance limits validated to the injury risk level defined are useful for assessing injury risk.

**Table 14: Relative Strengths and Weaknesses of Each Injury Assessment Method [223]<sup>1</sup>.**

	Humans			Human Surrogates		Numerical Models		
	Human Volunteers	PMHS	Human Exposure	ATD <sup>2</sup>	Animal	Brinkley Dynamic Response Model	ATD <sup>2</sup> Numerical Model	Human Numerical Models
<b>Extrinsic Injury Risk Factors</b>								
Vehicle Dynamic Profile	Yes	Yes	No <sup>3</sup>	Yes	Yes	Yes	Yes	Yes
Seat & Restraints	Yes	Yes	No <sup>3</sup>	Yes	No	No <sup>4</sup>	Yes	Yes
Suit & Helmet	Yes	Yes	No <sup>3</sup>	No <sup>5</sup>	Partial	No <sup>4</sup>	Yes	Yes
<b>Intrinsic Injury Risk Factors</b>								
Age	Yes	No <sup>6</sup>	No <sup>3</sup>	No	No	No	No	Possible <sup>7</sup>
Sex	Yes	Yes	No <sup>3</sup>	No	No	No	No	Yes
Anthropometry	Yes	Yes	No <sup>3</sup>	Yes	No	No	Yes	Yes
Spaceflight Deconditioning	No	Possible <sup>8</sup>	No	No	Yes	No	No	Possible <sup>7</sup>
<b>Other Considerations</b>								
Anatomy	Yes	Yes	Yes	Partial	No	No	Partial	Yes
Physiologic Response	Yes	No	Yes	No	Yes	No	No	Yes
Injurious Testing	No <sup>3</sup>	Yes	Yes <sup>3</sup>	Yes	Yes	Yes	Yes	Yes
Direct Observation of Injury	No	Yes	Yes	No	Yes	No	No	No
Technology Readiness Level <sup>9</sup>	High	High	High	High	High	High	Moderate <sup>9</sup>	Low

<sup>1</sup>Adapted from Crandall, et al. [223]

<sup>2</sup>Anthropomorphic Test Devices

<sup>3</sup>Not possible prospectively

<sup>4</sup>The Brinkley Dynamic Response Model was validated using specific seat and restraint setups and dynamics. The model may not predict injury accurately when extrapolating beyond this setup and dynamics.

<sup>5</sup>Not possible to assess localized injury potential

<sup>6</sup>Although possible prospectively, very difficult in practice due to limited subject pools

<sup>7</sup>Currently Available Human numerical models do not specifically address these factors, but could be modified to simulate the increased risk of injury

<sup>8</sup>Selection criteria could be used to select only subjects with similar bone mineral density (BMD), although this is not a true representation of spaceflight deconditioning.

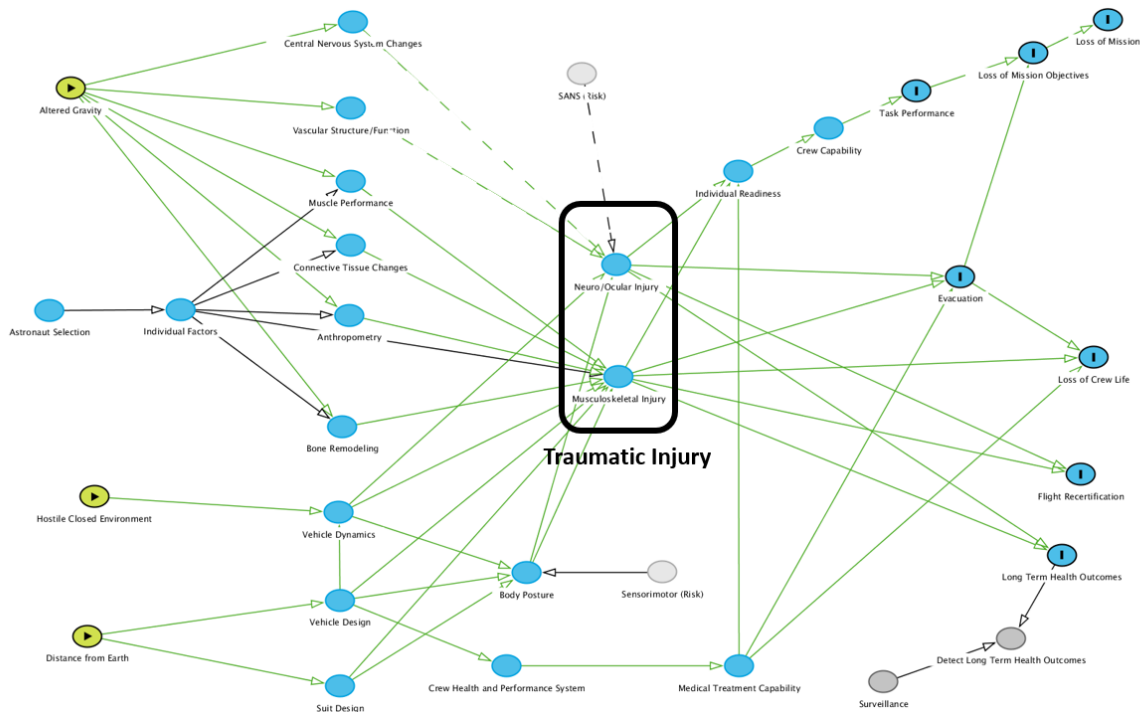
<sup>9</sup>Technology Readiness Level (TRL) is a measure of how ready each method is for immediate use. ATD models are at various levels of TRL depending on the solver, ATD family and size

## 2.0 RISK IN CONTEXT OF EXPLORATION MISSION AND OPERATIONS

Only one intrinsic factor will be affected during exploration missions—spaceflight-induced physiological deconditioning. Spaceflight-induced physiological deconditioning is related to amount of time in reduced gravity environments, thus without appropriate countermeasures, the risk of injury due to dynamic loads could increase. This is assuming that no other extrinsic factors have changed.

The extrinsic factors identified, while not directly affected by mission length or destination, can be used to mitigate the injury risk associated with spaceflight-induced physiological deconditioning.

### 3.0 DAG REVIEW



As of 5/13/2022

### 4.0 KNOWLEDGE BASE

#### 4.1 GAPS

Based on the evidence presented above, several knowledge gaps have been identified. These can best be discussed based on the related risk factors and assessment methods.

Significant research has been conducted to assess the risk from impacts aligned with the X and Z axes; however, very little research has been conducted in the anticipated orientations and complex dynamics expected during spaceflight. Additional research may be warranted to better understand the impacts of these orientations. It is also clear that more knowledge is required to understand the effects of the suit and helmet on the occupant while exposed to dynamic loads, and to determine the occupant, suit, and helmet interactions with the seat and restraints. This issue is somewhat unique to NASA and very little research has been conducted to directly address these issues.

Dynamic loading while standing is not well characterized in the context of landing on planetary surfaces. Although 6 Apollo missions landed crew on the lunar surface in a standing posture, there is insufficient evidence to develop appropriate reference values for injury. Currently, no sufficient analytical tools are available to assess a vehicle design incorporating a standing posture during landings.

In addition, investigations of human tolerance to dynamic loads have been primarily conducted on young, healthy males or on elderly male PMHS. The effects of sex, age, and anthropometric measures on injury risk has been addressed to varying degrees in the past, but more research is needed to understand the effect of sex on injury risk in the spaceflight context, particularly when coupled with risk from the suit and helmet. Finally, spaceflight-induced physiological deconditioning is a risk factor unique to spaceflight, and additional research is required to better understand how this affects the risk of injury during dynamic loads.

Although injury assessment methods have improved dramatically over the past 5 decades, no single assessment method satisfactorily addresses all the risk factors and other considerations. In addition, the prediction of the very low injury risks associated with dynamic loads requires additional research. The available numerical models have all been developed for other environments and additional research is required to adapt or validate these models for spaceflight injury prediction.

#### Knowledge Gaps:

- Quantification of the risk of injury due to vehicle orientations and complex dynamics including during a standing posture
- Quantification of the risk of injury related to the suit and helmet, particularly in relation to the seat, restraints, and crewmember anthropometry
- Quantification of the risk of injury related to sex, age and anthropometric measures
- Quantification of the risk of injury due to spaceflight-induced physiological deconditioning
- Determination of criteria for low injury risk (<5%)
- Adequate assessment methods (ATDs and FEMs) validated for the spaceflight environment

## 4.2 STATE of KNOWLEDGE/FUTURE WORK

The injury rates during Soyuz landings are underpredicted using our current analytical tools. Landing data show that 10% of crewmembers sustain minor or moderate injuries during nominal landings, whereas our tools predict less than 1%. This data is evidence that gaps exist in our understanding of injury tolerance during dynamic events. Improvements in our analytical tools and further research is needed to increase confidence in our current injury prediction processes. In preparation for future lunar and Mars missions, additional concerns must be addressed.

The crew may have to stand in planetary landers during dynamic phases of flight. Most previous research involves seated occupants, so there is very little additional data available in literature to inform human tolerances in a standing orientation. The ISS treadmill heel strike data provides evidence of deconditioned crewmembers' tolerance to repetitive accelerations through the lower extremities. Voluntary jumping task data collected from deconditioned crewmembers after their return to Earth also contributes to non-injury cases of repetitive loading through lower extremities. Military studies report lower leg injury due to blasts. During Apollo missions, 12 crewmembers landed on the Moon in a standing posture with no complications. Unfortunately, acceleration time history data is not available for these lunar landings, but

landing accelerations were approximated using touchdown conditions from each Apollo landing and assumptions about the landing dynamics. These data were used to propose initial standing acceleration limits for HLS, but additional data will give us more confidence.

It is possible that the crew will wear an EVA suit during planetary landings, and blunt force injuries could occur due to the crew impacting with rigid elements of the suit during dynamic events. The contribution of the suit to injury risk is unquantified. Future work is needed to define allowable accelerations for suited crewmembers.

We must also consider that the crew will be increasingly deconditioned during Mars missions and during extended missions to the lunar surface, which will affect injury tolerances during dynamic events.

To address these concerns, the following forward work is needed:

- Trade study of landing in xEMU vs. landing in shirt sleeves/Orion crew survival system (OCSS) suit
- Levy occupant protection requirements/verifications on xEMU and update vehicle interface to suit equipment (VISE) requirement/verification to mitigate crew injury
- Incorporate new human system requirements into document managed by human health and performance (HHP) exploration extravehicular activity (xEVA) that includes all human systems requirements that apply to all elements of xEVA, including intravehicular activity(IVA)
- Conduct thorough literature review of human injury in spaceflight analog environments to determine whether injury likelihood could be reduced
- Develop standing occupant models using initial conditions with VISE and EVA suit across minimum and maximum anthropometry ranges
- Validate standing occupant models using both ATD and human testing

## 5.0 CONCLUSION

During spaceflight, crewmembers are exposed to dynamic loads that can cause injury. Dynamic loads are transient loads ( $\leq 500\text{ms}$ ) that are most likely to occur during launch, launch or pad abort, and landing.

Several extrinsic factors affect the risk of injury including the dynamic profile of the vehicle, the design of the seat and restraint, and the design of the spacesuit and helmet. Because each vehicle can have different launch, abort, and landing dynamics, the risk of injury is greatly influenced by the vehicle design. Vehicles that minimize crew exposure to dynamic loads will be inherently safer than vehicles that introduce higher dynamic loads. The seat and restraint designs may either increase or mitigate risk of injury depending on how effectively they control movement of the body. Finally, the spacesuit and helmet may contribute to the risk of injury if the design is not configured to protect the occupant during dynamic loads. For instance, the suit can hinder the effectiveness of the restraints, increasing dynamic loads on the crewmember; rigid elements of the spacesuit can induce point loading; and the helmet can cause injury from blunt impact or it may overload the neck muscles if the neck is not properly supported.

In addition to these extrinsic factors, intrinsic factors such as age, sex, anthropometrics, and physiological deconditioning due to spaceflight can contribute to the risk of injury. Age affects the risk of injury in other situations that are analogous to spaceflight-induced dynamic loads, such as automobile collisions. Sex can influence the risk of injury from dynamic loads because men can have different body strength and have different geometry than woman. Anthropometric measures can affect injury risk because they can influence interaction with suits, helmets, seats, and restraints. Moreover, spaceflight-induced physiological deconditioning can cause decrements in BMD and muscle strength, which could affect the crewmember's tolerance to dynamic loads.

Multiple methods are available to assess injury risk from dynamic loads, and each has advantages and disadvantages. The methods can be divided into 3 categories: humans, human surrogates, and numerical models. Tests on humans would seem ideal for assessing the risk of injury because humans can provide subjective feedback, but tests on humans must be limited to sub-injurious levels only, which typically limits inference from the data. Injury metrics can be obtained from humans who have survived accidents; however, no prospective investigations of injury mechanisms are available in these type of situations, which typically limits inference from the data. PMHS can be tested at injurious levels but cannot be used to investigate how living tissue responses to trauma, and they do not include active muscle tone. Human surrogates include ATD and animal models. ATDs are manikins that vary in biofidelity depending on the design and the loading conditions. ATDs cannot be used to predict injury in all conditions, however, tests using ATDs are easy to perform and the data is reproducible. Although animal models can be used to test injury to living tissue, animals are, of course, not anatomically identical to humans, making it difficult to translate results from animals to risk of injury for humans. Numerical models can be used to assess risk of injury, although the fidelity of a model depends on the quality and the quantity of the human and/or human surrogate data used to validate the model. DR models are simple but have limited capabilities for predicting injury. FEMs of ATD have similar limitations as the actual ATD tests but they can be used to assess cases that cannot be tested physically. Human FEMs have great potential for predicting injury but currently these models are not validated in all necessary conditions. Finally, regardless of the method used to assess the risk of injury from dynamic loads, adequate criteria for assessing low risk of injury (<5 %) are needed.

Given this evidence, multiple knowledge gaps still exist in our understanding of the risk of injury due to dynamic loads: the effect of various body orientations on injury risk during spaceflight including in a standing posture; the effect of suit, seat and restraint designs on injury risk; the effects of the age, sex and anthropometry on injury risk; the effects of spaceflight-induced physiological deconditioning on injury risk; criteria to adequately assess low risks of injury; and adequate methods for assessing injury risk. These knowledge gaps highlight areas of needed research to assist in mitigating the risk.

## 6.0 REFERENCES

1. [Traffic Safety Facts 2011](#). 2012, National Highway Traffic Administration.
2. Air Force Safety Center. *Aircraft Statistics*. 2012; Available from: <http://www.afsec.afmil/organizations/aviation/aircraftstatistics/index.asp>.

3. [Columbia Crew Survival Investigation Report](#). 2008, National Aeronautics and Space Administration: Houston, TX.
4. Holcomb, G., [Human Experiments to Determine Human Tolerance to Landing Impact in Capsule Systems, in Ballistic Missile and Space Technology](#), D. LeGalley, Editor. 1960, Academic Press: New York, New York.
5. Kang, Y.-S., et al., [PMHS Lower Neck Load Calculation using Inverse Dynamics with Cervical Spine Kinematics and Neck Mass Properties](#), in *IRCOBI*. 2016.
6. Somers, J.T., N. Newby, and J. Wells, [Final NASA Panel Recommendations for Definition of Acceptable Risk of Injury due to Spaceflight Dynamic Events](#). 2015, National Aeronautics and Space Administration: Houston, TX.
7. Somers, J., et al., [Defining NASA Risk Guidelines for Capsule-based Spacecraft Occupant Injuries Resulting from Launch, Abort, and Landing](#). 2014, National Aeronautics and Space Administration: Houston, TX.
8. [Abbreviated Injury Scale 2005](#). 2005, Barrington, IL: Association for the Advancement of Automotive Medicine.
9. Hay, J., *The Biomechanics of Sports Techniques*. 1973, University of Michigan: Prentice-Hall.
10. Keaveny, T. and W. Hayes, [Mechanical Properties of Cortical and Trabecular Bone. Journal of Biomechanical Engineering, 1993](#). **115**(534-542).
11. Wismans, J., et al., *Injury Biomechanics Lecture Notes (4J610)*. 1994, Eindhoven University of Technology: The Netherlands.
12. [Apollo 12 Mission Report](#). 1970, National Aeronautics and Space Administration: Houston, TX.
13. [Apollo 15 Mission Report](#). 1971, National Aeronautics and Space Administration: Houston, TX.
14. Somers, J., *Lunar Landing Loads Discretionary Task Final Report*. 2019, NASA Johnson Space Center: Houston, TX.
15. Johnston, S.L., et al., [Risk of Herniated Nucleus Pulposus Among US Astronauts](#). *Aviation, Space, and Environmental Medicine*, 2010. **81**(6): p. 566-574.
16. Barer, A., et al., *Soyuz Spacecraft Crew Safety in the Landing Phase*. 2008.
17. Hall, R. and D. Shayler, *Soyuz: A Universal Spacecraft*. 2003, Chichester, UK: Springer - Praxis.
18. Rebrov, M., *A Difficult Re-Entry from Orbit*. *Krasnaya zvezda*, 1996. **5**.
19. Oberg, J.E., *Star-Crossed Orbits - Inside the U.S.-Russian Space Alliance*. 2002, New York: McGraw-Hill.
20. Xinhua, *First Taikonaut Marks 16th Anniversary of Space Trip*, in *China Daily*. 2019: Beijing, China.
21. Qiang, X. Xia Lin (夏林), *Xinhua Deputy Chief Editor, Reveals Secret Details of Old News Stories*. 2010; Available from: <https://chinadigitaltimes.net/2010/06/xia-lin-%E5%A4%8F%E6%9E%97-xinhua-deputy-chief-editor-reveals-secret-details-of-old-news-stories/>.
22. Stroud, K. and D. Klaus, *Spacecraft Design Considerations for Piloted Reentry and Landing*. *Journal of the British Interplanetary Society*, 2006. **59**: p. 426-442.
23. Baker, J., *The History of Manned Space Flight*. 1982, New York: Crown Publishers.
24. Air Research and Development Command, *Handbook of Instructions for Aircraft Designers (HIAD) (ARDVM 80-1)*. 1960, Air Research and Development Command: Wright-Patterson Air Force Base, Ohio.
25. Eiband, M., [Human Tolerance to Rapidly Applied Accelerations: A Summary of the Literature](#). 1959, National Aeronautics and Space Administration: Washington, DC.
26. Headley, R., et al., [Human Factors Responses During Ground Impact](#). *Aerospace Medicine*, 1962. **33**(2): p. 141-46.
27. Beeding, E. and J. Mosley, *Human Deceleration Tests*. 1960, AFMDC-TR-60-2: Holloman Air Force Base, New Mexico.



28. Beeding, E.L., *Daisy Track Tests: 520-707 (13 July 1959 - 13 April 1960)*. MDW Test Report No. 60-4. 1960, Air Force Missile Development Center: Holloman AFB, NM.
29. Weis, E., N. Clarke, and J. Brinkley, [\*Human Response to Several Impact Acceleration Orientations and Patterns\*](#). Aerospace Medicine, 1963. **34**(12): p. 1122-1129.
30. Schulman, M., et al., [\*Determination of Human Tolerance to Negative Impact Acceleration\*](#). 1963, United States Aerospace Crew Equipment Laboratory: Philadelphia, PA.
31. Stapp, J.P. and E.R. Taylor, [\*Space Cabin Landing Vector Effects on Human Physiology\*](#). Aerospace Medicine, 1964. **35**(12): p. 1117-1132.
32. Brown, W., J. Rothstein, and P. Foster, [\*Human Response to Predicted Apollo Landing Impacts in Selected Body Orientations\*](#). Aerospace Medicine, 1966. **37**(4): p. 394-398.
33. Zaborowski, A. *Lateral Impact Studies: Lap Belt Shoulder Harness Investigations*. in *9th Stapp Car Crash Conference, Society of Automotive Engineers*. 1966. Warrendale, PA.
34. Klopstein, H.W. *Compression Fracture of the Seventh Thoracic Vertebrae Caused by Experimental Impact: A Case Report*. in *40th Annual Meeting, Aerospace Medical Association*. 1969. San Francisco.
35. Payne, P., *Personal Restraint and Support System Dynamics*. 1965, Wright-Patterson Air Force Base: Dayton, OH.
36. Somers, J.T., et al., *ATD Injury Metric Development 2019 Annual Report*. 2019, NASA Johnson Space Center: Houston, TX.
37. Somers, J.T., et al., *Occupant Protection ATD Injury Metric Sensitivity Final Report*. 2019, NASA Johnson Space Center: Houston, TX.
38. Currie-Gregg, N. and C. Lawrence, *Analysis of Anthropomorphic Test Device (ATD) Response for Proposed Orion Crew Impact Attenuation System (CIAS)*. 2017, NASA Langley Research Center: Hampton, VA.
39. Somers, J., D. Gohmert, and J. Brinkley, *Application of the Brinkley Dynamic Response Criterion to Spacecraft Transient Events*. 2013, National Aeronautics and Space Administration: Houston, TX.
40. Air Force Research Laboratory. *Collaborative Biomechanics Data Network (CBDN)*. 2012 7/26/2013]; Available from: <https://biodyn.istdayton.com/CBDN/Default.aspx>.
41. Somers, J., et al., [\*Development of Head Injury Assessment Reference Values Based on NASA Injury Modeling\*](#). Stapp Car Crash Journal, 2011. **55**: p. 49-74.
42. Trammell, T.R.M. and H.M. Bock, *Spine Fractures in Open Cockpit Open Wheel Race Car Drivers: Reducing the Risk Through Seat Modification*. 2009.
43. Spine Research Institute of San Diego. *Epidemiology of Whiplash*. 2019; Available from: [http://www.srisd.com/consumer\\_site/](http://www.srisd.com/consumer_site/).
44. Danelson, K., J. Bolte, and J. Stitzel, [\*Assessing Astronaut Injury Potential from Suit Connectors Using a Human Body Finite Element Model\*](#). Aviation Space and Environmental Medicine, 2011. **82**(2): p. 79-86.
45. Schmidt, A., et al., *Establishing the Biodynamics Data Resource (BDR): Human Volunteer Impact Acceleration Research Data in the BDR*. 2010.
46. Melvin, J.W., et al., *Racing Car Restraint System Frontal Crash Performance Testing*. 1994, SAE Technical Paper.
47. Howland, W.J., J.L. Curry, and C.B. Buffington, [\*Fulcrum Fractures of the Lumbar Spine. Transverse Fracture Induced by an Improperly Placed Seat Belt\*](#). JAMA, 1965. **193**: p. 240-241.
48. Anderson, P.A., et al., [\*The Epidemiology of Seatbelt-Associated Injuries\*](#). Journal of Trauma, 1991. **31**: p. 60-67.
49. Viano, D.C., *Biomechanical Responses and Injuries in Blunt Lateral Impact*. 1989, SAE International.

50. Hearon, B.F., et al., [Knee Ligament Injury During Lateral Impact](#). Aviation Space and Environmental Medicine, 1985. **56**(1): p. 3-8.
51. Henzel, J.H., *The Human Spinal Column and Upward Ejection Acceleration: An Appraisal of Biodynamic Implications*. 1967, Aerospace Medical Research Laboratory.
52. Mohr, G.C., et al., [Variations of Spinal Alignment in Egress Systems and Their Effect](#). Aerospace Medicine, 1969. **40**(9): p. 983-988.
53. Brinkley, J., *Development of Aerospace Escape Systems*. Air University Review, 1968. **XIX**(5): p. 34-49.
54. Brinkley, J. and J. Schaffer, *Dynamic Simulation Techniques for the Design of Escape Systems: Current Applications and Future Air Force Requirements*. 1971, Wright-Patterson Air Force Base: Dayton, OH.
55. Brinkley, J., L. Specker, and S. Mosher. *Development of Acceleration Exposure Limits for Advanced Escape Systems*. in *Implications of Advanced Technologies for Air and Spacecraft Escape*, NATO AGARD Proceedings. 1990.
56. Kleinberger, M., et al., *Development of Improved Injury Criteria for the Assessment of Advanced Automotive Restraint Systems*. 1998, National Highway Traffic Safety Administration: Washington, DC.
57. Nahum, A. and J. Melvin, *Accidental Injury Biomechanics and Prevention*. Second Edition ed. 2002, New York: Springer Science and Business Media.
58. *Traffic Safety Facts 2009*. 2010, National Highway Traffic Safety Administration: Washington, DC.
59. Markogiannakis, H., et al., [Motor Vehicle Trauma: Analysis of Injury Profiles by Road-User Category](#). Emergency Medicine Journal, 2006. **23**(1): p. 27-31.
60. National Highway Traffic Safety Administration, *Final Economic Assessment, FMVSS No. 201, Upper Interior Head Protection*. 1995: Washington, DC.
61. Barer, A., [Medical Aspects of Cosmonaut Safety During Emergency Landings](#). *Respicere et prospicere*. Aviakosmicheskaja i Ekologicheskaja Meditsina, 2008. **42**(2): p. 3-20.
62. Snyder, R., et al., [Pathology of Trauma Attributed to Restraint Systems in Crash Impacts](#). Aerospace Medicine, 1968.
63. Brinkley, J., et al., [Evaluation of a Proposed, Modified F/FB-111 Crew Seat and Restraint System](#). 1981, Wright-Patterson Air Force Base: Dayton, OH.
64. Brinkley, J., *Man Protection During Landing Impact of Aerospace Vehicles*, in *Ballistic Missile and Space Technology*, D. LeGalley, Editor. 1960, Academic Press: New York, NY.
65. Caldwell, E. and J. Plaga, *The Characterization of Spinal Compression in Various-Sized Human and Manikin Subjects During +Gz Impact*. 2006, Biosciences and Protection Division Human Effectiveness Directorate with Air Force Research Laboratory.
66. Hearon, B. and J. Brinkley, [Effect of Seat Cushions on Human Response to +Gz Impact](#). Aviation, Space and Environmental Medicine, 1986. **57**(2).
67. Perry, C., D. Bonetti, and J. Brinkley, *The Effect of Variable Seat Back Angles on Human Responses to +Gz Impact Accelerations*. 1991: Wright-Patterson Air Force Base.
68. Hearon, B. and J. Brinkley, [Comparison of Human Response in Restraint Systems With and Without a Negative G Strap](#). Aviation, Space, and Environmental Medicine, 1986. **57**(4).
69. Asbun, H.J., et al., [Intra-Abdominal Seatbelt Injury](#). Journal of Trauma, 1990. **30**(2): p. 189-93.
70. Sato, T.B., [Effects of Seat Belts and Injuries Resulting from Improper Use](#). Journal of Trauma, 1987. **27**(7): p. 754-758.
71. SFI Foundation Inc., *Seatbelt Installation Guide for Upright Seating*. 2012: Poway, CA.
72. Bandstra, R., et al. *Seat-Belt Injuries in Medical and Statistical Perspectives*. in *Proceedings of the 16th International Enhanced Safety of Vehicles Conference (98-S6-W-25)*. 1998. Windsor, Ontario.

73. Clarke, N., et al., *Lateral Impact Tolerance Studies in Support of Apollo*. 1963, Wright-Patterson Air Force Base: Dayton, OH.
74. Stapp, J.P., *Human Exposures to Linear Acceleration: Part II. The Forward-Facing Position and Development of a Crash Harness*. 1947, Wright-Patterson Air Force Base: Dayton, Ohio.
75. Schall, D.G., [Non-Ejection Cervical Spine Fracture due to Defensive Aerial Combat Maneuvering in an RF-4C: A Case Report](#). *Aviation Space and Environmental Medicine*, 1983. **54**: p. 1111-1116.
76. Ewing, C.L. and A.I. King, *Structural Considerations of the Human Vertebral Column under +Gz Impact Acceleration*. NAMRL-1178. 1975, Naval Aerospace Medical Research Laboratory: Pensacola, FL.
77. King, A.I. and C.L. Ewing, [Mechanism of Spinal Injury due to Caudocephalad Acceleration](#). *Orthopedic Clinics of North America*, 1975. **6**(1): p. 19-31.
78. Perry, C.E., *Impact Evaluation of a Proposed B-2 Seat Cushion*. *SAFE Journal*, 1997. **27**(1): p. 24-31.
79. Cheng, Z. and J. Pelletiere. *Evaluation of the Safety Performance of Ejection Seat Cushions*. in *SAFE Symposium*. 2004. Salt Lake City, UT.
80. Miller, K. and L. Morelli, *Ejection Tower Evaluation of the Rate-Dependent Foam Cushions for the NACES Seat*. 1993, Naval Air Systems Command: Washington, D. C.
81. Kelly, T.J., *Moon Lander: How We Developed the Apollo Lunar Module*. Smithsonian History of Aviation and Spaceflight Series, ed. K. Kaufman. 2001, Washington, D.C.: Smithsonian Books.
82. McFarland, S. and M. Dub. *Suited Occupant Injury Potential During Dynamic Spacecraft Flight Phases (AIAA 2010-6230)*. in *40th International Conference on Environmental Systems*. 2010. Barcelona, Spain: AIAA.
83. Golman, A.J., et al., *Biomechanical Assessment of Astronaut Injury Potential from Suit Ring Elements Using a Full Human Body Finite-Element Model*, in *International Crashworthiness Conference*. 2012: Milan, Italy.
84. Radford, T., et al. *Next Generation Space Suit Injury Assessment (AIAA 2011-5107)*. in *Proceedings of the 41st International Conference on Environmental Systems*. 2011. Portland, OR: American Institute of Aeronautics and Astronautics.
85. Lau, I. and D. Viano. *The Viscous Criterion- Bases and Application of an Injury Severity Index for Soft Tissues*. in *30th Stapp Car Crash Conference* 1986.
86. Geddes, L. and R. Roeder, [Evolution of our Knowledge of Sudden Death Due to Commotio Cordis](#). *American Journal of Emergency Medicine*, 2005. **23**: p. 67-75.
87. Yoganandan, N., et al., [Role of Age and Injury Mechanism on Cervical Spine Injury Tolerance from Head Contact Loading](#). *Traffic Injury Prevention*, 2018. **19**(2): p. 165-172.
88. Burton, R., et al., *Cervical Spinal Injury from Repeated Exposures to Sustained Acceleration*. 1999, DTIC Document.
89. Deakin, R., *Military Aircrew Head Support System*. *Journal of Aircraft*, 1993. **30**(1).
90. Gil, J., et al., *Common Helmet Design for Launch, Entry and Abort and EVA Activities*. Society of Automotive Engineers International Journal, 2008.
91. Kornhauser, M., *Impact Protection for the Human Structure*, in *Advances in Astronautical Sciences*. 1958, Plenum: New York. p. Paper 3, Vol. 3.
92. Stitzel, J., J. Barretta, and S. Duma, *Predicting Fractures due to Blunt Impact: A Sensitivity Analysis of the Effects of Altering Failure Strain of Human Rib Cortical Bone*. *International Journal of Crashworthiness*, 2004. **9**(6): p. 633-642.
93. *Constellation Program Human-Systems Integration Requirements Revision D*. 2009, National Aeronautics and Space Administration: Houston, TX.
94. Pintar, F.A., et al., [Biomechanical Properties of Human Lumbar Spine Ligaments](#). *Journal of Biomechanics*, 1992. **25**(11): p. 1351-1356.

95. Foust, D., et al., *Cervical Range of Motion and Dynamic Response and Strength of Cervical Muscles*. 1973: Society of Automotive Engineers International Journal.
96. Yoganandan, N., et al., *Axial Tolerance of Human Foot-Ankle Complex*. 40th Stapp Car Crash Conference Proceedings, 1996.
97. Yoganandan, N., et al., [\*Biomechanics of Side Impact: Injury Criteria, Aging Occupants, and Airbag Technology\*](#). Journal of Biomechanics, 2007. **40**(2): p. 227-243.
98. Pintar, F.A., N. Yoganandan, and L. Voo, [\*Effect of Age and Loading Rate on Human Cervical Spine Injury Threshold\*](#). Spine, 1998. **23**(18): p. 1957-1962.
99. Evans, L., *Age and Fatality Risk From Similar Severity Impacts*. Journal of Traffic Medicine, 2001. **29**: p. 10-19.
100. Ebbesen, E.N., et al., [\*Age- and Gender-Related Differences in Vertebral Bone Mass, Density, and Strength\*](#). Journal of Bone and Mineral Research, 1999. **14**(8): p. 1394-1403.
101. Mosekilde, L. and L. Mosekilde, [\*Sex Differences in Age-Related Changes in Vertebral Body Size, Density and Biomechanical Competence in Normal Individuals\*](#). Bone, 1990. **11**(2): p. 67-73.
102. Singer, K., et al., [\*Prediction of Thoracic and Lumbar Vertebral Body Compressive Strength: Correlations with Bone Mineral Density and Vertebral Region\*](#). Bone, 1995. **17**(2): p. 167-174.
103. Cann, C.E., et al., [\*Quantitative Computed Tomography for Prediction of Vertebral Fracture Risk\*](#). Bone, 1985. **6**(1): p. 1-7.
104. National Aeronautics and Space Administration, [\*NASA Space Flight Human-System Standard Volume I: Crew Health\*](#). 2007.
105. Iida, T., et al., [\*Effects of Aging and Spinal Degeneration on Mechanical Properties of Lumbar Supraspinous and Interspinous Ligaments\*](#). The Spine Journal, 2002. **2**(2): p. 95-100.
106. Shim, V., J. Liu, and V. Lee, *A Technique for Dynamic Tensile Testing of Human Cervical Spine Ligaments*. Experimental Mechanics, 2006. **46**(1): p. 77-89.
107. NASA Human System Risk Board, *Risk of Injury from Dynamic Loads Board Decisions*. 2014, National Aeronautics and Space Administration: Houston, TX.
108. Evans, L. and P.H. Garrish, *Gender and Age Difference on Fatality Risk From the Same Physical Impact Determined Using Two-Car Crashes*. 2004, Society of Automotive Engineers: Warrendale, PA.
109. Evans, L., *Traffic Safety and the Driver*. 1991, New Yourk: Van Nostrand Reinhold.
110. Allnutt, R., *Gender Effects in Traumatic Injury*. SAFE Journal, 2007. **37**(1): p. 1-8.
111. Stemper, B., et al., [\*Anatomical Gender Differences in Cervical Vertebrae of Size-Matched Volunteers\*](#). SPINE, 2008. **33**(2): p. 44-49.
112. Gallagher, H., et al. *A Comparison of Cervical Stress and BMD as Related to Gender and Size During +Gz Acceleration*. in *Proceedings of the 44th SAFE Symposium*. 2006.
113. Gallagher, H., et al., *An Analysis of Vertebral Stress and BMD During +Gz Impact Accelerations*. 2007: Wright-Patterson Air Force Base.
114. Nightingale, R.W., et al., *The Dynamic Responses of the Cervical Spine: Buckling, End Conditions, and Tolerance in Compressive Impacts*. 1997, Society of Automotive Engineers: Warrendale, PA. p. 451-471.
115. Nightingale, R.W., et al., [\*Comparative Strengths and Structural Properties of the Upper and Lower Cervical Spine in Flexion and Extension\*](#). Journal of Biomechanics, 2002. **35**(6): p. 725-732.
116. Nightingale, R.W., et al., [\*Flexion and Extension Structural Properties and Strengths for Male Cervical Spine Segments\*](#). Journal of Biomechanics, 2007. **40**(3): p. 535-42.
117. Yoganandan, N., et al., [\*Preliminary Female Cervical Spine Injury Risk Curves from PMHS Tests\*](#). Journal of the Mechanical Behavior of Biomedical Materials, 2018. **83**: p. 143-147.

118. Perry, C., et al. *The Effects of Variable Helmet Weight on Head Response and Neck Loading during Lateral +Gy Impact*. in *Proceedings of the 41st Annual SAFE Symposium*. 2003. Jacksonville, FL.
119. Coa, P., et al., [\*Exercise within Lower Body Negative Pressure Partially Counteracts Lumbar Spine Deconditioning Associated with 28-Day Bed Rest\*](#). *Journal of Applied Physiology*, 2005. **99**: p. 39-44.
120. Brown, J., *The Apollo-Soyuz Test Project: Medical Report*. 1977, NASA: Washington, DC. p. 119-121.
121. Thornton, W.E. and T. Moore, *Height Changes in Microgravity In: Results of the Life Sciences DSOs Conducted Aboard the Space Shuttle 1981-1986*, M. Bungo, et al., Editors. 1987, Johnson Space Center: Houston, TX. p. 55-57.
122. Wing, P., et al., [\*Back Pain and Spinal Changes in Microgravity\*](#). *Orthopedic Clinics of North America*, 1991. **22**: p. 255-262.
123. Young, K.S. and S. Rajulu, [\*Changes in Seated Height in Microgravity\*](#). *Applied Ergonomics*, 2020. **83**: p. 1-7.
124. Chang, D.G., et al., [\*Lumbar Spine Paraspinal Muscle and Intervertebral Disc Height Changes in Astronauts After Long-Duration Spaceflight on the International Space Station\*](#). *Spine*, 2016. **41**(24): p. 1917-1924.
125. LeBlanc, A.D., et al., [\*Changes in Intervertebral Disc Cross-Sectional Area with Bed Rest and Space Flight\*](#). *Spine*, 1994. **19**(7): p. 812-817.
126. Belavy, D.L., et al., [\*Disc Herniations in Astronauts: What Causes Them, and What Does It Tell Us About Herniation on Earth?\*](#) *European Spine Journal*, 2016. **25**(1): p. 144-154.
127. Lewandowski, B., et al. *Risk Assessment of Bone Fracture During Space Exploration Missions to the Moon and Mars*. in *Space Systems Engineering and Risk Management Symposium*. 2008. Los Angeles, CA.
128. Vico, L., et al., [\*Effects of Long-Term Microgravity Exposure on Cancellous and Cortical Weight-Bearing Bones of Cosmonauts\*](#). *Lancet*, 2000. **355**(9215): p. 1607-1611.
129. LeBlanc, A., L. Shackelford, and V. Schneider, [\*Future Human Bone Research in Space\*](#). *Bone*, 1998. **22**: p. 113S-116S.
130. Feiveson, A., C. Mendez, and J. Somers. *Assessing the Effect of Spaceflight on the Propensity for Astronauts to Develop Disc Herniation*. in *NASA Human Research Program Investigator's Workshop*. 2015. Galveston, TX: National Aeronautics and Space Administration.
131. Sibonga, J.D., et al., *Risk of Bone Fracture due to Spaceflight induced Changes to Bone*. 2017, NASA Johnson Space Center: Houston, TX.
132. Black, D.M., et al., [\*Proximal Femoral Structure and the Prediction of Hip Fracture in Men: A Large Prospective Study Using QCT\*](#). *Journal of Bone and Mineral Research*, 2008. **23**(8): p. 1326-1333.
133. Loehr, J.A., et al., [\*Physical Training for Long-Duration Spaceflight\*](#). *Aerospace Medicine and Human Performance*, 2015. **86**: p. A14-A23.
134. Belavy, D.L., et al., [\*Countermeasures Against Lumbar Spine Deconditioning in Prolonged Bed Rest: Resistive Exercise with and Without Whole Body Vibration\*](#). *Journal of Applied Physiology*, 2010. **109**(6): p. 1801-1811.
135. Keyak, J.H., et al., [\*Reduction in Proximal Femoral Strength due to Long-Duration Spaceflight\*](#). *Bone*, 2009. **44**(3): p. 449-453.
136. Thornton, W. and J. Rummel, *Muscular Deconditioning and its Prevention in Spaceflight*, in *Biomedical Results of Skylab*, R.S. Johnston and L.F. Deitlein, Editors. 1977, NASA: Washington, DC. p. 191-197.
137. Stein, T., [\*Nutrition and Muscle Loss in Humans During Spaceflight\*](#). *Advances in Space Biology and Medicine*, 1999. **7**: p. 49-97.



138. LeBlanc, A., et al., [\*Muscle Volume, MRI Relaxation Times \(T2\), and Body Composition After Spaceflight\*](#). Journal of Applied Physiology, 2000. **89**: p. 2158-2164.
139. Zhou, M., et al., [\*Myosin Heavy Chain Isoforms of Human Muscle After Short-Term Spaceflight\*](#). Journal of Applied Physiology, 1995. **78**: p. 1740-1744.
140. Edgerton, V., et al., [\*Human Fiber Size and Enzymatic Properties After 5 and 11 Days of Spaceflight\*](#). Journal of Applied Physiology, 1995. **78**: p. 1733-1739.
141. Hackney, K.J. and L.L. Ploutz-Snyder, [\*Unilateral Lower Limb Suspension: Integrative Physiological Knowledge from the Past 20 Years\*](#) (1991-2011). European Journal of Applied Physiology, 2012. **112**(1): p. 9-22.
142. Sibonga, J.D., [\*Spaceflight-Induced Bone Loss: Is There an Osteoporosis Risk?\*](#) Current Osteoporosis Reports, 2013. **11**(2): p. 92-98.
143. National Aeronautics and Space Administration, *Orion Multi Purpose Crew Vehicle Program: Human-Systems Integration Requirements*. 2012, Johnson Space Center: Houston, TX.
144. Lang, T., et al., [\*Cortical and Trabecular Bone Mineral Loss from the Spine and Hip in Long-Duration Spaceflight\*](#). Journal of Bone and Mineral Research, 2004. **19**(6): p. 1006-1012.
145. Galante, J., W. Rostoker, and R.D. Ray, [\*Physical Properties of Trabecular Bone\*](#). Calcified Tissue Research, 1970. **5**(1): p. 236-246.
146. Ploutz-Snyder, L., et al., *Risk of Impaired Performance Due to Reduced Muscle Mass, Strength, and Endurance*. 2015, NASA Johnson Space Center: Houston, TX.
147. Bailey, J.F., et al., [\*Effect of Microgravity on the Biomechanical Properties of Lumbar and Caudal Intervertebral Discs in Mice\*](#). Journal of Biomechanics, 2014. **47**(12): p. 2983-2988.
148. Townsend, M.T. and N. Sarigul-Klijn, *Human Spaceflight and Space Adaptations: Computational Simulation of Gravitational Unloading on the Spine*. Acta Astronautica, 2018. **145**: p. 18-27.
149. Mertz, H.J. and L.M. Patrick, *Strength and Response of the Human Neck*. Stapp Car Crash Conference, 1971.
150. Scheuring, R., N. Holguin, and J. Sibonga, *Risk of Intervertebral Disc Damage*. 2008, NASA Human Research Program.
151. Maas, A.I., N. Stocchetti, and R. Bullock, *Moderate and Severe Traumatic Brain Injury in Adults*. Lancet Neurology, 2008. **7**(8): p. 728-741.
152. *Report to Congress on Mild Traumatic Brain Injury in the United States: Steps to Prevent a Serious Public Health Problem*. 2003, Centers for Disease Control and Prevention: Atlanta, GA.
153. Pellman, E.J., [\*Background on the National Football League's Research on Concussion in Professional Football\*](#). Neurosurgery, 2003. **53**(4): p. 797-798.
154. Pellman, E.J., et al., [\*Concussion in Professional Football: Recovery of NFL and High School Athletes Assessed by Computerized Neuropsychological Testing\*](#). Neurosurgery, 2006. **58**(2): p. 263-274.
155. Pellman, E.J. and D.C. Viano, [\*Concussion in Professional Football: Summary of the Research Conducted by the National Football League's Committee on Mild Traumatic Brain Injury\*](#). Neurosurgical Focus, 2006. **21**(4): p. E12.
156. Pellman, E.J., et al., [\*Concussion in Professional Football: Location and Direction of Helmet Impacts\*](#). Neurosurgery, 2003. **53**(6): p. 1328-1340.
157. Pellman, E.J., et al., [\*Concussion in Professional Football: Reconstruction of Game Impacts and Injuries\*](#). Neurosurgery, 2003. **53**(4): p. 799-814.
158. Pellman, E.J., et al., [\*Concussion in Professional Football: Helmet Testing to Assess Impact Performance\*](#). Neurosurgery, 2006. **58**(1): p. 78-96.
159. Viano, D.C., et al., [\*Concussion in Professional Football: Performance of Newer Helmets in Reconstructed Game Impacts\*](#). Neurosurgery, 2006. **59**(3): p. 591-606.

160. Funk, J., et al., [\*Biomechanical Risk Estimates for Mild Traumatic Brain Injury\*](#). Annual Proceedings of the Association for the Advancement of Automotive Medicine, 2007. **51**: p. 343-361.
161. Funk, J., et al., [\*Validation of Concussion Risk Curves for Collegiate Football Players Derived from HITS Data\*](#). Annals of Biomedical Engineering, 2012. **40**(1): p. 79-89.
162. Rowson, S., et al., *Rotational Head Kinematics in Football Impacts: An Injury Risk Function for Concussion*. Annals of Biomedical Engineering, 2012. **40**(1): p. 1-13.
163. Gennarelli, T.A. and L.E. Thibault, [\*Biomechanics of Acute Subdural Hematoma\*](#). Journal of Trauma, 1982. **22**(8): p. 680-686.
164. Post, A. and T.B. Hoshizaki, *Mechanisms of Brain Impact Injuries and Their Prediction: A Review*. Trauma, 2012. **14**(4): p. 327-349.
165. Gennarelli, T.A. and L.E. Thibault, *Experimental Production of Prolonged Traumatic Coma in the Primate*, in *Advances in Neurotrauma*, R. Villiani, Editor. 1983, Excerpta Medica: Amsterdam.
166. Ommaya, A.K. and T.A. Gennarelli, [\*Cerebral Concussion and Traumatic Unconsciousness: Correlation of Experimental and Clinical Observations of Blunt Head Injuries\*](#). Brain, 1974. **97**(4): p. 633-654.
167. Unterharnscheidt, F. and L.S. Higgins, [\*Pathomorphology of Experimental Head Injury due to Rotational Acceleration\*](#). Acta Neuropathologica, 1969. **12**(2): p. 200-204.
168. Ommaya, A.K., et al., [\*Cerebral Concussion in the Monkey: An Experimental Model\*](#). Science, 1966. **153**(3732): p. 211-212.
169. Ommaya, A.K. and A.E. Hirsch, [\*Tolerances for cerebral concussion from head impact and whiplash in primates\*](#). Journal of Biomechanics, 1971. **4**(1): p. 13-21.
170. Gennarelli, T.A., F.A. Pintar, and N. Yoganandan. *Biomechanical Tolerances for Diffuse Brain Injury and a Hypothesis for Genotypic Variability in Response to Trauma*. in *Annual Proceedings of the Association for the Advancement of Automotive Medicine*. 2003.
171. Rowson, S. and S.M. Duma, [\*Brain Injury Prediction: Assessing the Combined Probability of Concussion Using Linear and Rotational Head Acceleration\*](#). Annals of Biomedical Engineering, 2013. **41**(5): p. 873-882.
172. King, A.I., et al. *Is Head Injury Caused By Linear or Angular Acceleration?* in *IRCOBI*. 2003. Lisbon, Portugal.
173. Prasad, P. and H. Mertz, *The Position of the United States Delegates to the ISO Working Group 6 on the Use of HIC in the Automotive Environment*. 1985, SAE 851246.
174. Mertz, H., P. Prasad, and G. Nuscholtz. *Head Injury Risk Assessment Based on 15ms HIC and peak head acceleration criteria*. in *AGARD Meeting on Impact Head Injury*. 1996. NATO.
175. National Highway Traffic Administration, *Federal Motor Vehicle Safety Standards and Regulations*. 2008: Washington, DC.
176. Takhounts, E.G., et al., [\*Investigation of Traumatic Brain Injuries Using the Next Generation of Simulated Injury Monitor \(SIMon\) Finite Element Head Model\*](#). Stapp Car Crash Journal, 2008. **52**: p. 1-31.
177. Takhounts, E.G., et al., [\*On the Development of the SIMon Finite Element Head Model\*](#). Stapp Car Crash Journal, 2003. **47**: p. 107-133.
178. Takhounts, E., et al. *Kinematic Rotational Brain Injury Criterion (BRIC)*. in *Proceedings of the 22nd International ESV Conference*, 11-0263. 2011.
179. Takhounts, E., et al., [\*Development of Brain Injury Criteria \(BrIC\)\*](#). Stapp Car Crash Journal, 2013. **57**: p. 243-266.
180. McElhaney, J.H., et al., *Biomechanical Aspects of Cervical Trauma*, in *Accidental Injury: Biomechanics and Prevention*, A.M. Nahum and J.W. Melvin, Editors. 2002, Springer-Verlag: New York, N.Y. p. 324-373.

181. Myers, B.S. and B.A. Winkelstein, [Epidemiology, Classification, Mechanism, and Tolerance of Human Cervical Spine Injuries](#). Critical Reviews in Biomedical Engineering, 1995. **23**(5-6): p. 307-409.
182. McElhaney, J.H., et al., *Cervical Spine Compression Responses*. Stapp Car Crash J, 1983(27): p. 163-177.
183. Maiman, D.J., et al., [Compression Injuries of the Cervical Spine: A Biomechanical Analysis](#). Neurosurgery, 1983. **13**(3): p. 254-260.
184. Pintar, F.A., et al., [Cervical Vertebral Strain Measurements under Axial and Eccentric Loading](#). Journal of Biomechanical Engineering, 1995. **117**(4): p. 474-478.
185. Myers, B.S., et al., *The Influence of End Condition on Human Cervical Spine Injury Mechanisms*. Stapp Car Crash Journal, 1991. **35**: p. 391-400.
186. Shea, M., et al., [In Vitro Hyperextension Injuries in the Human Cadaveric Cervical Spine](#). Journal of Orthopaedic Research, 1992. **10**(6): p. 911-916.
187. Yoganandan, N., et al., [Human Head-Neck Biomechanics Under Axial Tension](#). Medical Engineering and Physics, 1996. **18**(4): p. 289-294.
188. Prasad, P. and R.P. Daniel, *A Biomechanical Analysis of Head, Neck and Torso Injuries to Child Surrogates due to Sudden Torso Acceleration*. Stapp Car Crash Journal, 1984. **28**: p. 784-799.
189. Bass, C., et al. *A New Neck Injury Criterion in Combined Vertical/Frontal Crashes with Head Supported Mass*. in IRCOBI Conference. 2006.
190. Yoganandan, N., A. Sances, and F. Pintar, [Biomechanical Evaluation of the Axial Compressive Responses of the Human Cadaveric and Manikin Necks](#). Journal of Biomechanical Engineering, 1989. **111**(3): p. 250-255.
191. Tran, N.T., et al., [Mechanism of the Burst Fracture in the Thoracolumbar Spine. The Effect of Loading Rate](#). Spine, 1995. **20**(18): p. 1984-1988.
192. Holmes, J.F., et al., [Epidemiology of Thoracolumbar Spine Injury in Blunt Trauma](#). Academic Emergency Medicine, 2001. **8**(9): p. 866-872.
193. Schmitt, K.-U., M.H. Muser, and P. Niederer, *A New Neck Injury Criterion Candidate for Rear-End Collisions Taking Into Account Shear Forces and Bending Moments*, in *Enhanced Safety of Vehicles*. 2001, National Highway Traffic Safety Administration. p. 1-9.
194. Bostrom, O., et al., *A New Neck Injury Criterion Candidate Based on Injury Findings in the Cervical Spinal Ganglia After Experimental Neck Extension Trauma*, in IRCOBI Conference. 1996: Dublin, Ireland.
195. Yoganandan, N., F.A. Pintar, and A. Banerjee, [Load-Based Lower Neck Injury Criteria for Females from Rear Impact from Cadaver Experiments](#). Annals of Biomedical Engineering, 2017. **45**(5): p. 1194-1203.
196. Ye, X., et al., [Computational Modeling and Analysis of Thoracolumbar Spine Fractures in Frontal Crash Reconstruction](#). Traffic Injury Prevention, 2018. **19**: p. S32-S39.
197. Yoganandan, N., et al., [Biomechanics of Human Thoracolumbar Spinal Column Trauma from Vertical Impact Loading](#). Annals of Advances in Automotive Medicine, 2013. **57**: p. 155.
198. Murphy, D.F., D.A.J. Connolly, and B.D. Beynon, [Risk Factors for Lower Extremity Injury: A Review of the Literature](#). British Journal of Sports Medicine, 2003. **37**(1): p. 13-29.
199. Hardy, W., et al., *Biomechanical Investigation of Airbag-Induced Upper Extremity Injuries*. 1997, Society of Automotive Engineers: Warrendale, PA.
200. Duma, S.M., et al., [Injury Criteria for Dynamic Hyperextension of the Female Elbow Joint](#). 2006, DTIC Document.
201. Duma, S.M., et al., [Dynamic Injury Tolerances for Long Bones of the Female Upper Extremity](#). Journal of Anatomy, 1999. **194**: p. 463-471.



202. Kuppas, S., et al. *Lower Extremity Injuries and Associated Injury Criteria*. in 17th ESV Conference Paper No. 457. 2001.
203. Manning, P., et al., *Dynamic Response and Injury Mechanism in the Human Foot and Ankle and an Analysis of Dummy Biofidelity*, in *Enhanced Safety of Vehicles*. 1998: Windsor, Canada.
204. Mertz, H.J., *Anthropomorphic Models*, in *The Biomechanics of Trauma*. 1993, Appleton-Century-Crofts Norwalk, CT. p. 31-60.
205. Schreiber, P., et al., *Static and Dynamic Strength of the Leg*, in *IRCOBI Conference*. 1997: Hannover, Germany.
206. Nyquist, G.W., et al., *Tibia Bending: Strength and Response*. SAE Transactions, 1985. **94**: p. 240-253.
207. Klopp, G.S., et al., *Mechanisms of Injury and Injury Criteria for the Human Foot and Ankle in Axial Impact to the Foot*, in *IRCOBI Conference*. 1997: Hannover, Germany.
208. Kitagawa, Y., et al., *A Severe Ankle and Foot Injury in Frontal Crashes and Its Mechanism*. SAE Transactions, 1998. **107**(2649-2660).
209. Parenteau, C.S., D.C. Viano, and P.Y. Petit, [\*Biomechanical Properties of Human Cadaveric Ankle-Subtalar Joints in Quasi-Static Loading\*](#). Journal of Biomechanical Engineering, 1998. **120**(1): p. 105-111.
210. King, A.I., [\*Fundamentals of Impact Biomechanics: Part I-Biomechanics of the Head, Neck, and Thorax\*](#). Annual Review of Biomedical Engineering, 2000. **2**: p. 55-81.
211. Neathery, R.F., C.K. Kroell, and H.J. Mertz, *Prediction of Thoracic Injury from Dummy Responses*. 1975, SAE Technical Paper.
212. Viano, D.C. and V.K. Lau, [\*Role of Impact Velocity and Chest Compression in Thoracic Injury\*](#). Aviation, Space, and Environmental Medicine, 1983. **54**(1): p. 16-21.
213. Cavanaugh, J.M., et al., *Biomechanical Response and Injury Tolerance of the Thorax in Twelve Sled Side Impacts*. 1990, SAE Technical Paper.
214. Eppinger, R.H., J.H. Marcus, and R.M. Morgan, *Development of Dummy and Injury index for NHTSA's Thoracic Side Impact Protection Research Program*. SAE Transactions, 1984. **93**: p. 359-387.
215. Arumugam, S., et al., [\*Frequency, Causes and Pattern of Abdominal Trauma: A 4-Year Descriptive Analysis\*](#). Journal of Emergencies, Trauma, and Shock, 2015. **8**(4): p. 193-198.
216. Hermans, E., et al., *Research on Relation of Mortality and Hemodynamics in Patients with an Acute Pelvic Ring Fracture*. Journal of Acute Disease, 2016. **5**(2): p. 117-122.
217. Cavanaugh, J.M., et al., *Abdominal Injury and Response in Side Impact*. 1996, SAE Technical Paper.
218. Trosseille, X., et al., [\*Abdominal Response to High Speed Seatbelt Loading\*](#). Stapp Car Crash Journal, 2002. **46**: p. 71-79.
219. Coughlin, T.A., et al., *Acetabular Fractures, Anatomy and Implications for Treatment*. Orthopaedics and Trauma, 2018. **32**(2): p. 116-120.
220. Horsch, J.D., et al., *Mechanism of Abdominal Injury by Steering Wheel Loading*. SAE Transactions, 1985. **94**: p. 210-219.
221. Novelline, R.A., J.T. Rhea, and T. Bell, [\*Helical CT of Abdominal Trauma\*](#). Radiologic Clinics of North America, 1999. **37**(3): p. 591-612.
222. King, A.I., et al., [\*Humanitarian Benefits of Cadaver Research on Injury Prevention\*](#). Journal of Trauma, 1995. **38**(4): p. 564-569.
223. Crandall, J.R., et al., [\*Human Surrogates for Injury Biomechanics Research\*](#). Clinical Anatomy, 2011. **24**(3): p. 362-371.
224. *CIREN Program Report*. 2002, National Highway Traffic Safety Administration: Washington, DC.

225. Anton, D.J., *The Incidence of Spinal Fracture on Royal Air Force Ejections 1968-1983*. 1986, RAF Institute of Aviation Medicine: Farmborough, UK.
226. Somers, J., D. Gohmert, and J. Brinkley, *Application of the Brinkley Dynamic Response Criterion to Spacecraft Transient Events*. 2017, National Aeronautics and Space Administration: Houston, TX.
227. Pintar, F.A., L. Voo, and N. Yoganadan. *Mechanisms of Hyperflexion Cervical Spine Injury*. in *IRCOBI Conference*. 1998. Goteborg, Sweden.
228. Mertz, H., P. Prasad, and A. Irwin. *Injury Risk Curves for Children and Adults in Frontal and Rear Collisions*. in *Forty-First Stapp Car Crash Conference*. 1997. SAE 973318.
229. *USAF Revision of MIL-HDBK-516C Section 9.1.1: Escape System Safety Compatibility Criteria Standard; Supporting Data And Legacy Criteria*. 2016, Air Force Life Cycle Management Center.
230. Perry, C., C. Burneka, and C. Alberly, *Biodynamic Assessment of the THOR-K Manikin*. 2013, DTIC Document.
231. Newby, N., et al. [\*Assessing Biofidelity of the Test Device for Human Occupant Restraint \(THOR\) Against Historic Human Data\*](#). in *Stapp Car Crash Conference*. 2013. Orlando, FL.
232. Somers, J.T., et al., [\*Investigation of the THOR Anthropomorphic Test Device for Predicting Occupant Injuries during Spacecraft Launch Abort and Landing\*](#). *Frontiers in Bioengineering and Biotechnology*, 2014. **2**: p. 1-23.
233. Currie, N., et al., *Crew Exploration Vehicle (CEV) (Orion) Occupant Protection*. 2012, NASA Engineering and Safety Center: Hampton, VA.
234. Humanetics Innovative Solutions. *BioRID (50th Male) Rear Impact*. 2020 [cited 2020 January 23]; Available from: <https://www.humaneticsatd.com/crash-test-dummies/rear-impact/biorid-ii>.
235. Robinson, F., et al., [\*Response of the Rhesus Monkey to Lateral Impact\*](#). *Aerospace Medicine*, 1963. **34**(1): p. 56-62.
236. Brinkley, J.W., *Acceleration Exposure Limits for Escape System Advanced Development*. *SAFE Journal*, 1985. **15**(2): p. 10-16.
237. Brinkley, J., *Personal Communication*. 2010.
238. Lewis, M.E., [\*Survivability and Injuries from Use of Rocket-Assisted Ejection Seats: Analysis of 232 Cases\*](#). *Aviation, Space and Environmental Medicine*, 2006. **77**(9): p. 936-943.
239. Putnam, J.B., et al., [\*Development and Evaluation of a Finite Element Model of the THOR for Occupant Protection of Spaceflight Crewmembers\*](#). *Accident Analysis and Prevention*, 2015. **82**: p. 244-256.
240. Toyota Central R & D Labs. *Human Body Model for Injury Analysis*. 2012; Available from: [http://www.tytlabs.co.jp/english/tech/thums/ethums\\_3.html](http://www.tytlabs.co.jp/english/tech/thums/ethums_3.html).
241. Gaewsky, J.P., et al., [\*Modeling Human Volunteers in Multidirectional, Uni-axial Sled Tests Using a Finite Element Human Body Model\*](#). *Annals of Biomedical Engineering*, 2019. **47**(2): p. 487-511.

## 7.0 RESOURCES

Additional Evidence- <https://humanresearchroadmap.nasa.gov/Evidence/>

Human Research Roadmap (HRR) risk page - <https://humanresearchroadmap.nasa.gov/Risks/>

NASA Technical Reports Server (NTRS) - <https://ntrs.nasa.gov/>

Life Science Data Archive (LSDA) - <https://lsda.jsc.nasa.gov/>

GeneLab - <https://genelab.nasa.gov/>

HRP Computational Model Repository (CMR) - <https://hrpcmr.ndc.nasa.gov/>